TRACKING CHANGES IN HYDRAULIC CONDUCTIVITY OF SOIL RECLAMATION COVERS WITH THE USE OF AIR PERMEABILITY MEASUREMENTS

A Thesis Submitted to the College of Graduate Studies and Research
In Partial Fulfillment of the Requirements for the
Degree of Master of Science
in the Department of Civil Engineering,
University of Saskatchewan, Saskatoon, Canada

By
Heather Alecia Rodger

PERMISSION TO USE

The author has agreed that the library, University of Saskatchewan, may make this thesis freely available for inspection. Moreover, the author has agreed that permission for extensive copying of this thesis for scholarly purposes may be granted by the professors who supervised the thesis work recorded herein or, in their absence, by the head of the Department or the Dean of the College in which the thesis work was done. It is understood that due recognition will be given to the author of this thesis and to the University of Saskatchewan in any use of the material in this thesis. Copying or publication or any other use of the thesis for financial gain without approval by the University of Saskatchewan and the author's written permission is prohibited.

Requests for permission to copy or to make other use of material in this thesis in whole or part should be addressed to:

Head of the Department of Civil Engineering
University of Saskatchewan
Engineering Building
57 Campus Drive
Saskatoon, Saskatchewan
Canada, S7N 5A9

ABSTRACT

The objective of this project was to design a prototype field air permeameter that can be used to track changes in the hydraulic conductivity within soil covers with time. The evolution of soil structure in reclamation soil covers at the Syncrude Canada Ltd. oilsands mine is currently being studied. The Guelph permeameter is currently used to measure hydraulic conductivity, but gathering the data is a very time consuming task due to the relatively low hydraulic conductivity of the cover materials. The use of a faster, more efficient method would increase the capabilities for tracking changes in hydraulic conductivity of reclamation soil covers with time.

Three air permeameter design options were evaluated. One design was chosen and a prototype was built. Preliminary field trials were conducted at the Syncrude Canada Ltd. oilsands mine in August 2005. Air permeability measurements were taken on various soil cover treatments and slope positions. Improvements to the air permeameter were implemented in 2006, and additional data gathered. Guelph permeameter testing was carried out alongside the air permeameter in both field seasons. The air permeameter and Guelph permeameter were also tested under controlled laboratory conditions and compared to standard constant head column tests.

Results include correlations of air and water permeability for various materials and soil structures. Using dry uniform sand in a laboratory setting, the full scale air permeameter provided permeability values within 21% of a standard constant head column test. Testing of the air and Guelph permeameters on a cover constructed of peat-mineral mix over tailings sand revealed a difference of approximately one order of magnitude in permeability values. A difference of approximately two orders of magnitude existed between permeability values measured with the air and Guelph permeameters on till/secondary soil covers.

Further investigation into the difference between values of permeability measured with both methods is necessary. If successful, the air permeameter could prove to be a viable alternative to the Guelph permeameter for use in long-term monitoring of soil covers

used in mine reclamation or waste containment. A more efficient air permeability method would allow a greater number of measurements to be made in a shorter time and could be used to track temporal as well as spatial variability in hydraulic conductivity.

ACKNOWLEDGEMENTS

First and foremost, I would like to thank Dr. Lee Barbour for giving me the opportunity to pursue this M.Sc. degree. Dr. Barbour has been both encouraging and very patient with me throughout the last few years. I am truly thankful for the mentorship and friendship he has provided to me. I would also like to thank my advisory committee, Dr. Malcolm Reeves, Dr. Ian Fleming, and Dr. Bruce Sparling (chair) for their guidance of my research work. A special thank you goes out to Dr. Lisa Feldman, who was asked to take on the position of Graduate Chair upon Dr. Sparling's sabbatical. Dr. Feldman kindly helped with defense arrangements to ensure timely completion of my degree.

Financial support for this project was provided by Syncrude Canada Ltd. and the NSERC Collaborative Research and Development Grant program for which I am thankful.

I would also like to thank our Civil Engineering laboratory technicians Alex Kozlow, Dale Pavier and Brennan Pokoyoway for kindly lending their assistance, tools, storage space and most of all great company time after time. I have thoroughly enjoyed working with all of you over the last couple years.

Throughout all of the phases of this project, many fellow graduate students as well as summer students have lent a helping hand to all of whom I owe a big thank you. These people include Dana Fenske, Chris Kelln, Randi Strunk, Sophie Kessler, Stephen Klemmer and Sheala Konecsni. Many fun times were had with all of you at our various field sites!

My parents, Bob and Peggy Rodger, have been a huge support to me from day one. Thank you both so much for your love and support throughout all of my academic experiences. And most of all, thank you to God for providing me with the strength and perseverance to accomplish this goal.

TABLE OF CONTENTS

LIST OF TABLES

LIST OF FIGURES

CHAPTER 1
INTRODUCTION

Soil covers are used extensively to reclaim overburden or waste deposits from mining operations. The properties of these covers will change with time as a result of changes in secondary structure caused by physical or biologic processes such as freeze-thaw or wet-dry cycling, settlement of the waste material below the cover, and vegetation rooting. These processes act to produce macropores and fractures which alter the hydraulic conductivity of the covers, which in turn controls the transport rates of both water and salt.

The only way of tracking these changes over time has been to undertake repeated measurements of the field saturated hydraulic conductivity. This was done to track the evolution of soil covers on overburden waste at the Syncrude Canada Ltd. mine in northern Alberta, Canada. The hydraulic conductivity was measured using the Guelph permeameter, which is a constant head well permeameter technique. The main study area of interest has been three prototype soil covers on the SW30 Dump. A monitoring program spanning five years has shown that the hydraulic conductivity of each cover soil increased significantly during the first three to four years, and appears to have reached a steady state (Barbour 2005).

Tracking changes in hydraulic conductivity with this method has been successful but has also been found to be extremely time consuming. The relatively low hydraulic conductivity of the cover materials often requires test durations of more than an hour for one location. The fine-grained materials of the soil covers are also prone to smearing upon installation of a Guelph permeameter well bore. This results in underestimated field measurements of hydraulic conductivity.

The method of using air permeability as an alternative to the Guelph permeameter to

track changes in hydraulic conductivity has been proposed. The method is based on the measurement of air permeability rather than saturated hydraulic conductivity. In an unsaturated condition, the air permeability of these soils is controlled by the same secondary structure (and larger pore sizes) that control the field saturated hydraulic conductivity. However, measurements of air permeability can be made much more rapidly, usually within minutes, without having to saturate the secondary structure with water. The pores of interest are empty during most of the summer in response to drainage and drying through evapotranspiration.

The objectives of this study were 1) to design a prototype air permeameter that can measure the hydraulic conductivity of reclamation soil covers using air as the test fluid, 2) compare permeability values calculated from hydraulic conductivity measurements using air and water as the test fluids and 3) evaluate the suitability of the air permeameter as an alternative to the Guelph permeameter.

Three alternatives for air permeability measurement were evaluated, with one design developed as a full scale field prototype. Measurements of permeability were conducted using the prototype air permeameter under controlled laboratory conditions. The results of this test were compared to those obtained by conventional constant head permeability tests to investigate the capability of the air permeameter method to provide reasonable values of permeability in a controlled environment.

Preliminary field trials were conducted at the Syncrude Canada Ltd. oilsands mine in August 2005. Improvements to the air permeameter were implemented in a second field season in August 2006. Field data from the air permeability tests were back analyzed using finite element simulations of steady-state, axisymmetric water flow under saturated and unsaturated conditions. Guelph permeameter testing was carried out alongside the air permeameter to provide comparative measurements. Permeabilities of the cover soils determined from measurements using the air and Guelph permeameters were compared. The performance of the air permeameter was then evaluated and recommendations made for future applications.

CHAPTER 2
LITERATURE REVIEW

2.1 Hydraulic Conductivity Measurement Using the Guelph Permeameter

Several in-situ and laboratory methods exist for measuring the hydraulic conductivity of soils. In-situ methods may include the tension infiltrometer, air-entry permeameter or constant head borehole technique. The Guelph permeameter (GP) is an example of a constant head borehole technique. The GP has been used repeatedly to track the evolution of hydraulic conductivity of three non-compacted clay soil covers over time at the Syncrude Canada Limited oilsands mine (Meiers et al. 2006).

2.1.1 Guelph Permeameter Method

The GP method measures the "field-saturated" hydraulic conductivity (K_{fs}) by determining the steady-state liquid recharge rate (Q) required to maintain a constant depth of water in an uncased, cylindrical auger hole in the unsaturated zone (Reynolds and Elrick 1986). The term "field-saturated" refers to the fact that air may be entrapped or encapsulated by the infiltrating water, causing the measured hydraulic conductivity to be lower than truly saturated hydraulic conductivity K_s (Constantz et al. 1988).

As shown in Figure 2.1, the GP method consists of a mariotte type bottle resting on the bottom of a well bore that has been augered in the unsaturated zone (Elrick and Reynolds 1992). This mariotte bottle supplies water to the well bore while maintaining a constant water depth and providing a means of measuring the rate of water flow into the surrounding soil. Infiltration takes place through a field-saturated "bulb" that extends in the radial direction from the borehole. This bulb is surrounded by an unsaturated "wetting" zone that extends to the wetting front (Elrick and Reynolds 1992).

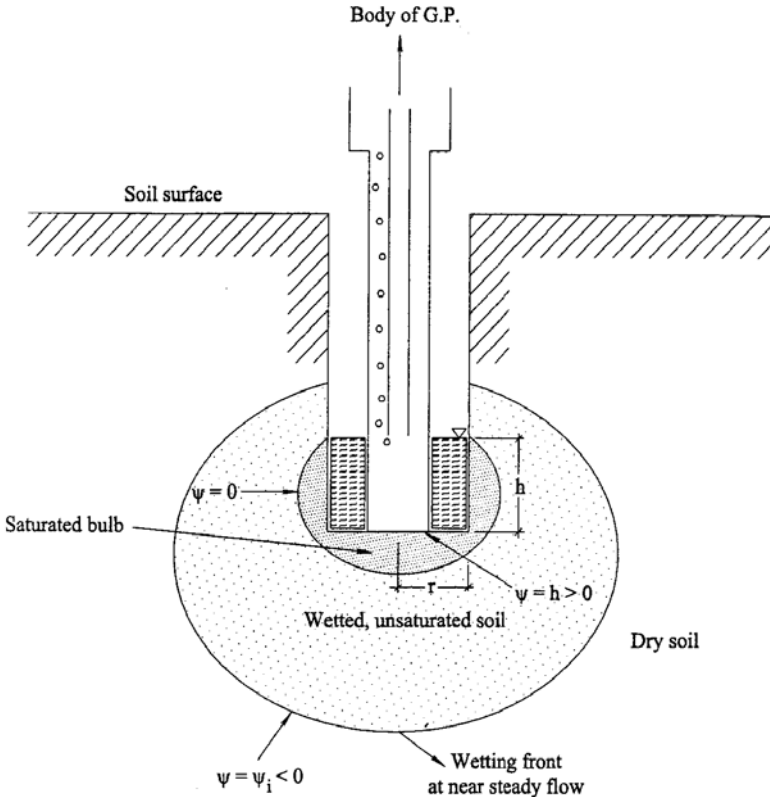

Figure 2.1. GP borehole, saturated bulb and wetting front, where: ψ is the soil water pressure head, h is the constant ponded height of water, and r is the well bore radius (from Giakoumakis and Tsakiris 1999).

2.1.2 Guelph Permeameter Data Analysis

Analysis methods for the GP technique have evolved from simple calculations using saturated flow and pressure head to calculations which take into account saturated-unsaturated flow and pressure, gravitational, and capillary pressure head contributions to flow (Elrick and Reynolds 1992). These contributions to flow are included in the single height analysis method used in this study.

The single height analysis technique was developed by Elrick et al. (1989) to take into account the saturated and unsaturated components of hydraulic conductivity measurement. Following a single water height measurement with the GP, K_{fs} [cm/s] can be determined by:

$$K_{fs} = \frac{CQ}{2\pi H^2 + C\pi r^2 + 2\pi \frac{H}{\alpha^*}} \quad [2.1]$$

where C is a dimensionless shape factor, Q is the steady state flow rate from the well bore [cm^3/s], H is the constant height of water ponded in the well [cm], r is the radius of the well [cm] and α^* is the ratio of K_{fs} to matric flux potential ϕ_m [cm^2/s]. Matric flux potential characterizes the soil's capillarity and represents the unsaturated component of flow (Elrick et al. 1989).

The parameter α^* can be calculated using the ratio of K_{fs}/ϕ_m but can also be estimated from a site evaluation because it is influenced by soil structure and texture. Elrick et al. (1989) state that when cracks or macropores are present in a soil, the value of α^* appears to be dominated by soil structure. A standard range of α^* values used in this study are shown in Table 2.1. A large value in α^* corresponds to a coarse or highly structured soil with low capillarity, whereas a small value of α^* corresponds to a fine, structureless soil with high capillarity (Elrick et al. 1989).

Table 2.1. Values of α^* based on structural/textural considerations (Elrick et al. 1989)

Material	α^* (cm^{-1})
Compacted clays (e.g. landfill caps and liners, lacustrine or marine sediments, etc.)	.01
Unstructured fine textured soils primarily	.04
Most structured soils from clays through clay loams; also includes unstructured medium and fine sands and sandy loams	.12
Coarse and gravely sands; may include highly structured soils with large cracks and macropores	.36

The dimensionless shape factor, C, is dependent mainly on the ratio of H/r, and also mildly dependent on the ratio of K_{fs}/ϕ_m (Elrick et al. 1989). C can be determined from a relationship with H/r depending on soil classification as shown in Figure 2.2. However, values of C can be estimated depending on material texture and structure, as shown in

Table 2.2, if the radius of the well and height of ponded water remain constant throughout the testing program.

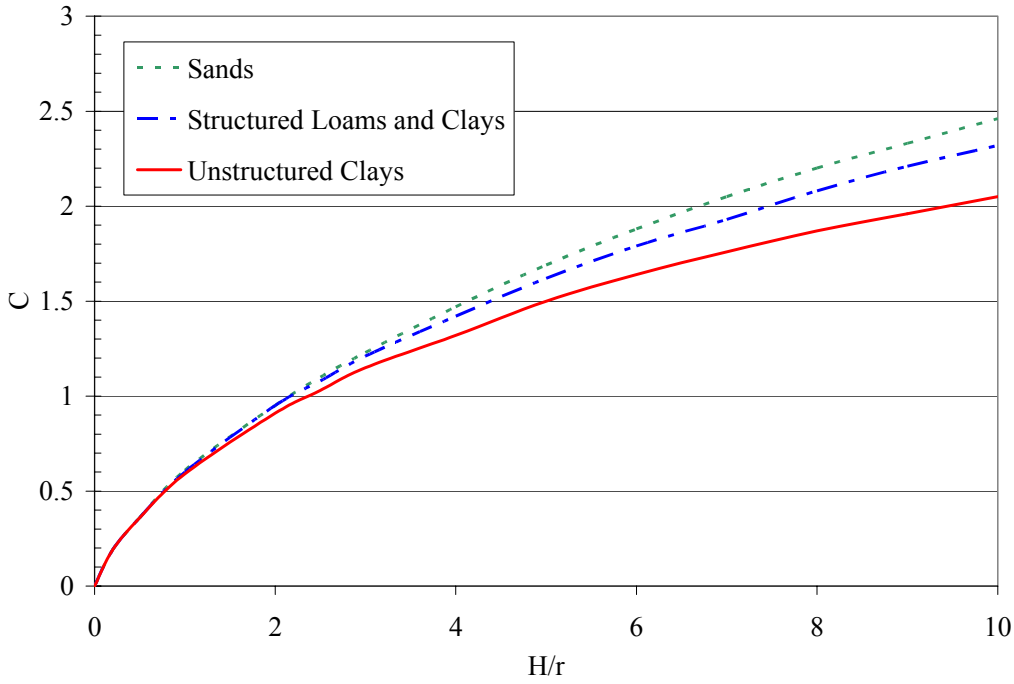

Figure 2.2. Relationship of shape factor C with ratio of H/r. H is height of ponded water in well and r is the radius of the well (after Soilmoisture Equipment Corp. 1991).

Table 2.2. Shape factor C derived from Giakoumakis and Tsakiris (1999).

Material	C_1 (H_1 = 5cm)	C_2 (H_2 = 10cm)
Sand	.84	1.3
Structured loams and clays	.84	1.28
Unstructured clay	.82	1.2

2.2 Factors Affecting Hydraulic Conductivity Measurement

Several factors may affect the magnitude of K_{fs} measurements in the unsaturated zone using the GP method. Elrick and Reynolds (1992) state that the calculated K_{fs} can be reduced up to a factor of 2 or more by:

- smearing, remolding, and/or compaction of the well surfaces during augering,

- gradual siltation of the well and well collapse during the course of the measurement,
- air entrapment by the infiltrating water,
- small scale soil heterogeneity,
- temperature and chemistry of the infiltrating water, and
- solar heating of the head space in the water reservoir.

Some of these effects are discussed in the following sections.

2.2.1 Well Bore Preparation Techniques

Underestimates of K_{fs} or test failures can occur due to inadequate well bore preparation prior to GP testing, especially when the antecedent moisture content is higher than field capacity in fine-grained soils. In an earlier study at the Syncrude Canada Limited oilsands mine, GP testing was completed on the SW30 Dump from 2001-2002 by Meiers (2002). The soil covers on this waste dump consisted of a peat-mineral mix overlying till secondary material. Meiers (2002) found higher success rates when the GP testing was completed during the dry summer months of the field season, when moisture contents were lowest. He also used a very sharp auger, and only took small "bites" with minimal downward pressure before emptying the auger. This technique was coined the "two-finger/two-turn rule."

Bagarello et al. (1999) investigated the potential use of the Guelph permeameter to characterize the hydraulic conductivity of cracking clay soils. They studied the impacts of smearing and compaction of the well bore and compared two well preparation techniques to alleviate those effects. The first technique was the standard technique prescribed by Soilmoisture Equipment Corp. (1991) which involved the use of a wire brush to scour the smear layer created by augering. The second technique was the use of a "plucking" instrument to manually pluck off smeared areas to expose undisturbed soil (Bagarello 1997; Campbell and Fritton 1994).

A study area of 1100 m^2 was used in Sicily, which included 69 standard "brushed" wells and 78 treated "plucked" wells. K_{fs} measurements were not possible on 54% of the standard wells and 68% of the treated wells because the upper operating limit was exceeded due to rapid emptying of the GP reservoir. According to Soilmoisture Equipment Corp. (1991), the GP operates reliably in a K_{fs} range of 1 x 10^{-8} m/s to 1 x 10^{-4} m/s. However, statistical analysis of all successful tests resulted in mean K_{fs} values of 3.4 x 10^{-6} m/s and 5.0 x 10^{-6} m/s for the standard and treated wells, respectively (Bagarello et al. 1999).

The differences in the test results for the two types of tests were not found to be significantly different. Given the clayey texture of the soil, however, these results were 1-3 orders of magnitude higher than expected. The combination of high K_{fs} measurements and the large percentage of failures due to high infiltration rates for both methods indicates that flow occurred primarily through the macrostructure and shrinkage cracks and not through the clay matrix (Bagarello et al. 1999).

If effects of smearing are not properly corrected, then the K_{fs} for cracking or fractured clay-rich soils will be largely underestimated (Elrick and Reynolds 1992). In other studies, K_{fs} measurements in well-structured clay soils have occurred in the expected K_{fs} range for structureless sands, 1 x 10^{-6} m/s to 1 x 10^{-4} m/s, instead of the K_{fs} range expected for structureless clay soils, 1 x 10^{-9} m/s to 1 x 10^{-7} m/s (Reynolds and Zebchuk 1996).

2.2.2 Effects of Macropore Flow

As mentioned in Section 2.1.1, air entrapment during infiltration can cause measured values of K_{fs} to be lower than the true saturated hydraulic conductivity K_s. Reynolds and Elrick (1986) found that K_{fs} can be up to 50 percent lower than K_s, the truly saturated hydraulic conductivity, depending on the amount of entrapped air. Effects of air inclusion may be insignificant when measuring K_s on sandy soils, but not necessarily when measuring K_s on clay soils when the flow may be governed by macropores. Daniel (1989) suggested that the value of hydraulic conductivity at complete saturation

compared to a value measured from an infiltration test may be up to two times larger for a sandy soil, and four times larger for a clayey soil.

Macropores are defined as pores that are significantly larger than those resulting from simple packing of elementary soil particles. The size of macropores is not as important as their continuity through the soil horizon, which allows for fluid transport (Bouma 1982). Total macroporosities have been found to typically occupy 1 to 8% of the soil volume (Beven and Germann 1982; Sollins and Radulovich 1988). However, water conducting macroporosities have been found to only occupy 0.01 to 0.04% of the total volume (Bodhinayake and Si 2004). Bouma and Wosten (1979) stated that water-conducting macropores usually occupy <1% of the total soil volume.

Macropore flow affects the transport capabilities of a soil horizon and has been quantified through field studies. Watson and Luxmoore (1986) used a double-ring infiltrometer and tension infiltrometer to estimate macroporosity in a forest watershed. They conducted infiltration measurements at thirty sites, using the double-ring infiltrometer to measure ponded flow followed by a tension infiltrometer to measure flow under tensions of 3, 6 and 15 cm (H_2O). According to capillary theory, measurements under these tensions limit water infiltration to pore diameters greater than 0.1, 0.05 and 0.02 cm, respectively.

The study concluded that all pores greater than 0.02 cm in diameter comprised 0.32% of the total soil volume, and transmitted approximately 96% of the total water flux. The macropores of 0.1 cm or larger in diameter comprised only 0.04% of the soil volume, but contributed to 73% of flux under ponded flow (Watson and Luxmoore 1986). If air entrapment occurs within macropore structure during a Guelph permeameter test, the resultant K_{fs} value may be much lower than the value of K_s which represents a fully saturated soil (Messing and Jarvis 1990).

2.2.3 Measurements in Anisotropic Soil

Flow initially occurs horizontally from the well bore during the GP test, followed by downward unsaturated infiltration into the surrounding soil. The GP equations are based on the assumption that the soil is isotropic and homogeneous; consequently, if the soil is anisotropic with respect to K_{fs} then this could affect the calculated value of K_{fs}. The hydraulic conductivity of a granular, unstructured soil is typically isotropic. In a structured soil, however, the GP measures an average of the vertical and horizontal K (Reynolds and Elrick 1986). This effect was quantified in a study by Reynolds and Elrick (1985) discussed below.

In the study by Reynolds and Elrick (1985), GP tests were carried out in a heterogeneous, anisotropic, structured loam soil and compared to laboratory saturated hydraulic conductivity tests on horizontal and vertically oriented undisturbed cores taken from the same site. At the time of testing, the antecedent water content of the soil was known to be near field capacity. Eleven GP tests were carried out in a 3 x 5 m test area, at depths varying between 0.25 m and 0.35 m below the soil surface, using a well radius of 0.03 m. Within this test area, fourteen vertical cores were taken from a top depth of 0.25 m to 0.35 m below the soil surface. Fourteen horizontal cores were also taken, with the upper sides of the samples located 0.20 m to 0.30 m below the soil surface.

The soil cores were saturated in the laboratory and K was measured using a constant head apparatus of Elrick et al. (1981). Comparisons of geometric mean K values for the GP and soil core tests are given in Table 2.3. The vertical and horizontal values of K calculated from the soil core tests were found to create upper and lower boundaries of the GP values.

Soil textures for the vertical and horizontal cores were compared, and no significant differences were found. Given the presence of vertical macropores, these results suggest the vertical-horizontal anisotropic effects of K are due to a macropore effect, and are not affected by sample size, texture or stratigraphy (Reynolds and Elrick 1985).

Lee et al. (1985) found similar results in a field comparison study of saturated hydraulic conductivity measurements, in which the Guelph permeameter was found to effectively average the matrix and macropore hydraulic conductivity in a structured soil.

Table 2.3. Comparison of GP test results to vertical and horizontal K test results (from Reynolds and Elrick 1985).

Parameter	Vertical core	GP test	Horizontal core
$10^6\ \overline{K}$ (ms^{-1})	6.39	3.35	1.08

2.3 Comparison of Hydraulic Conductivity Measurement Techniques

Several methods exist for the in-situ measurement of saturated hydraulic conductivity. These methods vary in geometry, operating ranges, boundary conditions and sample sizes and respond differently based on soil texture, structure and moisture conditions (Reynolds and Zebchuk 1996). Mohanty et al. (1994) conducted a study in which four in-situ methods and one laboratory method were compared at five sites located 50 meters apart in a glacial-till soil, using four depths of 15 cm, 30 cm, 60 cm and 90 cm. The soil tested in this study was under a no-tillage practice, with an area occupied by macropores varying between 2 and 12% (Singh et al. 1991).

The four in-situ methods included the Guelph permeameter, velocity permeameter, disk permeameter and double-tube method. The laboratory method used was the constant-head permeameter. Results from the double-tube method and constant-head permeameter were omitted from this discussion due to the small number of successful results available.

The velocity permeameter was a falling-head permeameter adapted for field use (Merva 1987), consisting of a cylinder 8.4 cm in diameter inserted 7 cm into the soil. The top of the cylinder was closed, with two hoses attached, one to allow water infiltration from a reservoir, the other to allow air to be vented. Cylinder geometry and rate of fall of the

water level in an observation tube were used to calculate saturated hydraulic conductivity. As the wetting front moved through the soil, estimates of K_s were made. These estimates were observed to approach a pseudo-constant value as the wetting front exited the soil core (Mohanty et al. 1994).

The disk permeameter was a constant-head infiltrometer which operated at a positive or negative head (Perroux and White 1988). Infiltration occurred vertically through the surface of the soil, using a 2 cm thick layer of 0.25 to 0.42 mm diameter sand inside a 25.4 cm diameter ring as an application surface. Four supply potentials were used to measure infiltration, and K_s was estimated using a calibrated empirical relationship at zero supply potential (Mohanty et al. 1994).

Geometric mean values for the Guelph, velocity and disk permeameter methods are shown in Figure 2.3. The Guelph permeameter produced the lowest estimates of hydraulic conductivity, approximately two orders of magnitude lower than the values produced by the disk permeameter.

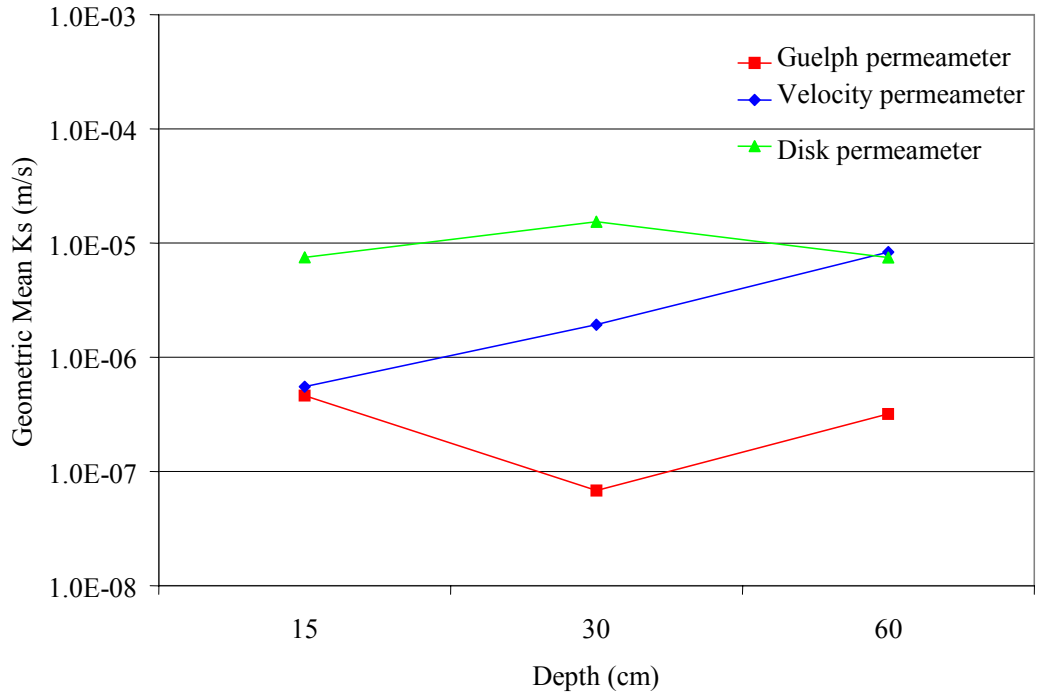

Figure 2.3. Comparison of geometric mean K_s values for different in-situ methods at individual depths (from Mohanty et al. 1994).

The velocity permeameter likely produced larger values of permeability than the Guelph permeameter because it measured vertical conductivity of the soil and utilized a larger macropore transport network. The disk permeameter yielded the highest values of hydraulic conductivity, because it was dominated by macropore flow and utilized a large undisturbed sample area (Mohanty et al. 1994).

2.4 Air Flow through Soil

As measuring saturated hydraulic conductivity of unsaturated, anisotropic soil produces numerous challenges, the use of air permeability as an indirect method has been viewed as a promising alternative. One of the challenges in measuring hydraulic conductivity is the entrapment of air within the macropore network during infiltration. As mentioned in Section 2.2.2, macropores occupy an extremely small volume of a soil horizon, yet contribute to the majority of the flow.

In the dry summer months, soil is typically at water contents less than field capacity, which suggests that the larger pores are fully drained and open for air flow. Iversen et al. (2001) states that field capacity typically occurs at matric water potentials of -5 to -10 kPa, which corresponds to available pore diameters of 60 to 30 μm and greater by the laws of capillary theory. According to Poiseuille's law, the flow rate of a fluid in fluid-filled continuous soil pores depends on the fourth power of the effective pore radius (Hillel 1998). Therefore, if a soil is at field capacity, the pores contributing to air flow are governing the overall flow rate through the soil horizon. Air flow measurement in unsaturated soil is therefore a more direct method to characterize permeability of the larger pores (Ball 1981).

Theoretically, the intrinsic permeability (k [m^2]) of soil to water and air should be equal at identical fluid phase contents. The intrinsic permeability will be represented by the term "permeability" from this point forward. The permeability of soil is related to hydraulic conductivity using properties of the test fluid according to the following equation:

$$k = \frac{\mu K}{\rho g} \qquad [2.2]$$

where μ is the dynamic viscosity of the test fluid [Ns/m^2], K is the hydraulic conductivity of the test fluid [m/s], ρ is the density of the test fluid [kg/m^3], and g is the gravitational constant [m/s^2] (Freeze and Cherry 1979). Therefore, measurements of hydraulic conductivity using air when the soil is near field capacity should provide a good prediction of permeability of the network of larger pores as well as the saturated hydraulic conductivity of water K_w (Iversen et al. 2003).

Differences between the value of permeability estimated from measurements of water hydraulic conductivity and air conductivity are quite likely due to the effect that water has on soil structure, although the error incurred may not be large. As water is a polar fluid, interactions may occur between the electrolytes in the water and exchangeable cations in the soil. For a perfect comparison to saturated water flow, air permeability measurements should be taken in soil which is completely dry. However, this could lead to drying and subsequent shrinkage of the soil and a change in soil structure (Iversen et al. 2001).

In order to use Darcy's law to quantify airflow in porous media, laminar flow conditions must be met. Laminar flow conditions are met for fluid flow through porous media when the Reynolds number is kept below a certain limit. Reynolds Number is defined as follows:

$$\mathrm{Re} = \frac{dq_m}{\mu\theta} \qquad [2.3]$$

where d is a representative pore-space diameter [cm], q_m is the specific mass flux for air [g/cm^2s], and θ is the air-filled porosity. Yu (1985) conducted column tests using sand, and determined that Darcy's law is valid for gas flow through porous media when the Reynolds numbers were less than 6 (Baehr and Hult 1991). To ensure that Darcy's law is valid following a specific air permeability measurement, the gas flux plotted against the pressure gradient should result in a linear relationship with an intercept of zero (Scanlon et al. 2002).

Deviations from Darcy's law can occur for air flow due to effects such as threshold gradient, gas compressibility and slip flow. Threshold gradients exist when the relationship of flux and pressure gradient is non-linear for very low and very high apparent velocities (Sinha et al. 1995). When air pressure is applied to a soil surface during an air permeability test, the flow rate initially remains zero or near zero, until a certain threshold gradient is reached, after which flow increases linearly with gradient according to Darcy's law. At high flow velocities, turbulence causes inertial effects on the air flow measurements. At this point, the relationship of flux and pressure gradient becomes non-linear, and the fluxes tend to be lower than what is predicted by Darcy's law (Scanlon et al. 2002).

Theoretically, a non-linear compressible flow equation should be used instead of Darcy's law for a compressible fluid. However, depending on the air pressures being applied in an air permeability test, the error incurred by ignoring compressibility may be small. As part of a soil vapor extraction test study, Massmann (1989) studied the possibility of modelling gas transport with equations for incompressible groundwater flow. He found that groundwater flow models could provide good approximations for gas transport if pressure variations between any two points in the flow field were approximately 0.5 atmospheres or less.

Kirkham (1946) also quantified the effects of ignoring compressibility in air flow calculations. He developed an air permeability measurement method which used a pressurized air tank with a water manometer to track pressure drop in a soil core in the laboratory, followed by a field application to measure air permeability in-situ. If the pressure applied to the soil was kept very small, relative to atmospheric pressure, he could remove the compressible flow terms from the flow equation with minimal error. The errors associated with neglecting compressibility for applied pressures of 25 cm and 50 cm H_2O were 1.25% and 2.5%, respectively (Kirkham 1946).

Slip flow, or the Klinkenberg effect, occurs as a result of the difference in flow behaviour of water and air in porous media. Water flows through soil according to

viscous fluid flow theory, which states that velocity is zero at solid surfaces (Scanlon et al. 2002). However, gas velocities are generally nonzero at solid surfaces, leading to an underestimation of flux according to Darcy's law.

Klinkenberg (1941) stated that "the permeability to a gas is a function of the mean free path of the gas molecules, and thus depends on factors which influence the mean free path, such as the pressure, temperature, and the nature of the gas." Slip flow is enhanced in fine-grained material with decreasing air-phase pressure (Ba-Te et al. 2005). However, as mean pressure increases, the permeability measured using gas flow decreases and approaches that calculated from permeability using liquid flow (Scanlon et al. 2002).

The relationship between slip-enhanced permeability, k_g, and permeability of a gas at infinite pressure, k, when gas behaves like a liquid (Klinkenberg 1941) is given by:

$$k_g = k\left[1 + \frac{b}{\overline{P}}\right] \qquad [2.4]$$

where b is the slip or Klinkenberg parameter which depends on the porous media and gas used in the measurement [Pa], and $\overline{P}$ is the mean pressure [Pa]. The Klinkenberg parameter b can be estimated using an empirical equation developed by Heid et al. (1950) as follows:

$$b = \left[3.98x10^{-5}\right]k^{-0.39} \qquad [2.5]$$

This parameter was adopted as the standard Klinkenberg correction of the American Petroleum Institute.

Scanlon et al. (2002) outlined a method in which to estimate the Klinkenberg parameter b and determine the true permeability. Measured values of permeability (k) can be plotted versus the reciprocal mean pressures ($1/\overline{P}$) at which the tests were performed. Rearranging [2.4] results in:

$$k_g = k + kb\left[\frac{1}{\overline{P}}\right] \qquad [2.6]$$

The slope of the graph is the product of k times b, and the intercept is the true permeability k_g.

Although the Klinkenberg effect should not be overlooked, the error associated with ignoring this effect is not necessarily significant, depending on the pore sizes and pressures involved in the air permeability test. Massmann (1989) stated that the effects of slip flow are small relative to viscous flow for pore diameters of 20 μm or greater. In air permeability tests conducted by Baehr and Hult (1991), the error associated with ignoring the Klinkenberg effect was found to become significant (> 10%) when intrinsic permeabilities are in the range of 1×10^{-12} m^2 or less.

2.5 Air Permeability Methods

Various methods have been used historically to measure air permeability in-situ. Three methods were investigated for this study and are discussed briefly. These methods include pneumatic tests, dual-probe dynamic pressure technique and the portable air permeameter. The portable air permeameter technique was found to be the most suitable alternative.

2.5.1 Pneumatic Tests

The first method considered was pneumatic tests, which are generally used to characterize sites for the design of soil vapor extraction (SVE) systems. A pneumatic test set-up generally consists of a well with a screened portion installed at some depth in the unsaturated zone, through which air is injected or extracted. An example of this configuration is shown in Figure 2.4. Although the diagram depicts a dual-well configuration, a single well configuration was considered for the current study.

Pressure, flow rate and temperature are measured within the well to calculate the mass flux into or out of the soil. Pressure probes are installed at various radial and vertical distances from the well screen in nested well formations which have screened intervals to observe the pressure distribution created by air injection or extraction. These screens

are surrounded by a granular material, and isolated vertically from other measurement probes with bentonite grout (Baehr and Hult 1991).

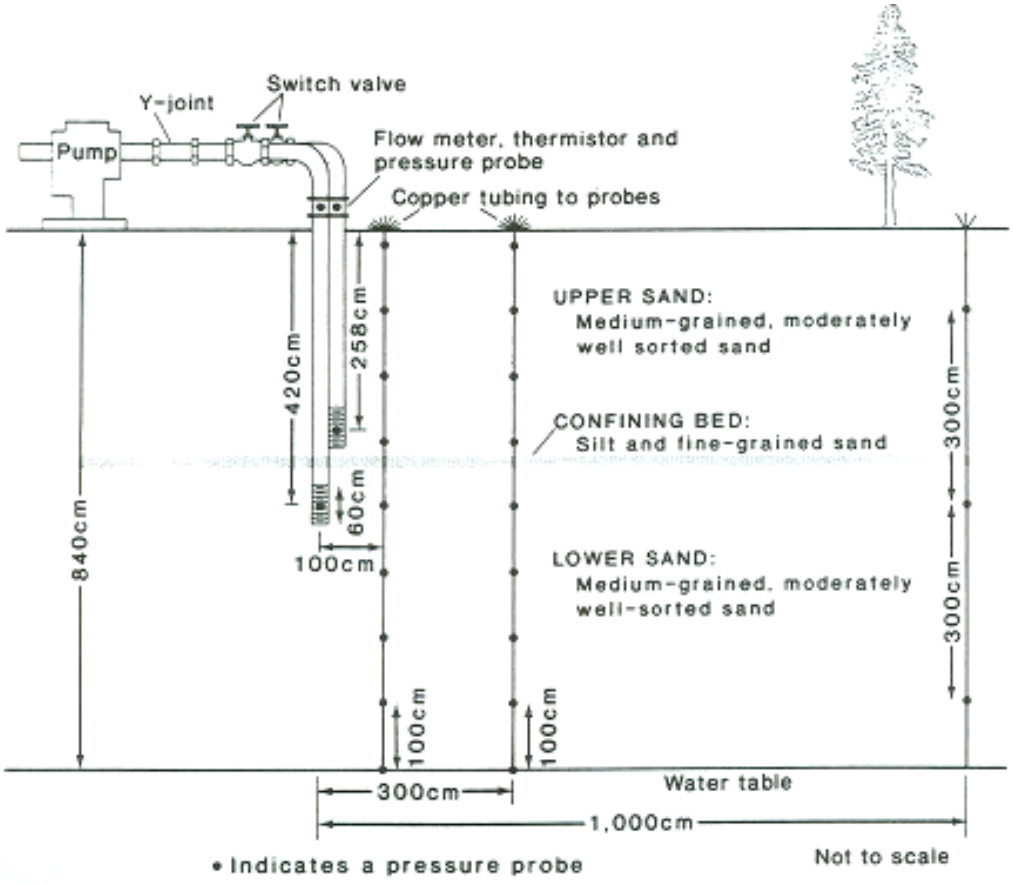

Figure 2.4. Typical pneumatic test set up (from Baehr and Hult 1991).

Several reasons exist for not choosing the pneumatic test method for the current study. The fine-grained nature of the soil cover material would have created challenges during installation of well bores due to smearing of fine-grained soil on the well face. The use of a well and nested pressure probes at various radial distances would have also eliminated the possibility of using this method in a portable nature for spatial analysis of permeability. Also, the reclamation covers in this study have a thickness of one meter or less, limiting the capabilities of quantifying a pressure distribution surrounding the well bore.

2.5.2 Dual-Probe Dynamic Pressure Technique

The dual-probe dynamic pressure technique was originally designed as a method to accurately measure air permeability while taking into account scale effects and spatial orientation. This method was implemented to quantify advective transport of soil gas contaminants into basements of houses. Although typical in-situ air permeability tests operate on a scale of approximately 1 x 10^{-1} m, houses interact with surrounding soil on a scale of approximately 1 to 10 m (Garbesi et al. 1996).

The dual-probe dynamic pressure (DDP) apparatus is shown below in Figure 2.5. The system consists of two probes: a source to provide a sinusoidal pressure oscillation; and a detector probe. The effective permeability of the pathway between the probes is determined by the time lag between source and detector signals.

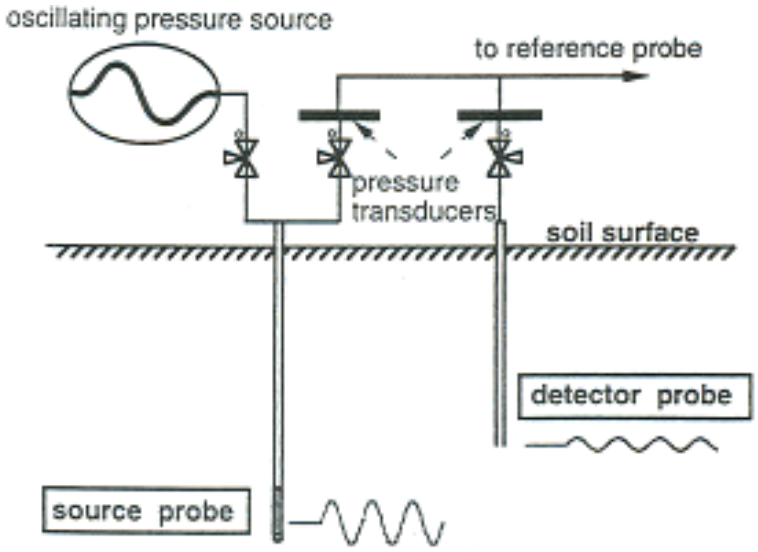

Figure 2.5. Dual-probe dynamic pressure technique (from Garbesi et al. 1996).

One advantage the dynamic pressure technique has over steady state pressure methods is that the pressure signal propagation speed is only weakly dependent on distance from the source. Therefore, effects of pressure loss caused by soil disturbance adjacent to the probe can be minimized by increasing the distance between the source and detector probes. However, this method also assumes the soil is homogeneous and isotropic (Garbesi et al. 1996). Given the heterogeneous, anisotropic nature of the reclamation

soil covers, these assumptions would be difficult to meet. An additional reason for not choosing this method is the cost of the components involved.

2.5.3 Portable Air Permeameter

Portable air permeameters have been used extensively to measure air permeability of shallow agricultural soils. A schematic of this method is shown in Figure 2.6. Air is supplied by a compressed gas cylinder, and its flow rate is measured by one of three flow meters of differing flow ranges. Air enters the soil within a metal cylinder that is pounded in to a shallow depth. To minimize air leakage along the inside boundary of the metal ring, the soil at this interface was kneaded carefully against the metal surface. The inner volume of the cylinder is isolated from atmosphere by the use of a packer. The pressure of the air entering the soil is measured with a water manometer.

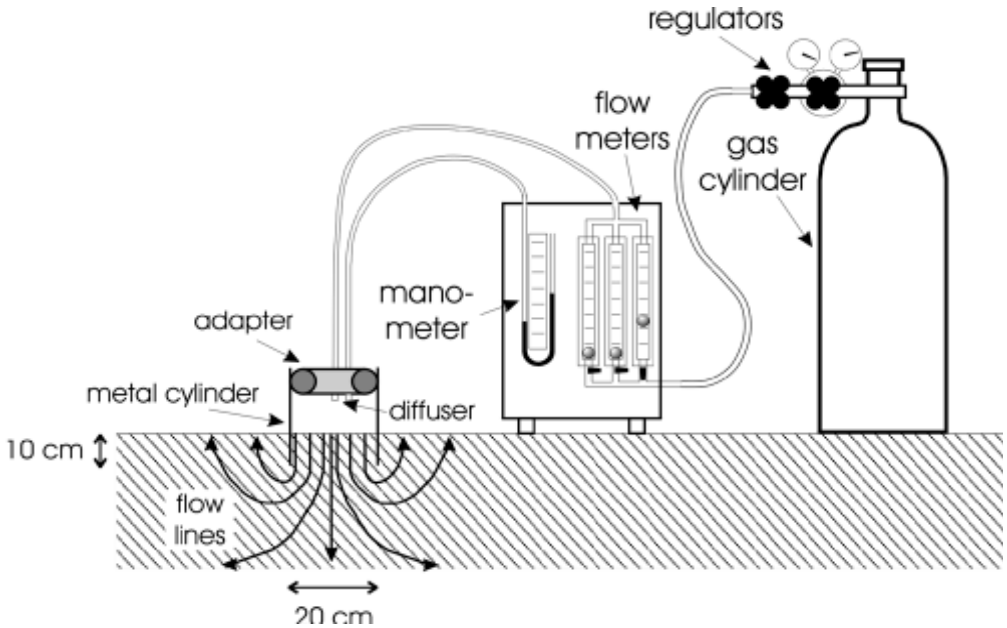

Figure 2.6. Portable air permeameter technique (from Iversen et al. 2001).

During the test, the flow rate of air is measured within the appropriate flow range, isolated from the other flow meters with the use of stopcock valves. The air pressure entering the system is set to a value between 0.5 and 1 kPa with the pressure regulator valves on the outlet of the air tank.

The portable air permeameter was chosen for this study for several reasons. The equipment involved is simple and inexpensive. The analysis required is straightforward and easily understood by an inexperienced operator. The portable nature of this permeameter allows multiple measurements to be taken across a reclamation cover. The use of an inserted vertical cylinder as compared to an augered well bore minimizes effects of soil structure disturbance on air permeability measurements.

2.6 Previous Applications of Portable Air Permeameter

The portable air permeameter has been used to predict saturated hydraulic conductivity for applications such as water infiltration modelling and determining spatial variability of hydraulic conductivity. As the nature of in-situ K_s tests is time consuming and not always reliable, in-situ measurements of air permeability have been seen as a fast and more reliable indirect method. Analysis methods of air permeability (k_a) data are discussed here. Predictive relationships of K_s from k_a data have also been developed and are discussed.

Calculations to determine air permeability using the portable air permeameter are simple and based on Darcy's law because the flow of air through porous media is similar to the flow of water at low pressure gradients (Iversen et al. 2003). The intrinsic permeability of soil, k [m^2], is estimated for either water or air flow using Darcy's law, according to:

$$q = -\left[\frac{k}{\eta}\right]\left[\frac{\Delta p}{\Delta x}\right] \qquad [2.7]$$

where q is flux density [m/s], η is dynamic viscosity [Ns/m^2], p is pressure [Pa], and x is distance along flow direction [m] (Iversen et al. 2003).

Air permeability measured on a cylinder of known dimensions and boundary conditions in the laboratory, $k_{a,lab}$ [m^2], would be determined using an integrated form of [2.7] (Kirkham 1947) as follows:

$$Q = -\frac{k_{a,lab}\Delta p a_s}{\eta L_s} \quad [2.8]$$

where Q is the volumetric flow rate [m^3/s], a_s is cross-sectional area [m^2] and L_s is the length of the sample [m]. When measuring air permeability using the portable air permeameter, the air pressure at the bottom of the cylinder is unknown, because the air must still flow through an unknown volume of soil before it reaches atmospheric pressure at the soil surface (see Figure 2.6).

To account for this lack of boundary condition at the bottom of the cylinder, a non-dimensional shape factor has been developed to take into consideration the pattern of flow lines for the air leaving the base of the cylinder. This shape factor was first determined for various combinations of sample diameters and insert depths (Grover 1955) and is incorporated into the calculation for in-situ permeability, $k_{a,in\text{-}situ}$ [m^2], as follows:

$$Q = -\frac{k_{a,in-situ}\Delta p A}{\eta} \quad [2.9]$$

where A is the non-dimensional shape factor.

The most recent improvement to the shape factor, A, was determined by Liang et al. (1995) using the finite element model ANSYS F. The shape factor equation is:

$$[A/D] = 0.4862[D/L_s] - 0.0287[D/L_s]^2 - 0.1106 \quad [2.10]$$

where D is the inside diameter of the soil core [m]. Iversen et al. (2001) demonstrated that calculations from air permeability measurements using the shape factor determined by Liang et al. (1995) provided reliable results for both structured and unstructured soils.

Measurements of k_a and k_w should theoretically be equal to each other if the same pore space is used in fluid flow. However, because differences may arise between permeability values measured using different fluids, empirical prediction relationships have been developed between k_a measured at -10 kPa and saturated hydraulic

conductivity K_s (Iversen et al. 2003).

Loll et al. (1999) developed a general predictive relationship between k_a and K_s based on the results from two studies (Riley and Ekeberg 1989; Schjonning 1986) which involved laboratory k_a and K_s testing on 1614 undisturbed 100 cm^3 soil cores. The data from these studies included multi-year sampling regimes, nine different Danish and Norwegian soils, six different soil treatments as well as sampling from the A, B and C horizons. Both Schjonning (1986) and Riley and Ekeberg (1989) found a log-log linear relationship to exist between the laboratory measurements of k_a at matric water potential of -10 kPa and K_s. Loll et al. (1999) fitted the prediction relationships using the Ordinary Least Squares method as follows:

$$\log[K_s] = \alpha \log[k_a] + \beta \qquad [2.11]$$

where α is the slope and β is the intercept of the log-log linear regression fit.

The predictive accuracy of this relationship was analyzed for various scenarios such as site-specific results, treatment-specific results as well as depth-specific results. Overall, the general relationship capturing trends of all data sets, and providing a prediction accuracy of ± 0.7 orders of magnitude is as follows:

$$\log[K_s] = 1.27 \log[k_a] + 14.11 \qquad [2.12]$$

where K_s and k_a are in units of [m/d] and [m^2], respectively (Loll et al. 1999).

The suitability of the prediction relationship developed by Loll et al. (1999) for predicting K_s from in-situ k_a measurements was determined in a study by Iversen et al. (2004). In-situ measurements of k_a were carried out using the portable air permeameter of Iversen et al. (2001) alongside K_s measurements using the tension infiltrometer (Ankeny et al. 1988). Values of K_s were predicted from the in-situ k_a measurements. The predicted values of K_s were found to compare well within a factor of two with the K_s values measured with the tension infiltrometer (Iversen et al. 2004).

CHAPTER 3
EXPERIMENTAL METHODS

3.1 Introduction

This chapter provides a detailed description of the prototype air permeameter (AP) as well as the analysis method used to process the results. A laboratory program was carried out to compare the values of permeability measured using the AP method to those measured using standard constant head permeability tests. The AP method was then applied to a field environment of reclamation soil covers of varying thicknesses and materials. Guelph permeameter (GP) testing was carried out alongside the AP in the field. An attempt was made to correlate values of permeability determined by both of these methods.

3.2 Prototype Design

The prototype AP was built prior to the 2005 field season using the basic design used for the portable AP method of Iversen et al. (2001) as shown in Figure 2.6. Iversen's method was typically used on shallow agricultural soils to a maximum depth of 10 cm. The prototype AP in this study was modified to allow testing to depths of 40 cm. A photograph of the prototype AP is shown in Figure 3.1. Air was supplied from a five gallon portable air tank, which was filled on site with a compressor. Air pressure from the tank was controlled with a pressure regulator. The flow rate of air used for each test was regulated with one of two flow meters, depending on the required range of flow rates. A 16 cm diameter steel cylinder was inserted into the ground in 10 cm intervals to a total depth of 40 cm, using a drop hammer on the cylinder cap.

A greased, rubber gasket was used as a seal between the metal cap and the cylinder during air permeability tests. Bolts were used to firmly attach the cap and cylinder through three sets of metal arms welded onto the cap and cylinder. Unfortunately, the

threads within the metal arms were exposed to moisture and soil early in the test program and became unusable. For the remainder of the testing program, the seal between the cap and cylinder relied on pressure created by the weight of the cap on the rubber gasket.

Figure 3.1. 2005 field season AP prototype design.

Two threaded ports machined through the metal cap allowed gas flow into the cylinder during an AP test and measurement of air pressure within the cylinder using a water manometer. A porous aquarium filter was threaded into the bottom of the gas flow port to ensure the air entering the cylinder was diffused. Flexible plastic tubing was used to connect the gauges and flow meters to the cylinder during air permeability trials. Once a full 40 cm profile was complete, a car jack was used to remove the cylinder from the ground. The soil within the cylinder was then removed using a soil auger and returned to the test hole.

Although the 2005 prototype AP seemed to work well, modifications were made prior to the 2006 field season to decrease the testing time, decrease possibilities for air leakage through system connections and incorporate temperature measurements of air within the cylinder. A photograph of the modified prototype AP can be seen in Figure 3.2.

Figure 3.2. 2006 field season AP prototype design.

During insertion of the 2005 prototype, the cylinder would quite frequently become skewed, likely due to hitting an obstruction such a small rock. A plastic support frame was incorporated in 2006 to guide the steel cylinder during insertion. This had the benefit of not only controlling orientation of the cylinder during insertion but also reduced disturbance of the soil along the side walls of the cylinder due to any rocking motion during insertion. The base of the frame was secured to the ground surface using metal stakes.

The five gallon carry tank used in 2005 could only be pressurized to 50 psi; consequently, the air supply had to be replenished quite frequently over the course of one day of testing. The use of a compressor on site also added challenges such as trying to start the compressor. For 2006, this tank was replaced by an industrial tank of nitrogen gas. The nitrogen tank was filled to 2000 psi by the distributor, allowing an entire week of testing before it had to be refilled. The tank was also made of lightweight aluminum, which was easy to move around.

One cap was used in 2005 to drive the cylinder into the ground and also provide flow and pressure ports. This required extra time between each depth interval to connect fittings and plastic hoses. A second cap was constructed in 2006 and the flow and pressure ports were permanently connected to this cap, decreasing the time required to attach and remove fittings. A greased rubber gasket was again used to create a seal between this cap and the cylinder. Clamps were used instead of bolts to firmly attach the cap to the cylinder and this worked effectively to seal the cylinder regardless of working conditions.

A flow meter manifold was built for the 2006 prototype, which allowed one flow meter in a bank of three to be isolated simply by using valves (Figure 3.3). This saved time by eliminating the need to disconnect and reconnect flow meters of various ranges during an air permeability test, similar to the 2005 design. All connections were sealed using Teflon tape in order to minimize the possibility of leakage.

The flexible plastic tubing used to connect the gauges and meters in the 2005 prototype was replaced by stiff plastic tubing and fittings. The hoses between the flow meters and the cylinder cap remained attached throughout all air tests, decreasing the possibility of leakage. A thermocouple, placed in the pressure measurement line for convenience, was also incorporated into the 2006 design to measure temperature within the cylinder during testing.

Figure 3.3. Flow meter manifold in 2006 AP design.

The car jack used for removing the cylinder from the ground was replaced with a Jackall in 2006. The Jackall operated more quickly and efficiently. A circular plastic base with a diameter equal to the inner diameter of the steel cylinder was fixed to the base of the Jackall. The Jackall could then be placed inside the cylinder, using wire cables to connect it to the arms on the cylinder, and used to extrude the intact soil core from the cylinder. Photographs of the cylinder removal process are shown in Figure 3.4. The ability to keep the soil core intact allowed it to be examined for structure as well as layer interfaces before returning it to the test hole. A record of these details is important in interpreting the air permeability results.

The modifications to the prototype for the 2006 field season allowed the air permeability testing to be conducted quickly and efficiently. Pounding the cylinder to the required depth and connecting the system took only a few minutes. When air flow was initiated, steady state was achieved within seconds, allowing for many

combinations of flow and pressure data to be collected quickly. Following the test, removal of the cylinder and extrusion of the soil core took approximately ten minutes. The efficient nature of this test allowed for many measurements to be completed at numerous sites within one day. Three 40 cm profiles could be tested within approximately two hours at one test location. The equipment necessary to do air permeability tests was also fairly affordable and accessible. With the use of a wagon, the system was also quite portable on the reclamation soil covers.

(a) (b) (c)

Figure 3.4. Cylinder removal process upon completion of an air permeability test: (a) removal of steel cylinder from ground, (b) extrusion of soil core from cylinder; and (c) examination of soil core before returning to test hole.

As the validity of AP measurements and the simplified analysis depend on the conditions of laminar flow, it is essential to monitor the pressure and flow rate. According to the literature discussed in Section 2.4 certain concerns such as compressibility or turbulence can be ignored if the pressure and flow rate are maintained within a certain range. Approximate ranges of suitable flow and pressure have been developed through past air permeability applications and were considered during the AP tests in the current study.

3.3 Data Analysis Method

Two methods were used to analyze flow and pressure data from air permeability tests. A numerical finite element analysis was performed on the data and compared to hand calculations performed using Darcy's law. It would be beneficial to have a simple hand calculation in order to make immediate interpretation of the AP test in the field. In this study all analyses were completed numerically; however, a comparison was made to a simple method of hand calculations.

The application of Darcy's law to interpret air permeability data requires some assumptions to ensure the validity of Darcy's law for gas flow. Laminar flow conditions must be met. The effects of slip flow and compressibility on gas flow must also be negligible. As discussed in Section 2.4, laminar flow conditions are met when the plotted relationship of pressure and flow is linear with an intercept of zero (Scanlon et al. 2002)

The majority of pressure-flow data sets were a linear relationship; however, several of the pressure- flow data sets resulted in an intercept very close to zero instead of through zero. Several reasons were investigated, such as incorrect flow recording or slip flow effects. A few data sets from tests in each reclamation cover were chosen, and a slip correction was applied to the test data according to the method described in Section 2.4. This adjustment to the data set resulted in a corrected pressure-flow relationship that did pass through the origin. However, the error in ignoring slip effects in permeability calculations was low.

Numerical modelling of air flow during the AP test shows that the majority of the head loss occurs within the soil within the column. The reason for this is that the volume of this soil is relatively small, due to the confinement provided by the column relative to the expansion of the air flow outside the column as it flows radially outward and back up towards the surface. A simple application of Darcy's law could be made in which it is assumed that the total pressure drop (Δp) occurs over the known length of a column (Δx). To use Darcy's law for this application, some error will occur in ignoring the

portion of the pressure drop between the base of the column and atmosphere. By comparing Darcy's law calculations to numerical simulations, this error can be quantified and used to correct hand calculations for future AP tests.

The program SEEP/W (GEO-SLOPE International 2004) was used for the finite element numerical analysis. This program simulates steady state or transient water flow through saturated or unsaturated soil. In this study it was used to simulate steady state air flow by representing the flow system as a saturated (constant K), steady state, axisymmetric flow system. The unit weight of air was used for the unit weight of water within the model. Air flow was assumed incompressible and the problem modeled as incompressible, saturated water flow.

An example of a single-layer analysis is shown in Figure 3.5. Insertion of the steel cylinder into the ground was represented by using null elements of zero hydraulic conductivity to represent the cylinder wall. Total head [m] boundary conditions were applied to ground surface both inside and outside the cylinder. Head values equivalent to the air pressure measured within the cylinder were applied to the soil surface inside the cylinder. A head of zero was applied to the soil surface outside of the column.

The value of K within the model (K_{model} [m/s]) was set to a value of unity. A boundary flux (Q_{model} [m^3/s]) was calculated through the cross-sectional area of the column. As flow and hydraulic conductivity are directly proportional for a given test geometry, the actual hydraulic conductivity (K_{actual} [m/s]) was calculated with the following equation:

$$Q_{actual} K_{model} = Q_{model} K_{actual} \qquad [3.1]$$

where Q_{actual} [m^3/s] is the recorded flow rate from an air permeability test. The hydraulic conductivity using air as the test fluid, K_{actual}, was then converted to a value of intrinsic permeability using [2.2]. Numerical simulations of the AP in layered soils were also conducted and are discussed in Chapter 4.

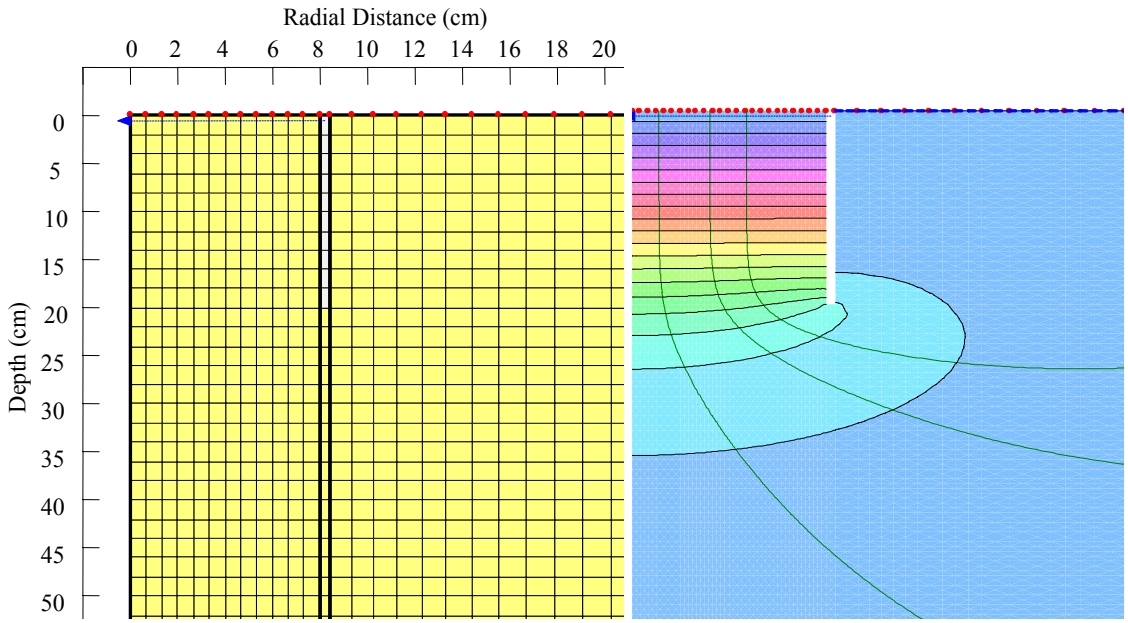

Figure 3.5. SEEP/W model of an AP test in a uniform material: (a) finite element mesh; and (b) resultant total head contours.

3.4 Laboratory Testing

Laboratory testing was initiated for two reasons. The first reason was to investigate whether constant head column tests using air and water as the test fluids could produce an equivalent value of intrinsic permeability under controlled conditions. The second reason was to carry out a full scale AP test on the same material, to determine whether this test method could provide a value of intrinsic permeability equivalent to that determined using a conventional column test. Results of this testing would provide a baseline case for all field based testing.

3.4.1 Column Tests

A plastic rigid wall permeameter filled with dry, uniform sand was used for the permeability tests. An air permeability test was conducted first. A pressure regulator was used to control air pressure. The flow meters used in the prototype AP design were used to control flow rate. A water manometer was used to measure air pressure at four vertical locations on the column. Darcy's law was used to calculate air hydraulic

conductivity. Laminar flow conditions were met based on the linear relationship of pressure and flow rate data, with an intercept of zero. The hydraulic conductivity was used with the properties of air to calculate permeability of the sand.

Once the air permeability test was complete, the column was saturated from the bottom with water. The water permeability test was conducted according to ASTM D2434-68 Standard Test Method for Permeability of Granular Soils (Constant Head) (American Society for Testing and Materials 2005). The permeability of the sand was calculated using the fluid properties of water. Photographs of the column tests using air and water as the test fluid are shown in Figure 3.6.

(a) (b)

Figure 3.6. Column permeability tests using (a) air as the test fluid; and (b) water as the test fluid.

Following both tests, comparisons were made of the intrinsic permeability determined using both methods. The void ratio (e) of the sand in the column was calculated according to:

$$e = \frac{G_s \rho_w}{\rho_d} - 1 \qquad [3.2]$$

where G_s is the specific gravity of the sand, ρ_w is the density of water [kg/m^3], and ρ_d is the dry density of the sand [kg/m^3].

3.4.2 Full Scale Tank Tests

A full scale test using the prototype AP was conducted in a tank of the dry, homogeneous sand used in the column tests. The boundary conditions of this test were well defined, and the effect of approaching the lower tank boundary during cylinder insertion was also investigated. A photograph of the full scale tank test is shown in Figure 3.7.

Figure 3.7. Full scale laboratory tank test of AP apparatus.

Analysis was completed using the same method as described in Section 3.3. The void ratio was calculated according to [3.2]. As permeability varies with void ratio for the same soil, a correction was applied to the permeability calculated for the full scale tank method using void ratios calculated for the column and tank. Many empirical relationships relate permeability and void ratio.

The one chosen for this application is:

$$k_2 = k_1 \frac{e_2^3(1+e_1)}{e_1^3(1+e_2)} \qquad [3.3]$$

where k_2 is the permeability of the tank at void ratio of the column, k_1 is the permeability calculated from the full scale test, e_2 is the void ratio of the column, and e_1 is the void ratio of the tank (Bowles 1992).

A GP test was also conducted in the sand tank following the air permeability test. This was done in an attempt to develop a correlation between the permeability determined using the AP and GP under ideal conditions. Results from the GP test are suspicious because the reservoir emptied quickly in this material, making accurate readings difficult. This is likely due to the fact that the hydraulic conductivity of the sand is on the upper end, or even above, the Guelph operating range, 1×10^{-8} to 1×10^{-4} m/s (Soilmoisture Equipment Corp. 1991).

3.4.3 Calibration of Flow Meters

The flow meters used as part of the AP apparatus are Dwyer Series RM Rate-Master flow meters, which operate as a variable area flow meter. As these flow meters are calibrated to operate under standard conditions, corrections must be applied if the flow meters are used for different pressures, temperatures and gases (Dwyer Instruments Inc. 2005). The correction equation uses conditions at the exit of the flow meter to compare to standard conditions. In this study, pressure and temperature measured within the steel cylinder were used for correction. The length of tubing between the flow meter and cylinder was kept as small as possible to minimize a drop in pressure.

The equation to correct for non-standard operating conditions is:

$$Q_2 = Q_1 x \sqrt{\frac{P_1 x T_2}{P_2 x T_1}} \qquad [3.4]$$

where Q_2 is the standard flow corrected for pressure and temperature [ft^3/h], Q_1 is the observed flow meter reading [ft^3/h], P_1 is the actual pressure (14.7 psia + gage pressure), T_2 is the standard temperature (530 R), P_2 is the standard pressure (14.7 psia) and T_1 is the actual temperature (460 R + Temp °F) (Dwyer Instruments Inc. 2005).

Compressibility may have an effect on volumetric flow readings because air behaves according to the ideal gas law. To determine the effects of compressibility, an electronic mass flow controller was used to test the values measured by the flow meters for typical test conditions. Standard operating conditions for the mass flow controller were 0 °C and 101.325 kPa. At these conditions the full capacity (100%) of the mass flow controller was 20 L/minute. The full capacity of the mass flow controller was adjusted to suit the temperature and atmospheric pressure in the laboratory on the day of testing.

The flow meters used in the AP apparatus were connected in series, one after the other, downstream from the mass flow controller. A backpressure was applied to the outlet line of the flow meter to simulate typical back pressures that might occur during a field trial. The flow meters were set to various flow rates that were measured during the air permeability trials. The percentage of full flow from the mass flow controller required to sustain these flow rates and backpressures was recorded. The actual mass flow rate determined from the mass flow controller for certain volumetric flow rate and pressure combinations was applied to the AP field data set, to ensure accuracy in the permeability calculations.

The difference between the flow rates measured by the Dwyer flow meters and those calibrated using the mass flow controllers were typically less than 10%, with a few values between 10 and 20% error. However, due to the nature of the flow meters, this is acceptable. Readings are taken by centering a round metal float on a scale gradation;

consequently, some error will occur in this reading if the ball is not perfectly centered on the gradation at which flow is recorded.

3.5 Field Trials

The AP was tested on three different reclamation soil covers in the oilsands mining region of Northern Alberta. The main objective of this testing was to determine how the AP could perform under non-ideal field conditions for various soil types and layered systems. Field based testing would also investigate the possibility of using the AP in place of the GP for monitoring changes in permeability of the soil covers over time. GP testing was completed alongside all air permeability tests to provide a reference value of permeability.

3.5.1 Soil Cover Prescriptions

The primary test site of interest was the SW30 Dump at the Syncrude Canada Limited oilsands mine. This site is a saline sodic overburden shale waste dump. Prototype reclamation covers were placed in 1999, consisting of a peat-mineral mix overlying till secondary material. Three 1 ha plots of varying thicknesses were created as shown in Figure 3.8. The D3 cover (20 cm peat-mineral mix overlying 80 cm of till secondary material) is the location at which all SW30 Dump air permeability testing took place in 2006.

The second test site was a deposit of petroleum coke at Syncrude Canada Limited, referred to as the Coke Beach. The prototype soil covers overlying the petroleum coke at this site were also a peat-mineral mix overlying till secondary material. Two cover thicknesses (shallow and deep) were placed in the winter of 2002-2003, as shown in Figure 3.9. The air permeability and GP tests were conducted on the deep cover (20 cm peat-mineral mix overlying 80 cm till secondary material).

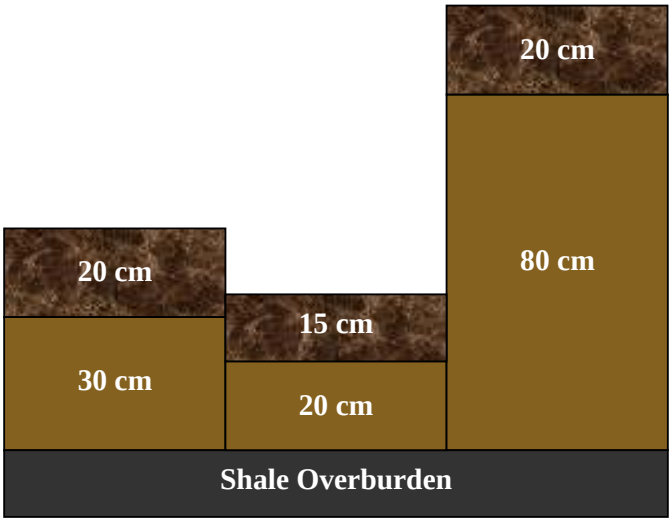

Figure 3.8. SW30 Dump prototype soil covers from left to right: D1, D2, and D3.

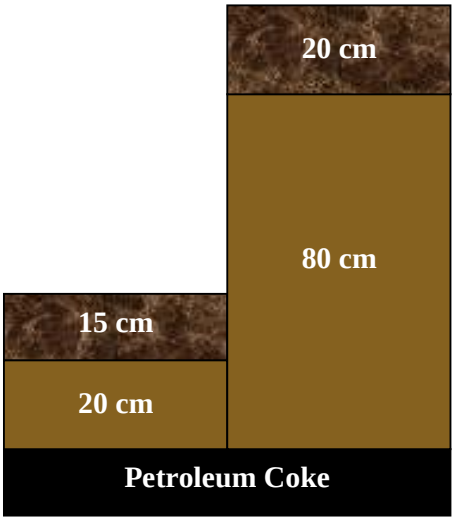

Figure 3.9. Syncrude Coke Beach prototype soil covers from left to right: shallow and deep covers.

The third test site was also a deposit of petroleum coke, at Suncor Energy. The soil covers at this site were a peat-mineral mix overlying tailings sand. The soil covers were placed on a 3:1 slope with a plateau at the top of the covers. The air permeability and GP tests were completed on the plateau of the shallow cover (30 cm peat-mineral mix overlying tailings sand). A schematic of these covers can be seen in Figure 3.10.

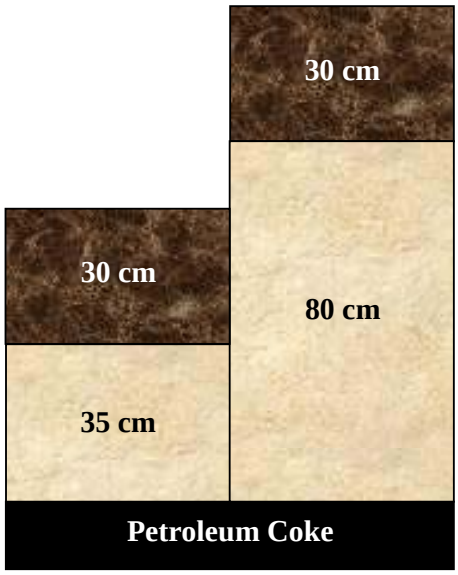

Figure 3.10. Suncor Coke Stockpile 3:1 prototype soil covers from left to right: shallow and deep covers.

3.5.2 Cover Soil Properties

Material properties for the peat/mineral mix summarized below are representative of the peat/mineral cover material at all three sites. Material properties discussed for the till/secondary material are representative of both the Syncrude SW30 Dump and Coke Beach cover materials. The properties of the sand layer (tailings sand) within the Suncor Coke Stockpile cover are also discussed.

Particle size distributions of the till/secondary material were completed in 2000 for three depths within the SW30D cover: 0-20 cm, 20-50 cm and 50-100 cm (Figure 3.11). The till/secondary material was 37% sand, 42% silt, and 21% clay particles (Kelln et al. 2007). PSD analysis was not performed on the peat/mineral mix because the organic fraction of the peat floated during the wet sieving process instead of passing through the sieve (Boese 2003).

A particle size distribution was also conducted on a sample of tailings sand in 2003. Test results were provided by MDH Engineered Solutions Laboratory (Figure 3.11). The average PSD of the tailings sand was 93% sand and 7% fines (silt and clay).

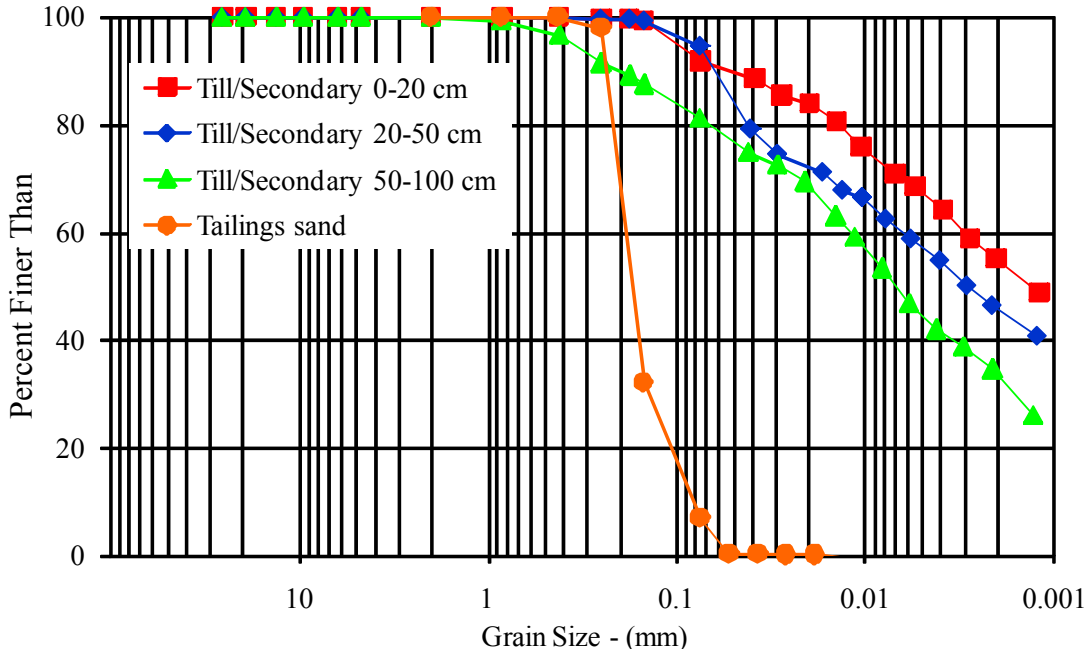

Figure 3.11. Particle size distribution for till/secondary material (Boese 2003) and tailings sand.

The in-situ density testing of cover soils on the SW30 Dump were measured in 2000 using a Troxler 3440 Density Probe (Boese 2003) (Table 3.1). The density of the peat was quite variable due to the nature of the material at the test location. The peat appeared soft and spongy in some areas, and denser when mixed with secondary (Boese 2003). The specific gravity of the peat and till materials was measured in 2000 by Boese (2003) (Table 3.1). Density and specific gravity data are not available for the tailings sand material.

Soil water characteristic curves were determined for the peat/mineral mix and till secondary by Boese (2003) in 2000 through laboratory testing. The soil water characteristic curve for the tailings sand was determined in 2003 through laboratory testing at MDH Engineered Solutions. Results from these tests are found in Figure 3.12.

Table 3.1. Bulk density and specific gravity test results for the peat/mineral mix and till secondary cover materials.

Parameter	Bulk Density (kg/m^3)		Specific Gravity
	Maximum	Minimum	
Peat/Mineral Mix	200	1400	2.62
Till/Secondary Material	930	1640	2.61

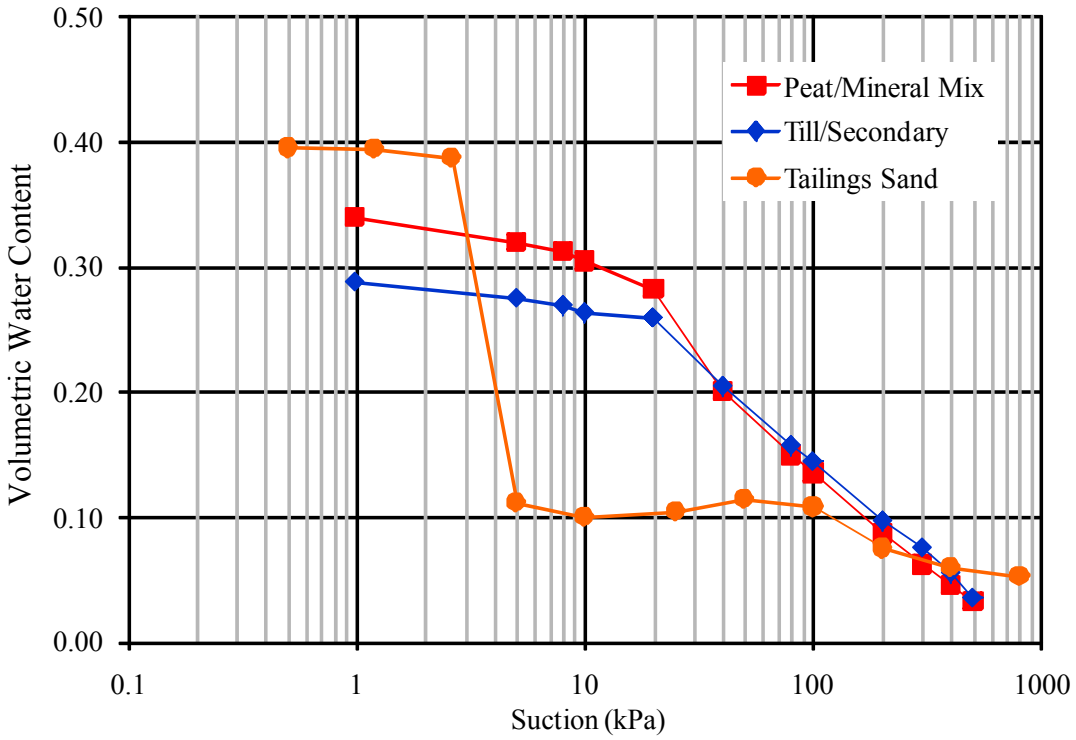

Figure 3.12. Soil water characteristic curve for peat/mineral mix and till/secondary materials (Boese 2003), as well as tailings sand.

3.5.3 Air Permeability Tests

In the 2005 field season, air permeability tests were completed at the SW30 Dump. Full profile tests were completed inserting the cylinder up to 45 cm through the peat-mineral and till layers to study permeability in a layered system. One complete profile was tested at the mid-slope location on each prototype cover. Four additional profiles were tested at various slope positions on the D3 cover. This was done to develop a

correlation between measurements and different moisture regimes of each location.

Additional tests were also completed for comparison after first scraping off the upper peat-mineral layer of the soil cover in order to test only the till layer. Seven tests of this nature were completed at the D3 mid-slope location. The 2005 field season was considered a wet year with higher than average rainfall throughout the summer. The AP field program was found to be challenging during that season, because the system cannot operate in the rain and ideal testing conditions would be reasonably dry soil.

Air permeability tests were also conducted on various slope positions of the SW30 Dump in 2005, to develop a correlation between measurements and different moisture regimes of each location. Most trials were still able to reach steady state within 10 seconds, which likely means the secondary structure was indeed drained, and the soil was near field capacity. Repeatability tests were also completed, by applying a range of flow rates more than once at a particular depth to ensure that the results were reproducible.

Air permeability tests were also conducted at the Syncrude Coke Beach in 2005. More difficulty was found at this location. Steady state air flow was either difficult to achieve, or impossible for some trials. This might be due to the fact that this watershed is relatively flat, decreasing the possibility of moisture drainage following the frequent rainfall events. This cover was also fairly new compared to the SW30 Dump, so it was possible that the secondary structure may not have fully evolved by 2005. According to Meiers et al. (2006), the SW30 Dump covers evolved over a period of approximately three years, resulting in a mean K increase of two orders of magnitude.

In 2006, several air permeability trials were completed at the Suncor Coke Stockpile test plots, which allowed investigation of a lower permeability layer overlying a higher permeability layer. Repeatability tests were also completed here as well as an examination of leakage. Air permeability tests were conducted at each cylinder depth. The soil next to the inner cylinder wall was then kneaded and air permeability tests

repeated to investigate the potential effects of leakage.

Air permeability tests were also completed at the Syncrude SW30 Dump and Coke Beach in 2006. Three full depth trials to 40 cm were completed at each site. At both locations, the peat-mineral layer was only 5 cm thick or less, so the measured permeability was considered to be that of the till layer. A leakage investigation was also conducted on these sites, doing air permeability tests before and after kneading the soil next to the cylinder wall. The soil at the Coke Beach was substantially drier than the previous season, and steady state air flow was reached almost immediately for all trials.

Results from the 2006 field season are presented in Chapter 4. Due to system modifications that were made between the 2005 and 2006 field seasons, presentation of 2006 results is more representative of true system operation. There was also substantially less rainfall during the late summer period of the 2006 field season. This adds confidence that the results are less affected by in-situ moisture, and that the soil was more likely drained to field capacity.

3.5.4 Guelph Permeameter Tests

Historical GP measurements were conducted at the SW30 Dump to track weathering from 2000 to 2004. An evolution of hydraulic conductivity for this site is shown in Figure 3.13. In 2005 and 2006, GP measurements were conducted at all three sites (Syncrude SW30 Dump, Syncrude Coke Beach and Suncor Coke Stockpile) to accompany AP measurements.

As shown in Figure 3.13, the hydraulic conductivity of the D3 cover till layer increased approximately two orders of magnitude between 2000 and 2003. The hydraulic conductivity of the D3 cover peat-mineral layer also increased approximately one order of magnitude over this time period.

As mentioned previously, GP measurements were taken alongside AP measurements in

order to compare the results from these two methods. A photograph of a test site on the Coke Beach in 2006 with GP and AP tests set up is shown in Figure 3.14. Typically, two Guelph test holes with two single height measurements in each hole were completed in each cover material to compare to air permeability tests.

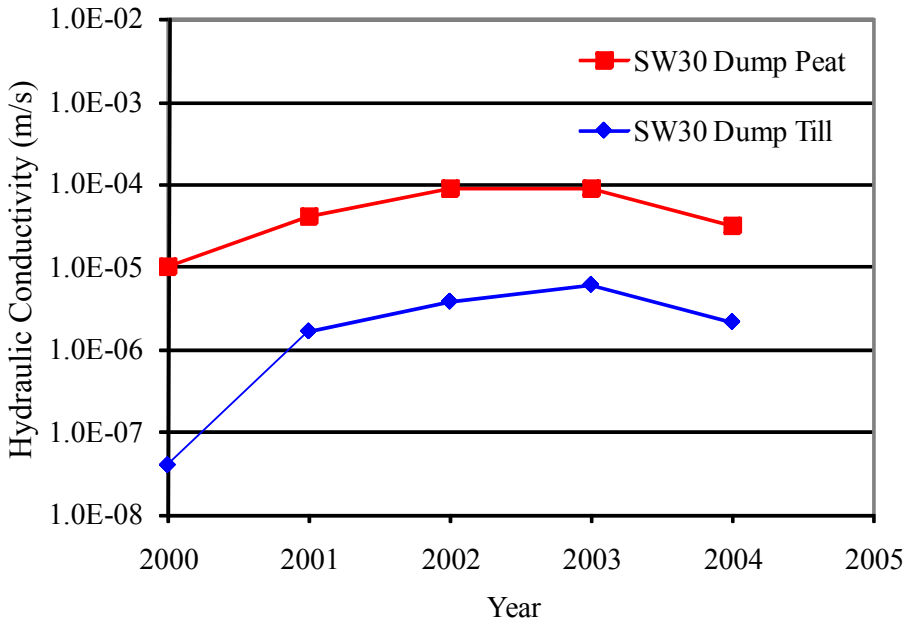

Figure 3.13. GP measurements for the Syncrude SW30 Dump D3 cover (Meiers et al. 2006).

For well preparation prior to the GP tests in 2005 and 2006, the wire brush technique introduced in Section 2.2.1 was used on the fine-grained materials to remain consistent with historical GP measurements. This technique was used to alleviate smear-induced underestimations of K_{fs}. The time required to set up the GP apparatus and prepare the well bore was approximately 20 to 30 minutes. The average testing time to complete a test at one depth in the peat-mineral or sand materials was approximately 15 to 20 minutes. The average testing time to complete a test at one depth in the till material was approximately 30 to 40 minutes.

GP measurements of the peat-mineral layer on the D3 cover were not taken during the 2006 field season because the hydraulic conductivity stabilized to a relative constant hydraulic conductivity previous to that field season. Also, the air permeability tests in

2006 focused mainly on the till material, because the peat-mineral layer was thin in the testing region- only 5 to 7 cm thick. GP measurements were taken at an average total depth of 30 cm in the till layer (ponded infiltration over a depth of 20-30 cm) to capture a representative measurement of the AP region tested.

Figure 3.14. GP and AP tests on Coke Beach in 2006 field season.

GP measurements of the Coke Beach cover peat-mineral layer were not taken in 2005 or 2006 because the layer was not thick enough to allow for set up of the GP apparatus in the AP testing area. GP measurements were taken at an average depth of 25 cm within the till (ponded infiltration over depth of 15-25 cm) to capture a representative measurement of the AP region tested.

GP measurements of the Suncor Coke Stockpile cover were taken within the peat-mineral and tailings sand layers for 2005 and 2006 at depths representative of individual layers. Measurements within the peat-mineral layer were taken at an average depth of 20 cm (ponded infiltration over a depth of 10-20 cm). Measurements within the sand layer were taken at an average depth of 51 cm (ponded infiltration over a depth of 41-51 cm).

CHAPTER 4
RESULTS AND DISCUSSION

4.1 Introduction

The data from the laboratory and field tests described in Chapter 3 will be presented in this chapter. The test data from the 2006 field season will be discussed including the analyses and comparison of the various permeability methods using air and water as the test fluid.

All permeability test data are presented using the method of box plots. Box plots are a graphical display of the exploratory data analysis procedures developed by Tukey (1977). The statistical computer program SPSS (2006) was used to produce the box plots. An example of the box plot method is shown in Figure 4.1.

Each box is constructed by plotting the first and third quartiles (q_1 and q_3 respectively) and drawing a box around these points. This box shows the spread of the middle 50% of the data. The range between the first and third quartiles is also known as the interquartile range (IQR). The median (q_2) is represented by a horizontal bar dividing this box. The location of the median within the box represents the symmetry of the middle 50% of the data. The median is usually less affected by the presence of outliers than the sample mean (Ostle et al. 1996).

Theoretical inner and outer "fences", which are not plotted in this study, are located at distances of 1.5*IQR and 3*IQR, respectively, from both ends of the box. The minimum and maximum values between the inner fences are represented by whiskers, which are joined by vertical lines to the box. Any data points located outside of the inner fences are called "outliers" and are represented by the symbol "○". Any data points located outside of the outer fences are called "extreme outliers", and are represented by the symbol "*".

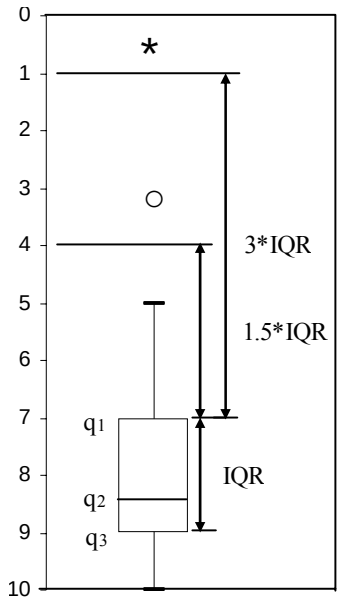

Figure 4.1. Box plot construction as per descriptive statistical method of Tukey (1977).

4.2 Laboratory Test Results

The first components of laboratory testing were the constant head air and water permeability tests using a column of uniform sand. A set of measurements were taken with loosely placed dry sand using air as the test fluid. The column was then saturated and permeability tests using water were performed. The same dry sand was loosely placed in a tank to perform a full scale trial using the air permeameter (AP) apparatus. The method used to analyze the AP data is described in Section 3.3. A Guelph permeameter (GP) test was also conducted on this sand tank, but the results are not comparable because the measured permeability exceeds the upper limit of the GP operating range. A detailed explanation of these methods can be found in Section 3.4. Results of all three tests are shown in Figure 4.2.

The median permeability values measured using the air and water column tests are 7.9×10^{-11} m^2 and 7.6×10^{-11} m^2, respectively. The relative difference of 4% between these values supports the assumption that the permeability to air or water at identical fluid phase contents should be equal. The median value of permeability determined using the AP in a full scale test was 9.2×10^{-11} m^2. This value has a relative difference

of 21% from the water column test. Although this percent difference is higher than that calculated between the column tests, the error is seen as acceptable in terms of using the AP to predict permeability of a uniform soil.

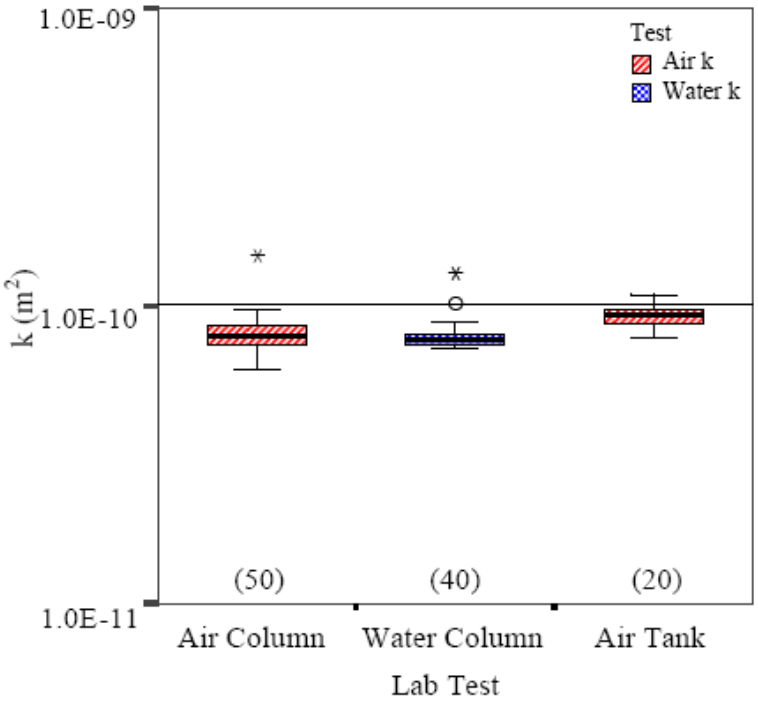

Figure 4.2. Comparison of permeability measurements using a column with air as the test fluid, a column with water as the test fluid, and the AP in a sand tank, where (n) is number of tests.

One extreme outlier was calculated for the air column test as well as one outlier and two extreme outliers for the water column test. For both column tests these values of permeability were calculated from a flow rate which was too low to maintain a linear relationship of flow and pressure throughout the column. This resulted in an excessively high measurement of permeability at those particular points.

4.3 Air Permeameter Field Trial Results

Results of AP trials on reclamation covers in the oilsands region are included in the following subsections. The field data were analyzed according to the method described in Section 3.3. The soil covers tested include the Suncor Coke stockpile cover (Suncor

cover), Syncrude SW30 Dump cover (SW30 Dump cover) and Syncrude Coke Beach cover (Coke Beach cover). As described in Section 3.5, the soil cover tested on the Suncor Coke stockpile consisted of a uniform peat-mineral mix over sand tailings. The soil covers on the SW30 Dump and Coke Beach consisted of a peat-mineral mix over till secondary. Although the prescriptions of these covers required 20 cm of peat-mineral mix overlying the till, the peat-mineral layer was found to be only a few centimeters thick in the 2006 testing region on both covers, likely due to factors such as weathering or inconsistent placement thickness.

Air permeability measurements were taken after each 10 cm advance of the cylinder to a total depth of 40 cm. Three flow rates were typically applied at each depth and the resulting air pressure within the AP cylinder was recorded. The flow rate and pressure data was plotted to ensure that laminar flow was occurring. Additional flow rates were applied in some cases to investigate repeatability. Bulk permeability values for the soil profile within the cylinder were calculated for each flow and pressure combination.

Three complete depth profiles were tested on each soil cover. Additional profiles were completed on the Suncor Coke Stockpile cover to investigate leakage and repeatability. The median permeability values at each depth in the profile are summarized in tables in the following sections. Box plots are displayed for each cover prescription with a summary of all permeability measurements according to depth. GP testing was also carried out alongside each AP trial. A comparison of AP and GP measurements for all sites are discussed in Section 4.6.

4.3.1 Suncor Coke Stockpile Soil Cover

Median permeability values according to depth for each individual test profile are shown in Table 4.1 and 4.2. Values of "N/A" are reported for specific profiles which were used for repeatability testing at shallow depths only. The overall median values based on these values were 4.9 x 10^{-12} m^2, 2.9 x 10^{-12} m^2, 5.0 x 10^{-12} m^2 and 4.3 x 10^{-12} m^2 for the 10 cm, 20 cm, 30 cm and 40 cm test depths, respectively. A visual summary of the overall permeability for each depth is shown in Figure 4.3. All tests were

conducted primarily in the peat-mineral layer, because the transition from the peat/mineral mix to tailing sand occurred at an average depth of 30 cm.

Table 4.1. Median permeability values for Trials 1-4 on the Suncor Coke Stockpile cover and number of measurements (n) for each test depth.

Test Depth (cm)	Trial 1 k (m^2)	Trial 2 k (m^2)	Trial 3 k (m^2)	Trial 4 k (m^2)
10 cm	7.2×10^{-12} (8)	5.3×10^{-12} (7)	1.2×10^{-11} (7)	5.3×10^{-11} (7)
20 cm	N/A	3.5×10^{-12} (4)	2.2×10^{-12} (4)	N/A
30 cm	N/A	5.1×10^{-12} (4)	5.2×10^{-12} (5)	N/A
40 cm	N/A	4.7×10^{-12} (4)	4.3×10^{-12} (5)	N/A

Table 4.2. Median permeability values for Trials 5-8 on the Suncor Coke Stockpile cover and number of measurements (n) for each test depth.

Test Depth (cm)	Trial 5 k (m^2)	Trial 6 k (m^2)	Trial 7 k (m^2)	Trial 8 k (m^2)
10 cm	1.6×10^{-12} (5)	8.0×10^{-13} (6)	4.4×10^{-12} (10)	3.5×10^{-12} (5)
20 cm	1.9×10^{-12} (4)	4.3×10^{-12} (5)	6.7×10^{-12} (11)	1.6×10^{-12} (3)
30 cm	3.9×10^{-12} (5)	4.9×10^{-12} (10)	N/A	N/A
40 cm	3.2×10^{-12} (5)	N/A	N/A	N/A

Several outliers were determined for the 10 cm profile. The high permeability outliers correspond with field notes explaining that a rock was encountered while pounding the cylinder in the first 10 cm. When the cylinder is disturbed during pounding, the seal between the soil and the cylinder is affected, which leads to overestimated values of permeability.

The low permeability outliers all occurred within one test profile. It is possible that either a dense or wetter layer existed near the surface, because the pressure measurements taken for this depth were much higher than all depths below it. Two extreme outliers occurred at the 30 cm depth. These extreme outliers are not of large concern because the variability of measurements at this depth was low, which is supported by the narrow interquartile range shown in Figure 4.3.

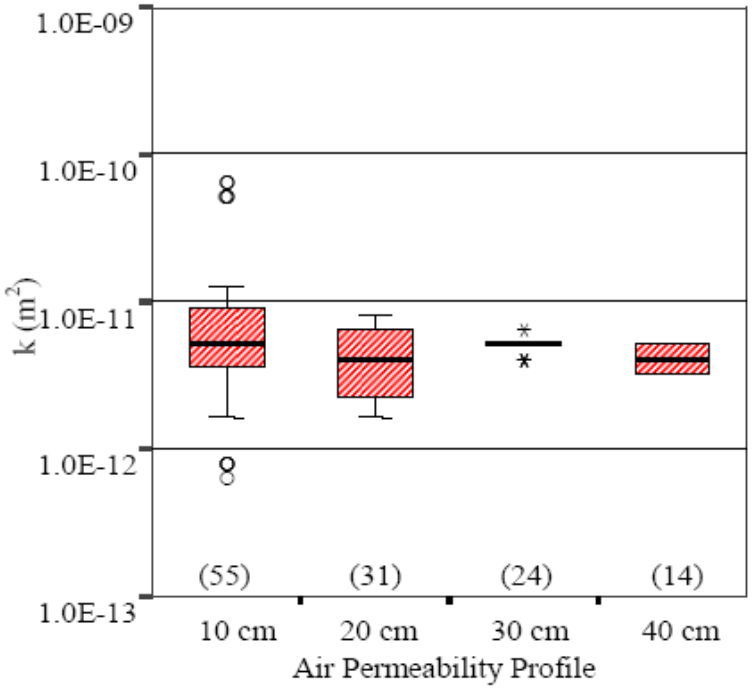

Figure 4.3. Overall results of air permeability measurements on the Suncor soil cover, where (n) is the number of tests. Average thickness of the peat-mineral mix was 30 cm.

4.3.2 SW30 Dump Soil Cover

Median permeability values according to depth for each individual test profile are shown in Table 4.3. The overall median values based on these values were 4.0 x 10^{-11} m^2, 6.8 x 10^{-11} m^2, 7.8 x 10^{-11} m^2 and 6.6 x 10^{-11} m^2 for the 10 cm, 20 cm, 30 cm and 40 cm test depths, respectively. A visual summary of all permeability values according to depth is shown in Figure 4.4. These measurements were taken primarily within the till layer, because the average depth of the peat-mineral layer was 5.7 cm.

Table 4.3. Median permeability values for the Syncrude SW30 Dump cover and number of measurements (n) for each test depth.

Test Depth (cm)	Trial 1 k (m^2)	Trial 2 k (m^2)	Trial 3 k (m^2)
10 cm	6.3×10^{-11} (6)	4.0×10^{-11} (3)	2.2×10^{-11} (3)
20 cm	1.6×10^{-10} (3)	6.8×10^{-11} (12)	3.1×10^{-11} (3)
30 cm	1.6×10^{-10} (3)	7.8×10^{-11} (3)	3.6×10^{-11} (3)
40 cm	N/A	8.8×10^{-11} (8)	4.4×10^{-11} (9)

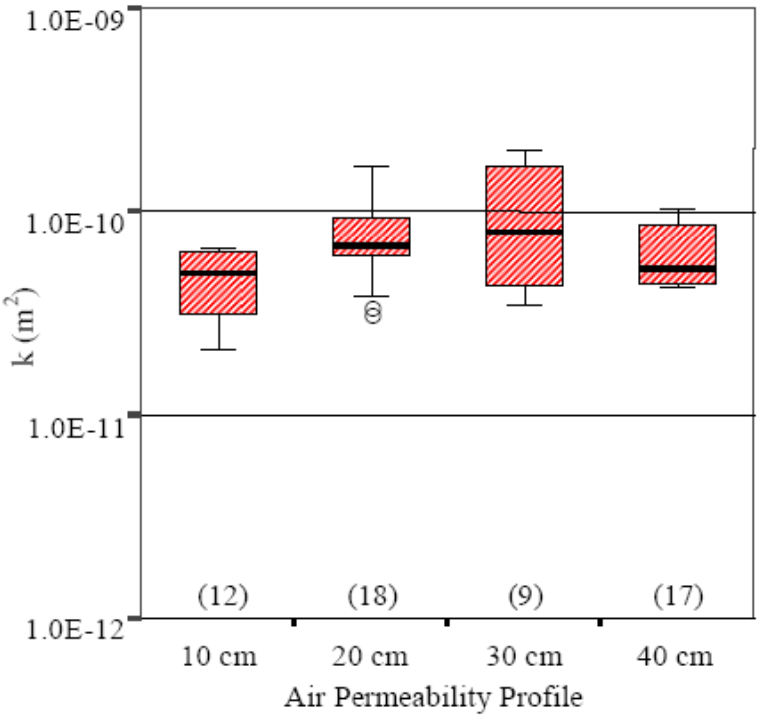

Figure 4.4. Overall results of air permeability measurements on the Syncrude SW30 Dump soil cover for four depth trials, where (n) is the number of tests. Average thickness of the peat-mineral mix was 5.7 cm.

The permeability values determined on this cover were more variable than those determined on the Suncor soil covers. This is likely due to the heterogeneous nature of the weathered secondary till soils at the SW30 Dump. The measured permeabilities

have more variability than those measured in a uniform soil because the macropores and fractures in this soil do not occur at a regular interval. The existence of a macropore network may also cause anisotropy in the soil. A numerical simulation of AP tests in soils of varying degrees of anisotropy is shown in Section 4.7.3.

Two low permeability outliers were calculated for the 20 cm profile, but are not of large concern. Those outliers are data points from a trial in which the soil was kneaded against the cylinder walls. The magnitude of the values of permeability measured for a weathered till appear high, which means data points occurring below the data set are more realistic for this material.

4.3.3 Coke Beach Soil Cover

Median permeability values according to depth for each individual test profile are shown in Table 4.4. The overall median permeabilities based on these values were 1.2 x 10^{-10} m^2, 1.0 x 10^{-10} m^2, 1.0 x 10^{-10} m^2 and 1.4 x 10^{-10} m^2 for the 10 cm, 20 cm, 30 cm and 40 cm test depths, respectively. A summary of all permeability values according to depth is shown in Figure 4.5. These permeability measurements were taken primarily in the till layer, because the average depth of the peat-mineral layer was 4 cm.

Table 4.4. Median permeability values for the Syncrude Coke Beach cover and number of measurements (n) for each test depth.

Test Depth (cm)	Trial 1 k (m^2)	Trial 2 k (m^2)	Trial 3 k (m^2)
10 cm	1.2 x 10^{-10} (4)	1.8 x 10^{-10} (4)	3.7 x 10^{-11} (5)
20 cm	1.0 x 10^{-10} (10)	2.5 x 10^{-10} (4)	6.9 x 10^{-11} (10)
30 cm	1.0 x 10^{-10} (5)	2.8 x 10^{-10} (9)	7.1 x 10^{-11} (5)
40 cm	1.4 x 10^{-10} (5)	3.6 x 10^{-10} (4)	8.0 x 10^{-11} (5)

The variability of these permeability values is similar to the variability of the SW30 Dump permeability values. The till materials of both of these covers have weathered to the same degree, explaining the similar behaviour in the AP tests. Three high permeability outliers were determined for the 20 cm profile, but there are no comments in the field notes to explain this occurrence.

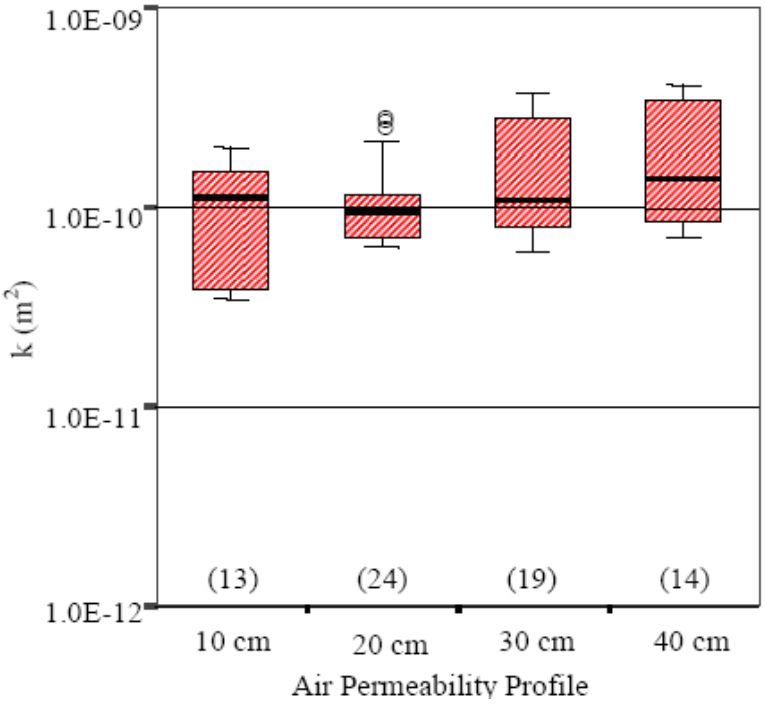

Figure 4.5. Overall results of air permeability measurements on the Syncrude Coke Beach soil cover for four depth trials, where (n) is the number of tests. Average thickness of the peat-mineral mix was 4 cm.

4.4 Guelph Permeameter Field Results

Guelph Permeameter test results for the Syncrude SW30 Dump and Coke Beach covers in 2005 and 2006 are shown in Figure 4.6. The SW30 Dump data includes GP measurements on the D3 cover only. As mentioned in Section 3.5.3, measurements in the peat-mineral mix were taken in 2005 only for the SW30 Dump cover. Results for the SW30 Dump till layer are shown to remain approximately constant over the study period.

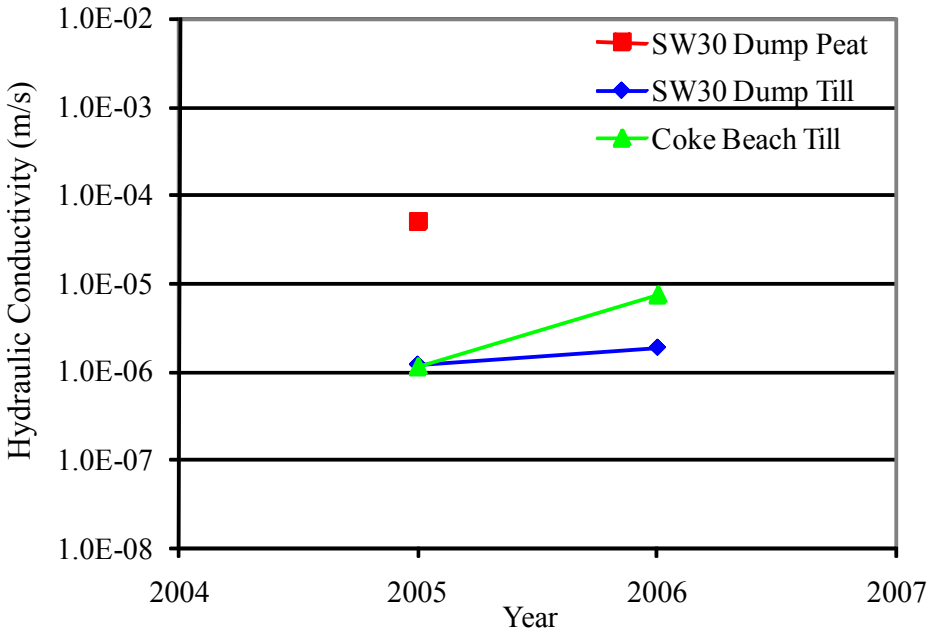

Figure 4.6. GP results for the Syncrude SW30 Dump and Coke Beach soil covers.

Measurements of the Coke Beach till layer were found to be consistent with the D3 cover till layer in 2005 and higher than the D3 till layer in 2006. These results are consistent with the air permeability measurements at these sites. The secondary structure of the soil at each site was also found to be similar. The peat-mineral layer at the Coke Beach cover was found to be thin and dry at the test locations, likely due to wind erosion. As a result, the underlying till layer has weathered quickly to a state which is similar to the D3 cover after eight years of weathering.

GP measurements were completed at the Suncor Coke watershed in 2005 and 2006. Measurements of the peat-mineral and sand layers on the plateau of the 3:1 shallow cover are shown in Figure 4.7. Neither the peat-mineral nor sand materials were shown to weather significantly between the 2005 and 2006 field seasons. Although the hydraulic conductivity of the sand was shown to decrease over time, this is likely due to factors such as operator error or variability in the material. As the sand is a granular material, the hydraulic conductivity is not expected to change substantially over time.

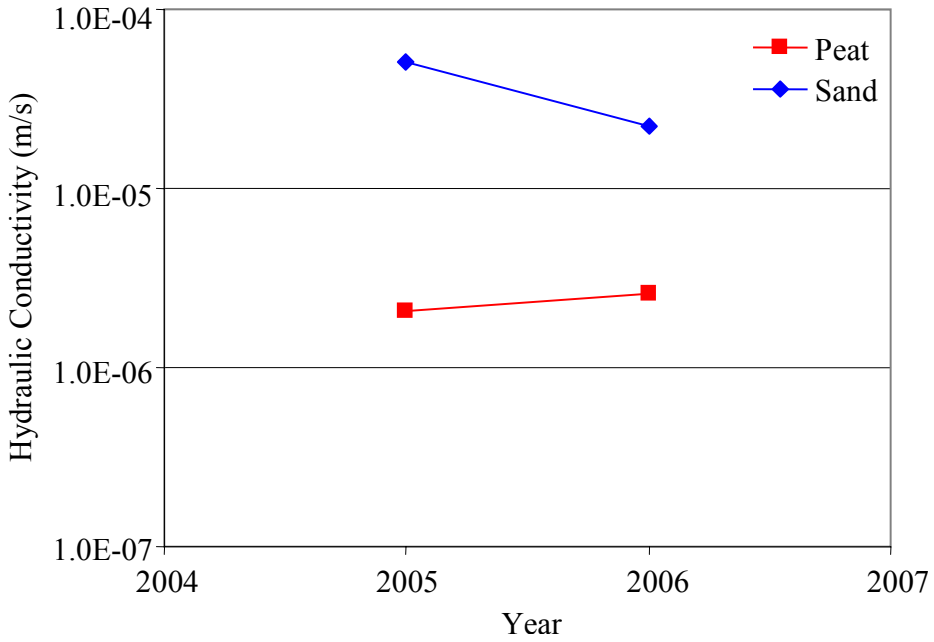

Figure 4.7. GP results for the Suncor Coke Stockpile soil cover.

4.5 Discussion of Air Permeability Analysis Method

The possibility of using a simple Darcy's law hand calculation in place of the axisymmetric numerical analysis as used in Section 4.3 was investigated. A comparison was made to highlight the differences in these methods of analysis. The suitability of using a hand calculation to determine permeability is discussed.

The values of permeability presented in this study represent bulk soil profiles for each successive insertion depth. However, an individual permeability calculation for each incremental 10 cm depth, although time consuming, may more accurately describe the soil conditions. A comparison of these two methods is made to determine if a simple bulk permeability calculation adequately describes the condition of the soil profile.

4.5.1 Simplification of Analysis with Hand Calculation

The numerical analysis method described in Section 3.3 is accurate but time consuming. The capabilities of the AP method would be greatly increased if an acceptable estimate of permeability could be made using a hand calculation. In order to use a hand

calculation to analyze the air permeability data, the AP method must be assumed to behave similar to a column test.

As discussed in Section 3.3, a column test requires that the assumption be made that the pressure at the base of the column is approximately equal to atmospheric pressure. This is not true in the case of the AP, because once the air leaves the base of the column, it will still need to travel to the soil surface before it is equilibrated with atmosphere. If the error of ignoring this fraction of the pressure drop can be quantified, a correction can be applied to the hand calculated value of permeability.

The entire data set from the Suncor soil cover was used to compare the values of permeability determined by the SEEP/W analysis method and those obtained from a simple Darcy's law hand calculation. Median values and percent differences calculated for both methods are shown in Table 4.5. To visualize these results, a graph of these permeability values is shown in Figure 4.8.

Table 4.5. Comparison of median air permeabilities determined with SEEP/W and hand calculation methods for the Suncor soil cover.

Test Depth	k (m^2)- SEEP/W Method	k (m^2)- Hand Calc Method	Relative Difference (%)
10 cm	5.0×10^{-12}	3.5×10^{-12}	43
20 cm	4.3×10^{-12}	4.2×10^{-12}	2
30 cm	5.0×10^{-12}	4.9×10^{-12}	2
40 cm	4.3×10^{-12}	4.8×10^{-12}	12

On the basis of individual permeability values, there is a typical trend according to depth in the error of using a hand calculation in place of numerical analysis. At a depth of 10 cm, values from the numerical analysis are typically a factor of 1.4-1.5 larger than the hand calculated values. This error decreases with increasing cylinder insertion

depth, where typically at a test depth of 40 cm, the error is negligible.

To validate these results a theoretical numerical simulation was conducted to quantify the error expected by assuming that the entire pressure drop occurs within the AP cylinder. A finite element mesh similar to that shown in Figure 3.5 was used. A hydraulic conductivity function of K = 1 m/s was applied to all of the elements, except the cylinder walls which were represented by null elements.

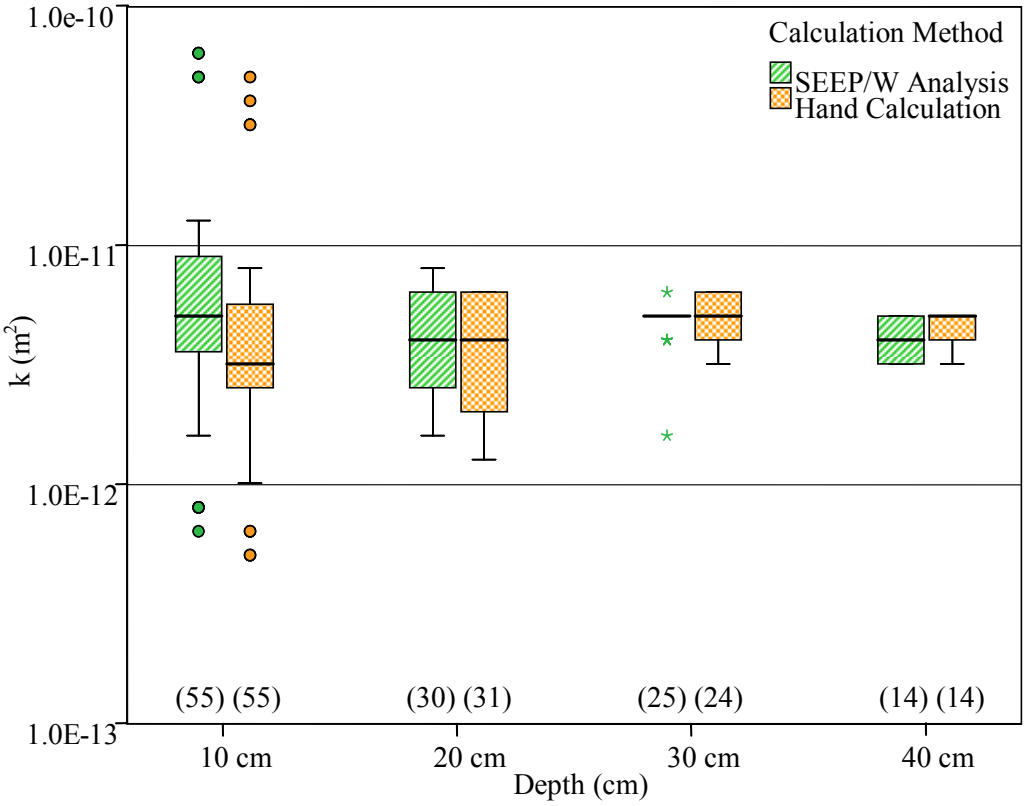

Figure 4.8. Comparison of permeabilities determined using the SEEP/W and hand calculation methods for the Suncor soil cover, where (n) is the number of calculations.

Head boundary conditions were set by applying theoretical values of head, H = 10 m and H = 0 m to the soil surface inside and outside the cylinder, respectively. These values were chosen to be representative of an air permeability test in which Darcy's law was obeyed. Cylinder insertion was simulated in 10 cm increments to a total depth of 50 cm. At each interval the boundary flux (Q) through the cylinder cross-section was

used to calculate a resultant value of hydraulic conductivity (K) assuming that the entire pressure drop occurred over the length of the cylinder.

The simulation was then repeated to calculate the value of hydraulic conductivity when the drop in total head actually occurred over the length of the column. This was simulated by placing a boundary condition of H = 0 m across the base of the cylinder. The boundary flux was again used to calculate a resultant value of hydraulic conductivity. A comparison of these K values can be seen in Table 4.6. This theoretical comparison of permeability values supports the permeability value trend with depth found in the Suncor data set. Therefore, a correction factor could be applied to hand calculated permeability values determined at various depths, eliminating the need for a numerical finite element analysis.

Table 4.6. Comparison of theoretical hydraulic conductivities (K) calculated by: a) assuming ΔH occurs through cylinder, and b) forcing ΔH to occur through cylinder.

Cylinder Depth	K (m/s)-(Assumption)	K (m/s) (Actual)	Relative Difference (%)
10 cm	0.7	1.0	50
20 cm	0.8	1.0	20
30 cm	0.9	1.0	20
40 cm	0.9	1.0	10
50 cm	0.9	1.0	10

4.5.2 Bulk Permeability Calculation

The use of one bulk permeability calculated for each progressive insert depth is the simplest approach to data analysis, and is the method used in this study. Using one value of permeability to represent the entire 40 cm soil profile may not adequately characterize the extent of weathering throughout the soil profile. To compare the values

of permeability obtained for each layer within the soil profile to the overall bulk permeability values, Darcy's law for a system of homogeneous, isotropic layers was applied to air permeability data sets. Freeze and Cherry (1979) state that a system of homogeneous, isotropic layers behaves as a single homogeneous, anisotropic layer according to:

$$K_z = \frac{vd}{vd_1 / K_1 + vd_2 / K_2 + \ldots + vd_n / K_n} = \frac{d}{\sum_{i=1}^{n} d_i / K_i} \qquad [4.1]$$

where K_z is an equivalent vertical hydraulic conductivity for the layered system [m/s], v is the specific discharge through the system [m/s], d is the depth of the entire system [m], d_1, d_2,…d_n are the depths of the consecutive layers [m], and K_1, K_2,…K_n are hydraulic conductivity values of each consecutive layer [m/s]. Although [4.1] uses values of hydraulic conductivity K [m/s] to compute values for individual layers, K was substituted for permeability k [m^2] in this study.

The permeability calculated at the first depth d_1 of 10 cm becomes k_1 for the system. As the cylinder is advanced, the overall permeability calculated becomes k_z and the above equation can be rearranged to determine the permeability of the consecutive layers k_2…k_n. This individual layer approach to permeability calculations could be used for analysis of layered reclamation soil covers. Although the exact location of these layer interfaces is unknown until after an AP test is complete, an individual permeability calculation could be used to define discrete regions of various textured material (e.g. peat-mineral to till transition).

To investigate the differences in permeability calculated using the bulk or individual layer methods, one AP profile was selected from each soil cover. At each depth several flow and pressure combinations were recorded in the field, with bulk values of permeability calculated for each combination. This data was regrouped according to flow rate, so that successive calculations of k_n could be done on individual data sets to depths of d_n. This resulted in three or four individual sequences of k_n calculations for each profile. Median values of individual and bulk permeability were then calculated

for each depth of the separate profiles. A comparison of individual and bulk permeabilities is shown in Figure 4.9.

Calculations of k_n for the Suncor peat-mineral data set were found to produce negative values at a depth of 30 cm. Similar results were found for the permeability at 40 cm (e.g. k_n) calculations from the Coke Beach data set. A negative k_n calculation is a result of lower pressure resistance at depth and a higher calculation of k_z, because flow rates are controlled in the air permeability tests.

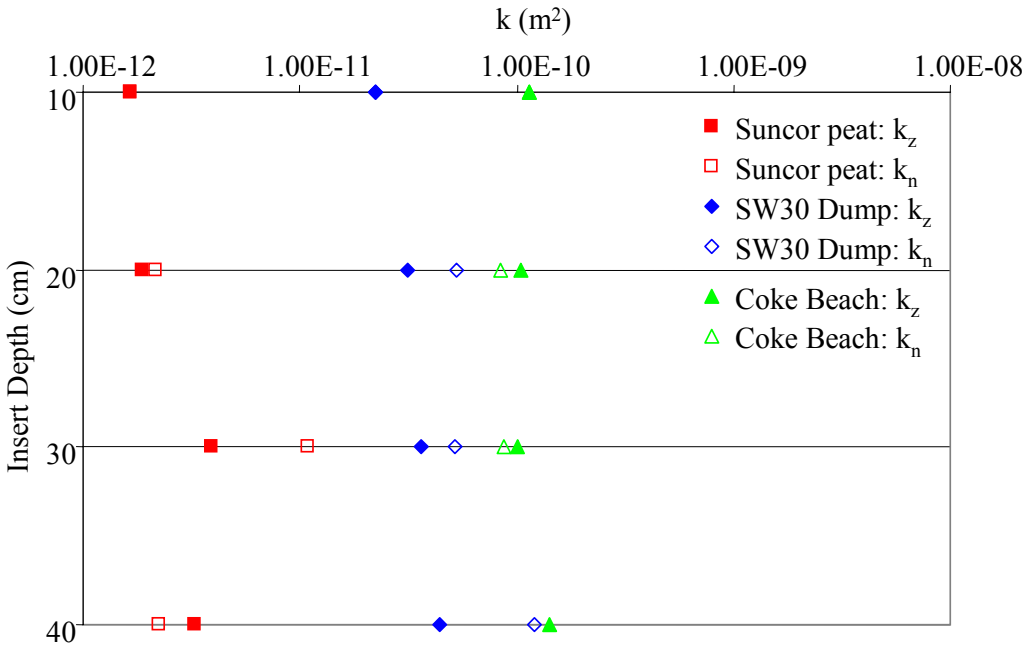

Figure 4.9. Comparison of bulk permeability (k_z) calculations to permeability calculations of individual soil layers (k_n).

One possible reason for higher permeability at depth could be that the cylinder encountered an obstruction while pounding, causing it to go slightly off vertical and damaging the seal between the soil and the cylinder. Another explanation could be that a zone of higher permeability was encountered at depth because the reclamation soil material is heterogeneous. The SW30 Dump and Coke Beach till layers have been found to contain envelopes of granular material.

The calculations of k_n are expected to decrease with depth, because weathering would

be expected to be more prevalent near the surface. However, because soil variability and obstructions such as rocks or wood cause leakage along the cylinder wall, this does not always occur. Examination of the soil profile following AP testing at the SW30 Dump and Coke Beach showed that the weathered zone can extend to depths of 40 cm. This was demonstrated by macropores extending throughout the entire profile. Therefore, the permeability is not expected to drop with depth. At the Suncor soil cover, the underlying sand layer is of higher permeability than the peat-mineral, so a drop in permeability with depth is unlikely.

Based on the results shown in Figure 4.9, calculations of bulk permeability provide a reasonable estimate of permeability for the reclamation soil covers. Due to the nature of the soils used in this study, variation is found regardless of the calculation method. Depending on the objective of the AP application, a bulk permeability calculation will be sufficient. However, if a more accurate description of permeability is desired, a calculation of permeability for each layer is recommended.

4.5.3 Effect of Soil Layering

Layered soil cover systems generally consist of two soil layers of differing hydraulic properties. The SW30 Dump and Coke Beach covers consist of a peat-mineral mix overlying a till secondary material, with the upper material having a value of hydraulic conductivity approximately one order of higher than the lower material. The Suncor cover consists of a peat-mineral mix overlying a sand material, with the lower material having a value of hydraulic conductivity approximately one order of magnitude higher than the upper material.

The location of the layer interface will have an effect on hydraulic conductivity (of air) tests using an apparatus such as the AP. It is important to know how the flow and pressure measurements are affected as the cylinder approaches and passes through the interface between materials of differing hydraulic conductivity. To quantify this effect, theoretical axisymmetric numerical simulations of the layered scenarios mentioned above were conducted with the program SEEP/W.

4.5.3.1 Layering of Higher Above Lower Hydraulic Conductivity

The scenario of the peat-mineral mix over till material was modeled first. Two layers of decreasing hydraulic conductivity with depth were created, and a region of vertically advancing null elements represented insertion of the AP cylinder. The top of the second soil layer was located at 25 cm. An image of the finite element mesh and resulting contour lines and flow paths is shown in Figure 4.10.

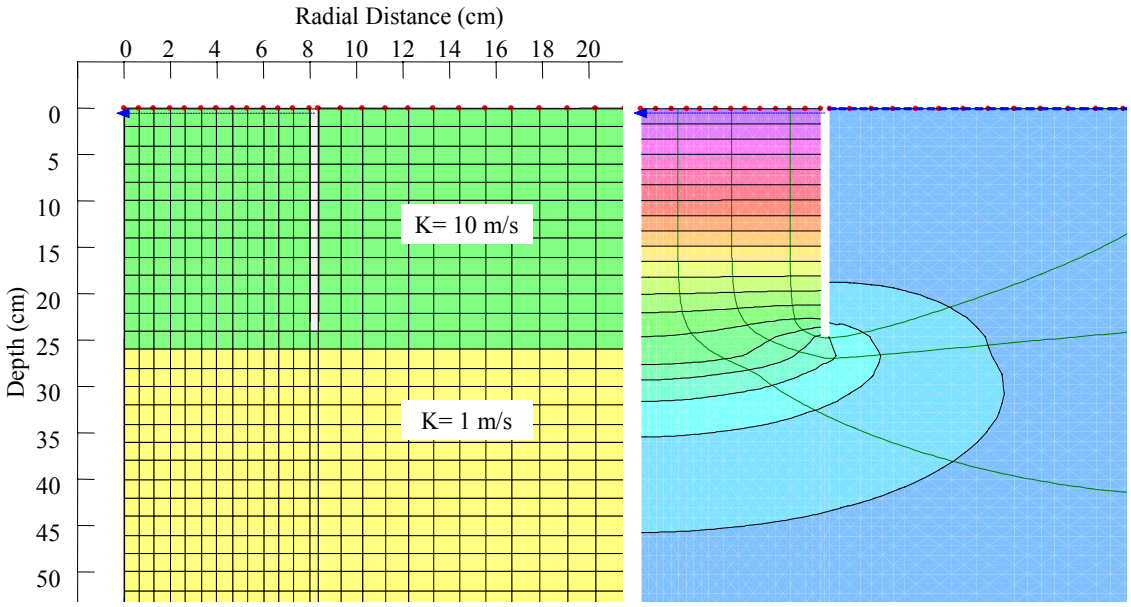

Figure 4.10. SEEP/W simulation of AP insertion into a layered soil system: (a) finite element mesh and (b) resulting contour lines and flow paths.

Three sets of simulations were run. The first simulation was a reference, with the values of hydraulic conductivity of the upper and lower layers set to 1 m/s. Total head boundary conditions were applied to the ground surface of the model, with H = 10 m inside the column, and H = 0 m outside the column. These boundary conditions were used in all simulations. The unit weight of air, 11.22 N/m^3, was applied as the unit weight of water. A boundary flux was calculated through the diameter of the soil column and used to calculate a resultant hydraulic conductivity, K, using a Darcy's law column calculation. Two successive simulations were run using K_1 = 5 m/s and K_2 = 1 m/s, and K_1 = 10 m/s and K_2 = 1 m/s.

Results from the simulation of K_1:K_2 ratios of 1:1 and 10:1 can be seen in Figure 4.11. Reference lines are drawn signifying the theoretical change in hydraulic conductivity at 25 cm depth between the upper and lower layers. The results of bulk K calculations to a depth of 40 cm are represented by the "1:1 Bulk K" data series. As mentioned in Section 4.5.1, an error occurs when the total head is assumed to drop over the length of the soil column within the cylinder.

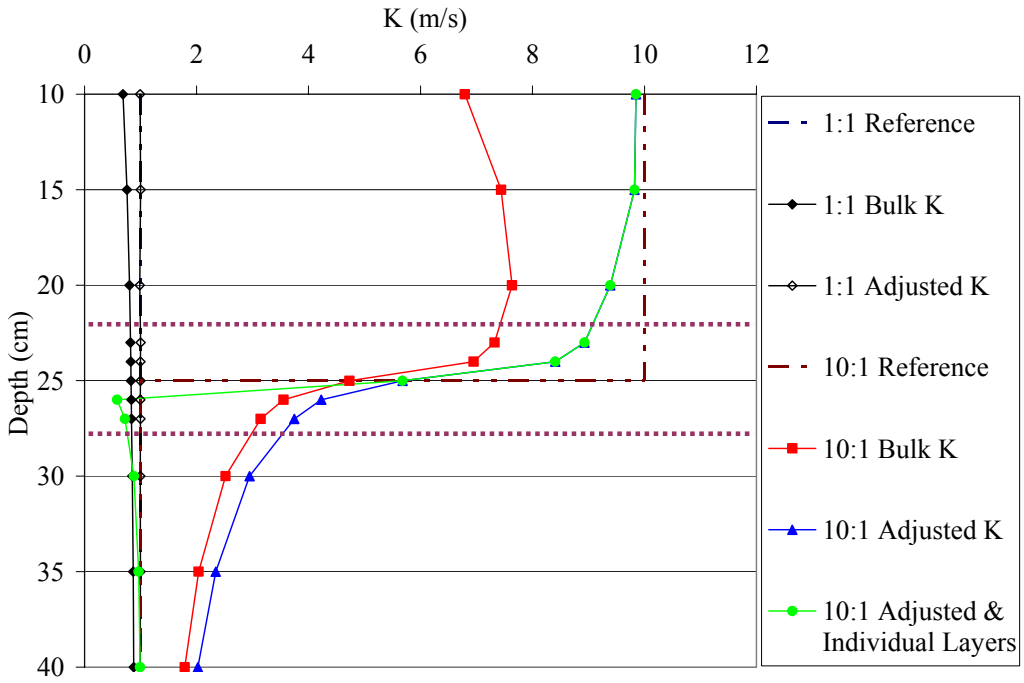

Figure 4.11. Results of theoretical simulation of air permeability measurements in a system of layers with higher above lower hydraulic conductivity.

A correction factor was applied to these values in order to produce a K equivalent to the 1:1 reference line, represented by the data series "1:1 Adjusted K". This correction factor was based on the relative difference between hydraulic conductivities when assuming or forcing the total head drop to occur over the length of the column, as shown in Table 4.6 for various insert depths. Minor adjustments were made to these values to ensure the "1:1 Adjusted K" series replicated the 1:1 reference line.

Three sets of data are shown for the K_1:K_2 ratio of 10:1. The first set of data, "10:1 Bulk K", is a set of K values calculated for each progressive depth to a total depth of

40 cm, ignoring the change in K at 25 cm depth. The correction factor derived for the "1:1 Adjusted K" data set was applied to the 10:1 data set, resulting in the series "10:1 Adjusted K". That correction brings the values of K significantly closer to the reference value of K = 10 m/s in the top layer. The third data set, "10:1 Adjusted & Individual Layers" is a data set that includes the correction for the error in Darcy's law as well as a calculation of K for individual layers, using [4.1].

As shown by the second and third data sets for the 10:1 K simulation, the calculated hydraulic conductivity profile is affected by the presence of the layer interface. For the case of K calculated for individual layers, the error in the calculated value of K only becomes significant (> 10%) within 2-3 cm on either side of the boundary. This region is denoted on Figure 4.11 by purple dashed lines.

In the "Bulk K" case for the 10:1 K ratio, the error in K calculation for Layer 1 is the same; however, the overall values of K calculated for Layer 2 are overestimated. This is something to take into consideration when measuring the K of a layered system. At the end of an AP trial, the cylinder is extruded, which allows for boundaries between soil layers to be identified in the profile and accounted for in analysis.

In this study, the upper peat-mineral layers of the Syncrude SW30 Dump and Coke Beach covers were so thin, that the layer interface was passed within the first 10 cm of the test. According to historical GP measurements, the K of the peat-mineral layer was approximately one order of magnitude higher than the K of the till layer. The upper peat-mineral layer was therefore modeled as having a K value 10 times higher than that of the till.

4.5.3.2 Layering of Lower Above Higher Hydraulic Conductivity

The Suncor cover of peat-mineral mix overlying sand was modeled next. The method described in Section 4.5.3.1 was used to model this scenario. First a reference test was simulated using a hydraulic conductivity of 1 m/s throughout the depth of the domain. A second set of simulations were then conducted with the lower layer having a

hydraulic conductivity of 10 m/s.

Results from the simulation of K_1:K_2 ratios of 1:1 and 1:10 can be seen in Figure 4.12. Reference lines are drawn signifying the theoretical change in hydraulic conductivity at 25 cm depth between the upper and lower layers. The results of bulk K calculations to a depth of 40 cm are represented by the "1:1 Bulk K" data series. The correction factor used in Section 4.5.3.1 was also applied to these values in order to produce a K equivalent to the 1:1 reference line, represented by the data series "1:1 Adjusted K".

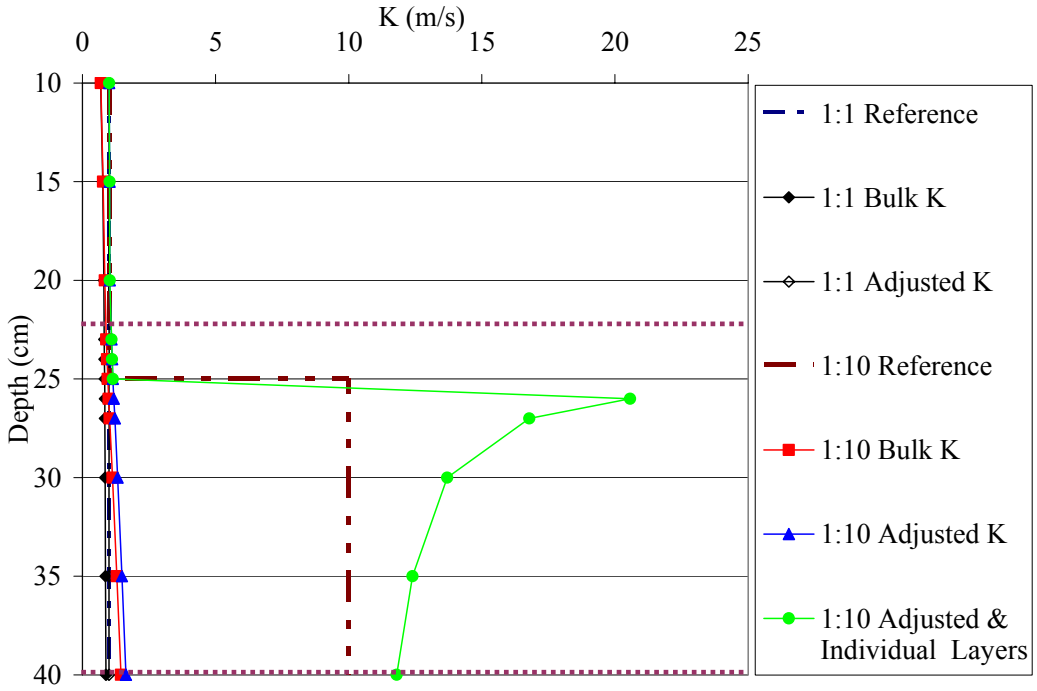

Figure 4.12. Results of theoretical simulation of air permeability measurements in a system of layers with lower above higher hydraulic conductivity.

Three sets of data are shown for the K_1:K_2 ratio of 1:10. The data sets "1:10 Bulk K", "1:10 Adjusted K" and "1:10 Adjusted & Individual Layers" were derived in a similar fashion as described for the corresponding data sets in Section 4.5.3.1. Similar to the simulation in Section 4.5.3.1, the hydraulic conductivity calculated above the layer change is not affected significantly (> 10%) until the cylinder is inserted within 2-3 cm of the interface.

However, the behaviour of the hydraulic conductivity calculations below the boundary is different in this situation. In a calculation of bulk hydraulic conductivity throughout the entire 40 cm profile, the values change minimally, disguising the fact that a layer of higher hydraulic conductivity exists at depth. When the hydraulic conductivity for individual layers is calculated and the adjustment factor applied (1:10 Adjusted K & Individual Layers) the hydraulic conductivity of the lower layer is greatly overestimated, resulting in a difference greater than 10% from the theoretical value of K = 10 m/s for the entire depth.

4.6 Comparison of Values of Permeability Measured with Air and Water

Results for AP tests on all materials involved in this study are shown in Figure 4.13. For each soil cover, the AP results include values from all depth profiles in all trials. Comparative permeability values determined by the water column method in the laboratory and GP in the field cases are also shown.

As discussed in Section 4.2, the results from the laboratory tests show that there is little difference in the values of permeability measured using air or water as the test fluid in the case of uniform dry sand. The measurements using the AP in the laboratory were compared to permeability determined using the constant head permeameter, which is accepted as an ASTM standard. This suggests that the AP technique does provide an accurate measurement of permeability.

There is approximately one order of magnitude difference in the median values of permeability measured with the AP and GP methods for the peat-mineral mix at the Suncor Coke Stockpile cover. The median values for the AP and GP tests are 5.0×10^{-12} m^2 and 4.2×10^{-13} m^2, respectively. One explanation for this difference may be the large difference in surface area available to flow between the two methods.

Vertical flow is possible through the entire undisturbed 16 cm diameter AP cylinder. However, disturbance to the soil structure during GP well installation may decrease the surface area available for flow out of the 6 cm diameter well bore. This is important

because the AP method measures strictly vertical permeability and the GP measures the net result of infiltration in both the vertical and horizontal directions. As discussed in Section 2.1.1, effects such as air entrapment during infiltration are also known to create underestimates of saturated hydraulic conductivity when using the GP (Reynolds and Elrick 1986).

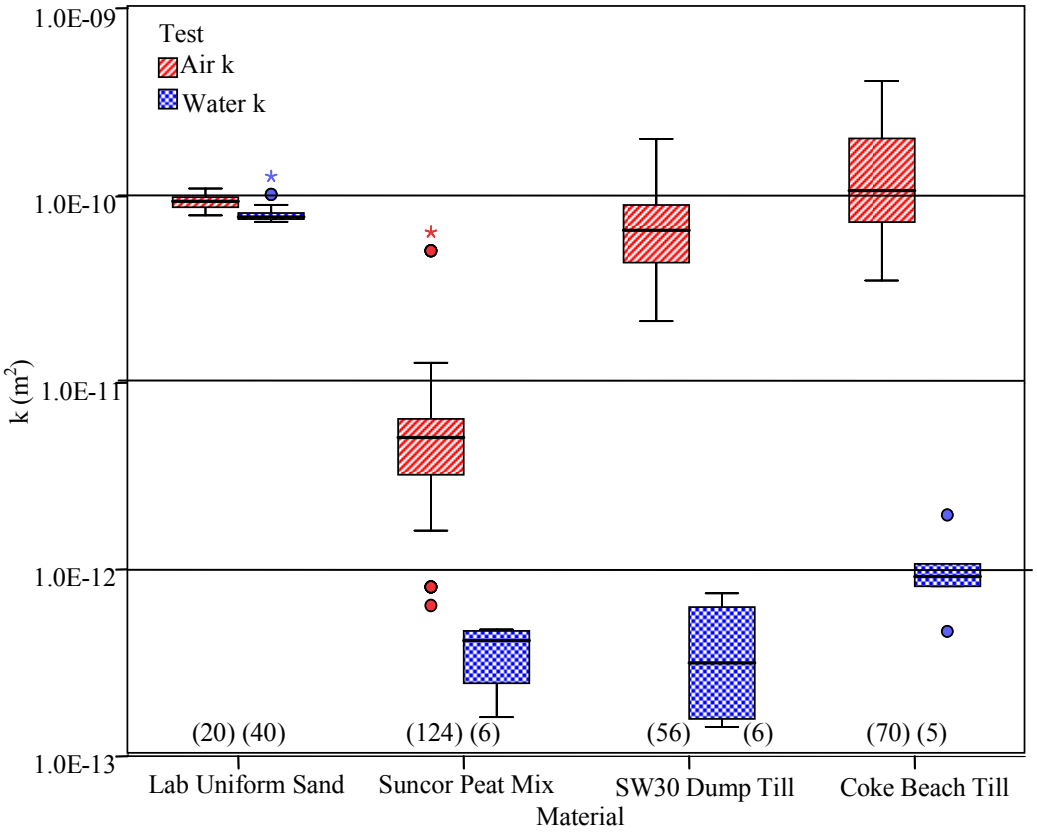

Figure 4.13. Comparison of values of permeability for all materials tested using the AP and water column in the laboratory or GP in the field, where (n) is the number of tests.

The Suncor soil cover was found to be fairly uniform in terms of soil structure, so the likelihood of macropore flow occurring in the AP and GP methods is unlikely. A photograph of a portion of a Suncor peat-mineral core extruded from the AP cylinder can be seen in Figure 4.14. The soil at this site was extremely dry, which lends itself to AP testing, although it is not weathered to the same degree as the other two sites studied.

Figure 4.14. Photograph of a portion of an AP core from the Suncor soil cover.

The median values of permeability at the two till covers as measured using the AP and the GP are consistently two orders of magnitude different. The median values of permeability on the SW30 Dump soil cover for the AP and GP tests are 6.6 x 10^{-11} m^2 and 3.7 x 10^{-13} m^2, respectively. The median values of permeability on the Coke Beach soil cover for the AP and GP tests are 1.0 x 10^{-10} m^2 and 9.9 x 10^{-13} m^2, respectively.

Differences of this magnitude may be due to the high degree of anisotropy in these soils as a result of weathering. The SW30 Dump soil cover was placed in 1999 and a substantial network of macropores and fractures has formed over these eight years. The Coke Beach soil cover was only placed during the winter of 2002-2003; however, climatic conditions of high heat and wind speed have caused erosion of the peat-mineral layer and consequently rapid weathering of the till layer (Fenske In Progress).

These effects can be seen in photographs that were taken of the soil profiles following the completion of an AP test (Figure 4.15). These photographs show that the soil texture is predominantly fine-grained, with an extensive macropore network. Smearing of the fine-grained materials of these covers can easily occur while augering the well bore for a GP test, sealing off some of the macropores that dominant flow. As a result, the surface area of the well bore available to flow is decreased and the value of K_{fs} can

be substantially underestimated. Likewise, the AP method involves vertical flow into the soil through a large undisturbed surface area. The surface area available to flow is not affected, and the macropore network is utilized for air transport.

(a) (b)

Figure 4.15. Photographs of soil profiles following removal of the AP cylinder for the Syncrude: (a) SW30 Dump and the (b) Coke Beach soil covers.

4.7 Factors Affecting Air and Water Permeability Measurements

Questions arise about the validity of the air permeability values when a difference of two orders of magnitude exists between the AP and GP values. Several possible explanations were mentioned in Section 4.5. In terms of air permeability values one possible explanation for the high values is the Klinkenberg effect. Another explanation is that Darcy's law is not valid for air flow through soil. Operational concerns such as leakage in the AP system could also cause an overestimated prediction of permeability. All of these effects are discussed in the subsequent sections.

4.7.1 Slip Flow Effects and Darcy Flow

As discussed in Section 2.4, the permeability of soil can be overestimated for gas flow though fine-grained soils at low pressures. Although the soil covers in this study consist of fine-grained soils, the existence of a macropore structure significantly increases the size of the air transport pathways and decreases the likelihood of slip-enhanced flow. However, the possibility of slip enhanced flow should not be

overlooked.

The method of Scanlon et al. (2002) to determine the true gas permeability of a soil (Section 2.4) was applied to the data sets of various materials to investigate the effects of slip flow. This equation can be written as follows:

$$k_g = k + kb\left[\frac{1}{\overline{P}}\right] \qquad [2.6]$$

where the calculated permeability k_g is plotted against the inverse of the mean applied pressure ($1/dH_{mean}$). A trend line is fitted to the data, with the y-axis intercept resulting in the true permeability k. An example of this correction applied to 10 cm and 20 cm depth interval tests on the Coke Beach soil cover is shown in Figure 4.16.

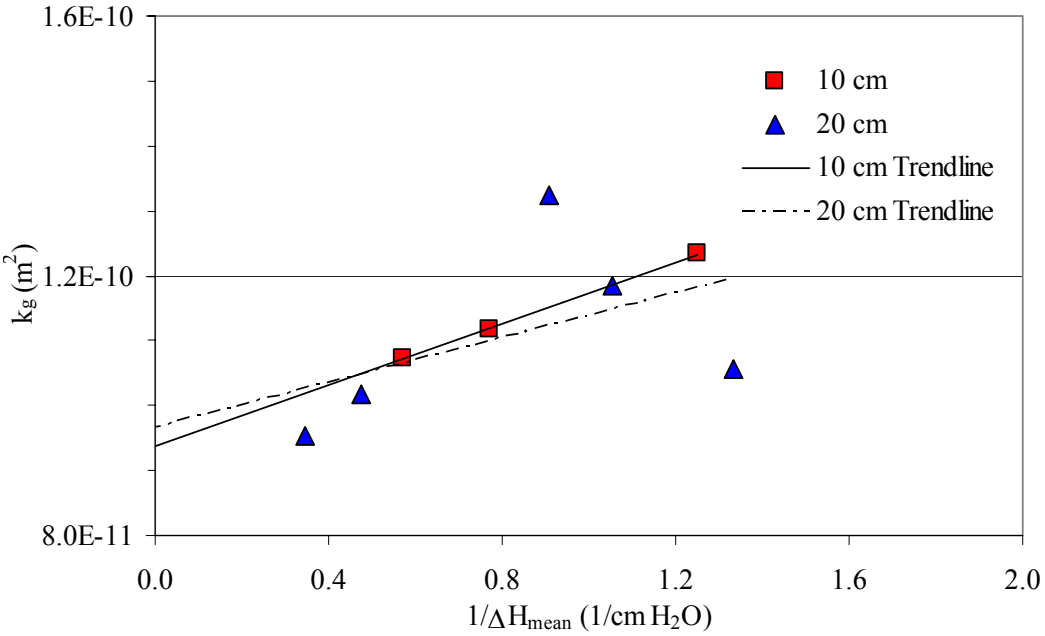

Figure 4.16. Slip correction procedure for Coke Beach soil cover permeability measurements.

As explained in Section 2.4, deviations from Darcy's law can occur for gas flow through soil due to effects such as slip flow or compressibility. Most commonly a non-linear, compressible flow equation is used to analyze gas permeability. However, assumptions have been made in this study to allow the use of Darcy's law to calculate permeability. According to Scanlon et al. (2002) a simple check can be made to

establish whether Darcy's law is being obeyed - the gas flux when plotted against pressure gradient should result in a linear relationship with an intercept of zero.

A graph of flow and pressure data from the 10 cm data set (from Figure 4.16) on the Coke Beach soil cover can be seen in Figure 4.17. The raw test data are represented by square symbols with a solid trend line passing backwards through the y axis. The relationship of flow and pressure is linear; however, the intercept is not zero. The slip corrected permeability that was determined by the graph in Figure 4.16 for the 10 cm depth was used with the test pressure data to back calculate values of flux and hydraulic conductivity through the soil core.

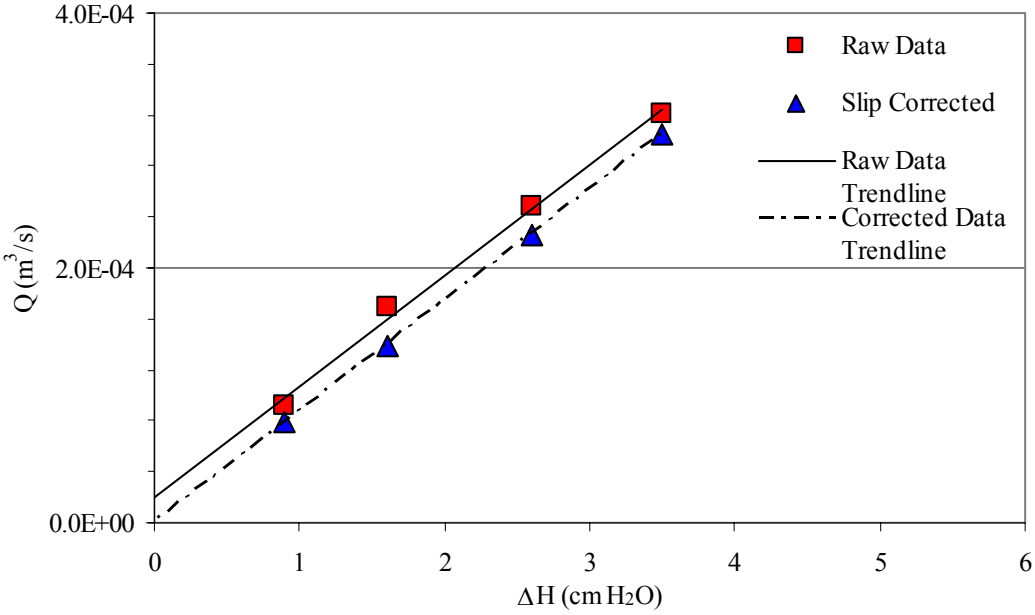

Figure 4.17. Air permeability test data for Coke Beach soil cover before and after slip correction applied.

The resulting relationship of flow and pressure denoted by the triangular symbols and dashed trend line is linear, with an intercept of zero. The difference in permeability before (1.2×10^{-10} m^2) and after (1.1×10^{-10} m^2) the slip correction was applied is approximately 9%. Therefore, compensation for slip effects will ensure Darcy flow behaviour is met; however, it can also safely be ignored without large errors in the analysis.

The slip correction procedure was applied to several data sets from the Suncor and Coke Beach soil covers to determine the effects of slip-enhanced flow on various materials. Individual data sets compared to corresponding slip-corrected values of permeability can be found in Figure 4.18. The first two pairs of data correspond to measurements taken on the Suncor soil covers. The last two pairs of data correspond to measurements taken on the Coke Beach soil covers.

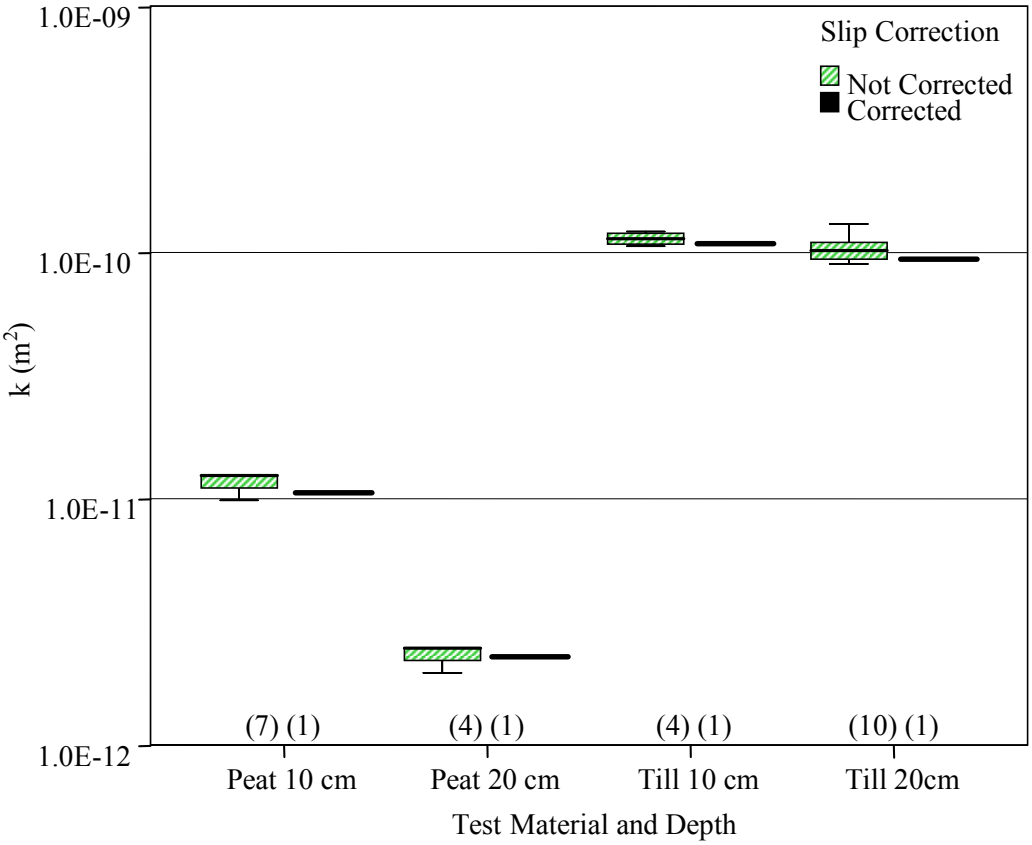

Figure 4.18. Comparison of slip-enhanced (non-corrected) permeability to true (corrected) permeability for Suncor peat-mineral and Coke Beach till AP tests, where (n) is the number of calculations.

A comparison of the median values of permeability and slip corrected permeability for all four data sets as well as relative differences can be found in Table 4.7. The differences between median values and the single slip corrected permeability are similar for both peat-mineral and till materials. Although it would be expected that the slip correction would have a greater effect for the finer grained till cover, the existence of

the macropore structure could decrease the tendency of slip flow occurring with decreasing pore size.

Table 4.7. Comparison of median values of permeability before slip correction to slip corrected permeability for the Suncor peat-mineral and Coke Beach till materials.

Test Material and Depth	k (m^2) - Median - Not Corrected	k (m^2) – Median - Slip Corrected	Relative Difference (%)
Peat 10 cm	1.2×10^{-11}	1.1×10^{-11}	9
Peat 20 cm	2.3×10^{-12}	2.2×10^{-12}	5
Till 10 cm	1.2×10^{-10}	1.1×10^{-10}	9
Till 20 cm	1.0×10^{-10}	9.5×10^{-11}	5

4.7.2 Leakage Effects

During AP tests, a support frame is used to ensure vertical insertion into the soil profile. However, due to factors encountered during the test such as stones in the path of the cylinder, some disturbance occurs, creating a pathway along the inner cylinder wall which may cause air flow to bypass the soil core.

In order to quantify this leakage, two sets of data were gathered for individual test depths at one location on the Suncor soil cover and one location on the SW30 Dump soil cover. The first set of data was three measurements of flow and pressure according to the standard test procedure. Following the measurements a stake was used to knead the soil around the inside perimeter of the cylinder wall to block off any potential bypass flow. A second set of flow and pressure measurements were taken. Median permeability values of untreated and kneaded trials are compared in Table 4.8. Visual results from this experiment can be seen in Figure 4.19.

The difference in values for the peat-mineral cover is small, 2 and 3%. However, the

difference in values for the till cover is substantially larger, 45%. One explanation for this behaviour could be the larger probability of encountering stones during installation of the column in the till covers. Greater disturbance could occur relative to installation in the peat-mineral covers, increasing the difference between untreated and kneaded values.

Table 4.8. Comparison of median permeability values for untreated and kneaded soil.

Test Material and Depth	k (m^2) – Median – Untreated	k (m^2) – Median - Kneaded	Relative Difference (%)
Peat 10 cm	4.4×10^{-12}	4.3×10^{-12}	2
Peat 20 cm	6.8×10^{-12}	6.6×10^{-12}	3
Till 20 cm	9.3×10^{-11}	6.7×10^{-11}	45

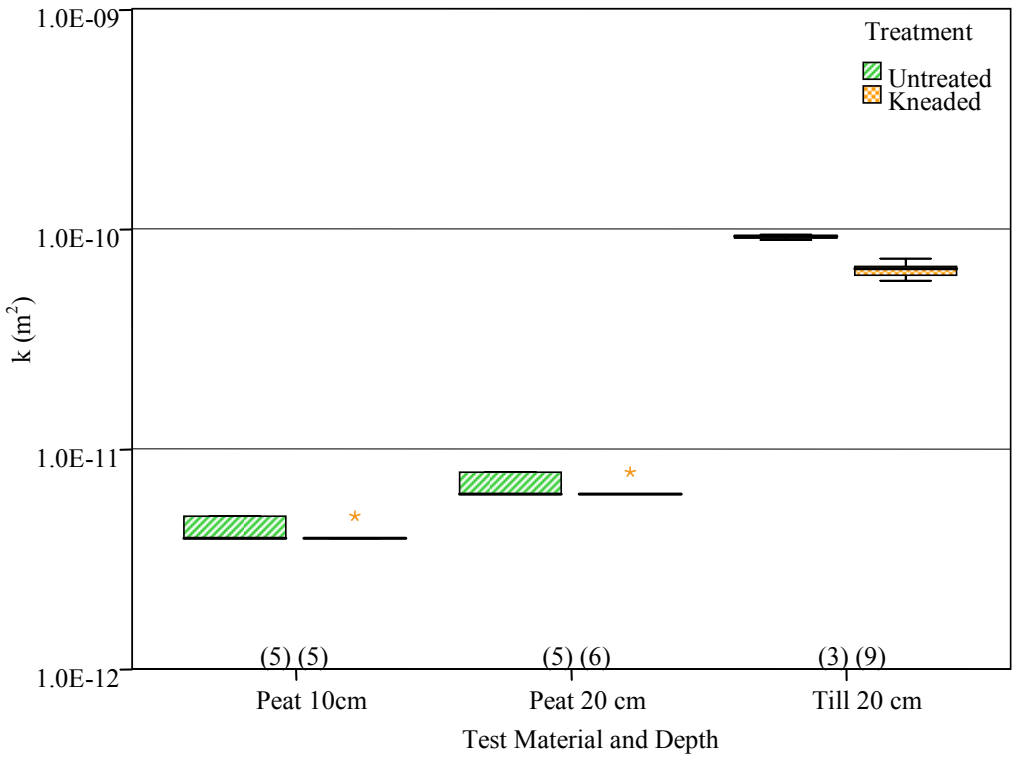

Figure 4.19. Comparison of air permeability tests for soil untreated, followed by soil "kneaded" against the cylinder wall, where (n) is the number of tests.

4.7.3 Effect of Anisotropy on Air and Guelph Permeameter Methods

The factors that cause the difference in AP and GP permeability values for the Suncor soil covers are likely common to the Syncrude SW30 Dump and Coke Beach covers. However, at these latter sites an additional order of magnitude difference in permeability values between methods must be explained. The cause of this difference is specific to this material, because results of both sites exhibited similar characteristics.

Anisotropy may be one explanation for this difference in permeability. In this case, anisotropy is caused by a macropore network formed in a fine-grained till matrix with macropores occurring predominantly in a vertical direction. The AP measures flow in the vertical direction; consequently, it will measure the maximum permeability within the soil while the GP will be affected by the lower horizontal permeability. Also, insertion of a cylinder of 16 cm diameter vertically causes minimal disturbance on the macropore network within the cylinder. Any smearing shut of this macropore network will cause an underestimation of permeability, because the majority of flow out from the GP well bore must occur horizontally prior to vertical drainage.

The effect of anisotropy on both of these tests was investigated through a SEEP/W numerical simulation. Ratios of vertical to horizontal permeability (K_v/K_h) of 10 and 100 were simulated. A typical value of air permeability expected for the till material was chosen (7.5×10^{-11} m^2) and converted into hydraulic conductivities for air (K_{air} = 4.9×10^{-5} m/s) and water ($K_w = 7.3 \times 10^{-4}$ m/s). Separate simulations were conducted to represent the geometry and fluid properties for both AP and GP test methods.

An AP simulation was conducted first, using null elements to represent the column walls of the AP cylinder in an axisymmetric analysis. Images of this simulation are shown in Figure 4.20. A simulation using assumed isotropic conditions was then developed and the value of K varied until the flow rate matched the flow rates for the anisotropic simulation case.

The saturated hydraulic conductivity of the model was set equal to K_{air} [m/s]. Head

boundary conditions (H) were set to force flow to occur downward through the soil surface within the cylinder. A value of flux that would be expected for a permeability of 7.5 x 10^{-11} m^2 was used as a reference flux ($Q_{reference}$).

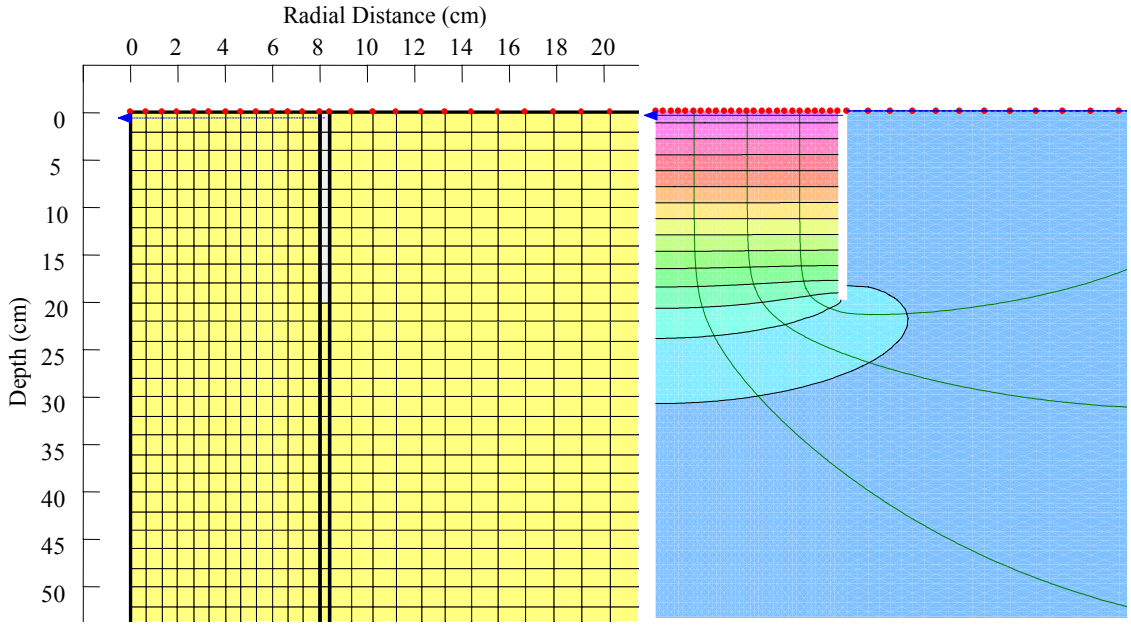

Figure 4.20. SEEP/W simulation of AP insertion into an anisotropic soil system: (a) finite element mesh and (b) resulting contour lines and flow paths.

A boundary flux (Q_{output}) was calculated through the cross-sectional area of the cylinder. As K and Q vary linearly in Darcy's law, the resultant K (K_{actual}) was calculated using the method described in Section 3.3. An example of this procedure is shown in the following equation:

$$K_{air} Q_{output} = K_{actual} Q_{reference} \qquad [4.2]$$

where K_{air} is the reference hydraulic conductivity of this simulation.

Once the set of boundary conditions was calibrated so that $K_{actual} = K_{air}$ for insertion depths of 10, 20 and 30 cm on isotropic soil, the anisotropic investigation was completed. The same set of H boundary conditions was used for each insert depth. However, to simulate a K_v/K_h ratio of 10, the horizontal K value in SEEP/W (K_h) was set one order of magnitude lower, to 4.9 x 10^{-6} m/s, to produce a K_v/K_h ratio of 10. This

combination of hydraulic properties was used to simulate flow from the AP. This procedure was repeated for the case of a K_v/K_h ratio of 100.

This data was then interpreted in a new simulation assuming that the soil was isotropic with respect to K. The H boundary conditions remained unchanged, but the values of K_{air} within SEEP/W were adjusted for each data set so that the Q_{output} was equal to the Q that had been produced in the anisotropic cases.

A similar simulation was then conducted for the GP as illustrated in Figure 4.21. The well bore geometry was represented by null elements to a test depth of 30 cm. The typical ponded water heights of 5 cm and 10 cm in a GP test were simulated by applying H boundary conditions of -.25 m and -.20 m, respectively, along the surface of the well bore through which water would infiltrate. An H boundary condition of -1.0 m was set at the base of the finite element mesh, located at a y coordinate of -1.0 m, to force flow to occur in the downward direction.

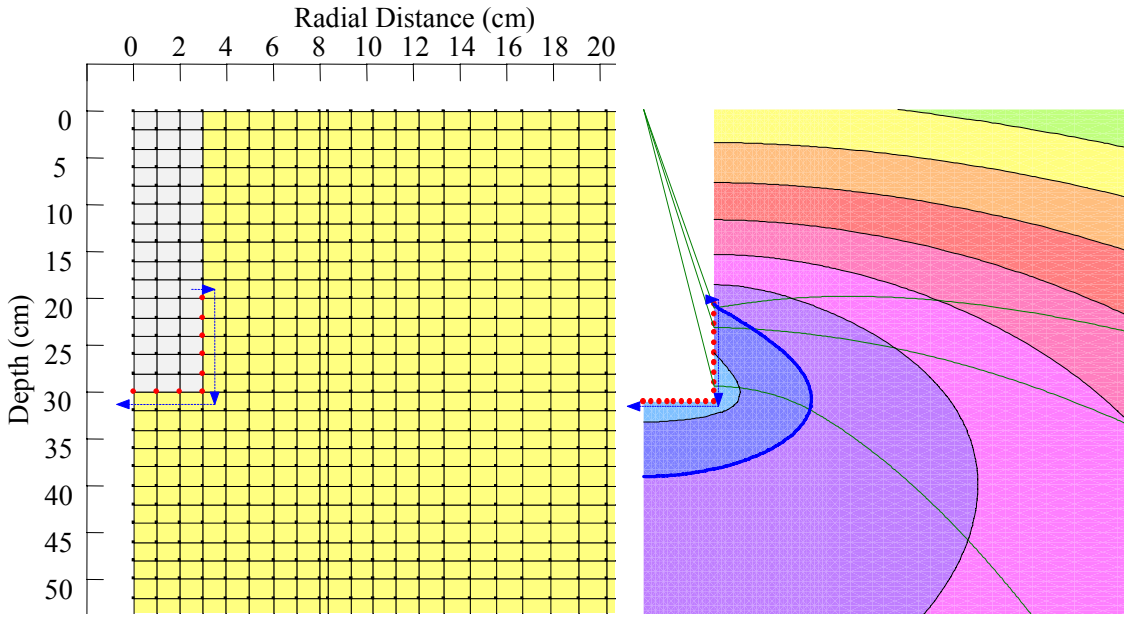

Figure 4.21. SEEP/W simulation of GP test in an anisotropic soil system: (a) finite element mesh and (b) resulting contour lines and flow paths.

A boundary flux (Q), which is denoted by the blue arrows in Figure 4.21 (a) was calculated through the entire height of the ponded water and also the width of the well bore. This output value of Q was used in the single height analysis equation defined in Chapter 2:

$$K_{fs} = \frac{CQ}{2\pi H^2 + C\pi r^2 + 2\pi \frac{H}{\alpha^*}} \qquad [2.1]$$

to determine a value of K_{fs}. The K_w used in SEEP/W was initially set as a saturated K value of 7.3 x 10^{-4} m/s. However, because the GP is operated in an unsaturated system, the K function in SEEP/W was adjusted until Q could be used in the single height equation to produce a K equivalent to K_w. The resultant K function is shown in Figure 4.22.

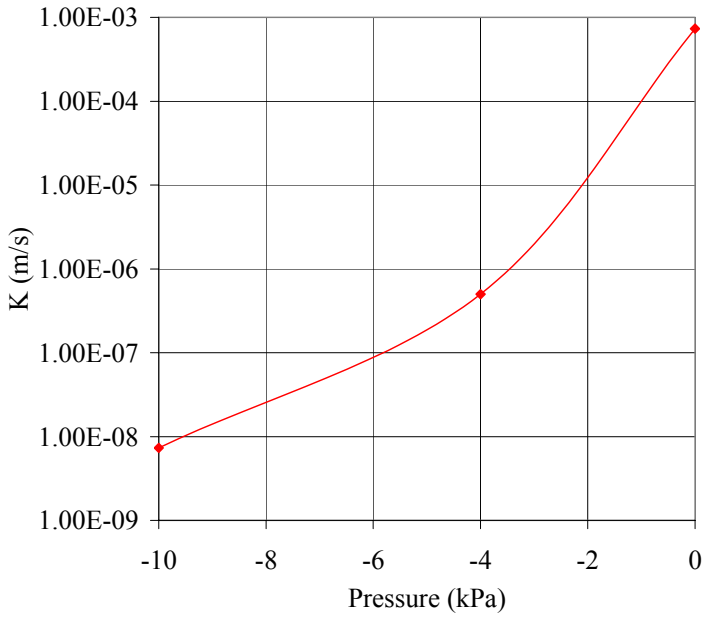

Figure 4.22. SEEP/W K function necessary to produce K_{fs} = K_w using single height analysis equation for isotropic soil condition.

Once the K function was adjusted to produce the same from both the equation (K_{fs}) as for the simulation (K_w) for the isotropic case, the anisotropic cases were conducted. To simulate this scenario for K_v/K_h ratio of 10, the entire K function (K_x) was lowered by one order of magnitude and the degree of anisotropy was set to 10, to produce a K_v/K_h

ratio of 10. A value of Q was computed for both the simulated 5 cm and 10 cm ponded water heights. The corresponding K_{fs} was calculated for each scenario. This procedure was repeated for an anisotropic scenario of K_v/K_h ratio of 100.

Results of the AP and GP simulations in isotropic and anisotropic soil are found in Figure 4.23. A green, dashed reference line is set at 7.5 x 10^{-11} m^2, which signifies the theoretical permeability of the soil in the simulations. Values of permeability for the three depth simulations of the AP are represented by the square symbols. The two ponded water heights for the GP are represented by diamond symbols.

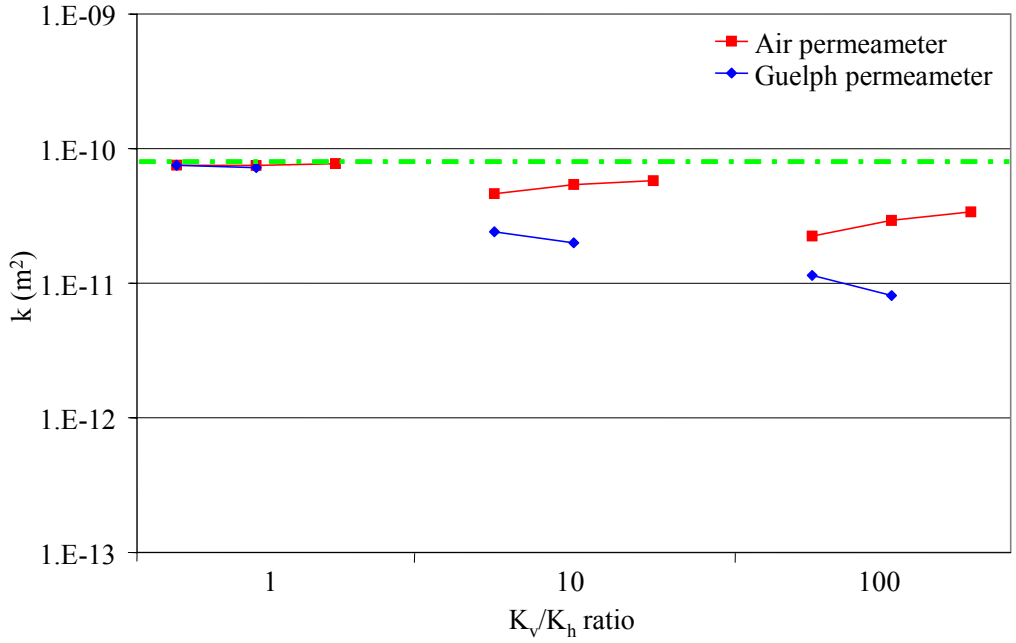

Figure 4.23. Results of numerical simulation of anisotropy for the AP and GP methods.

The values for both simulations are plotted with increasing degrees of anisotropy. As shown in the plot, both the AP and GP methods are affected by anisotropy. The GP is affected to a higher degree than the AP, which possibly explains some of the difference between the values of permeability determined through field measurements. However, because the difference between the results is not a full order of magnitude, other factors must be affecting the field results.

4.7.4 Effect of Well Bore Smearing on GP Measurements

Two numerical simulations were performed to investigate the potential underestimation of permeability as measured with the GP due to well bore smearing during the augering process. The first simulation assumes that smearing of the well bore walls has been treated; however, a smeared layer still exists on the bottom of the well bore. The second simulation investigates the possibility that smearing was not properly treated, resulting in a smeared layer on the well bore walls and bottom.

The walls of the well bore can be treated to remove a smear layer; however, it is difficult to treat the base of the well bore. This would cause a layer of soil at the bottom to the well bore to act as a material of lower hydraulic conductivity (K_{well}) than the region in which the test is being conducted (K_{region}). The first SEEP/W numerical simulation was used to investigate these effects.

The finite element mesh described in Section 4.7.3 was used, but modified to include a thin layer of soil below the well bore in which the hydraulic conductivity was lowered by factors of 10 and 100 relative to the surrounding soil to represent possible effects of smearing (Figure 4.24). The elements which experienced a decrease in hydraulic conductivity were 0.5 cm thick. The K function shown in Figure 4.22 was used for K_{region}. This K function was lowered by factors of 10 and 100 to represent K_{well} ().

The second simulation was used to model the case in which smearing on the walls of the well bore was not properly treated. This was modeled by creating a thin layer of soil of lower hydraulic conductivity through which all of the ponded water must infiltrate before entering the surrounding region. Although the standard treatment procedures were followed in this study, it is not guaranteed that all macropores and fractures were opened up to water flow upon treatment.

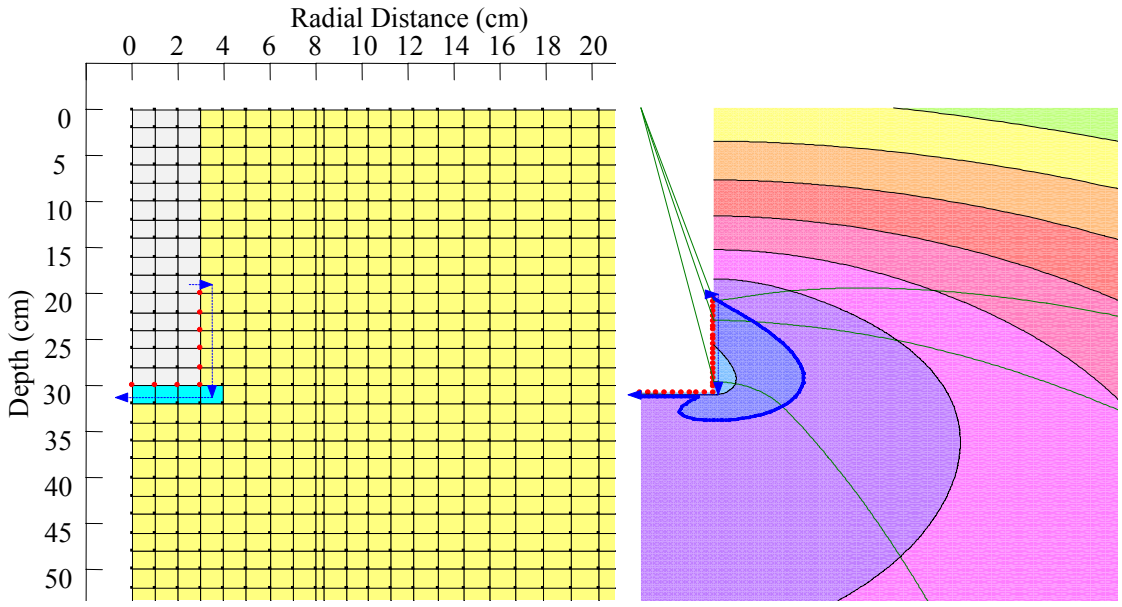

Figure 4.24. SEEP/W simulation of GP test with "smeared" well bore base, represented by a lower permeability region below the well bore: (a) finite element mesh and (b) resulting contour lines and flow paths.

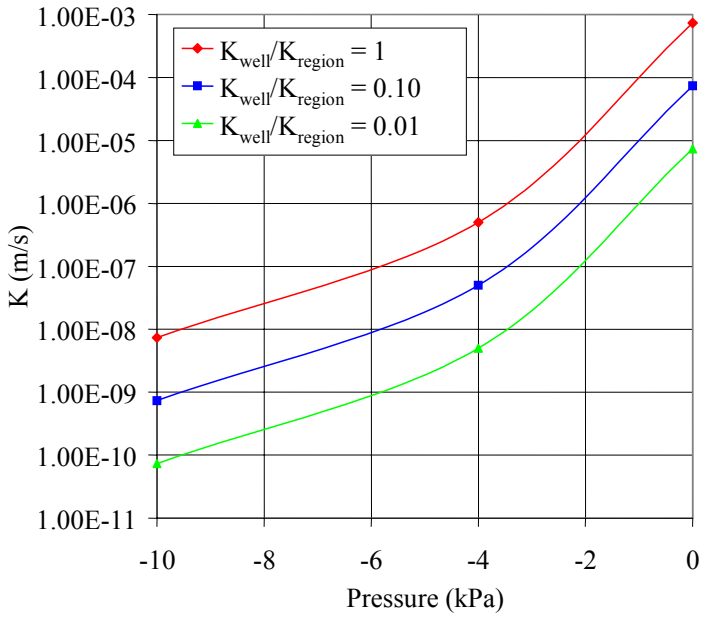

Figure 4.25. SEEP/W K functions for soil below well bore: with K_{well} equal to K_{region}, 10 times lower, and 100 times lower.

The finite element mesh used in this simulation is shown in Figure 4.26. Similar to the first simulation, the hydraulic conductivity was lowered by factors of 10 and 100 for elements of thickness 0.3 cm along the height of the well bore (under ponded water). The K function shown in was used for the material directly surrounding the well bore.

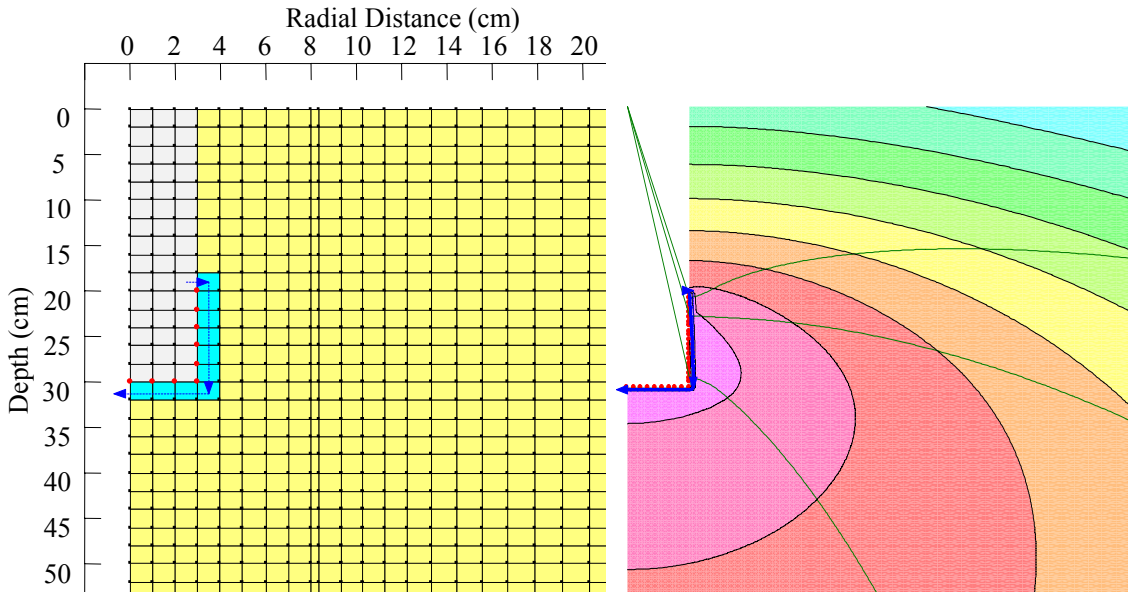

Figure 4.26. SEEP/W simulation of GP test with "smeared" well bore surface, represented by a lower permeability region surrounding well bore: (a) finite element mesh and (b) resulting contour lines and flow paths.

As the soil from two sites investigated in this study were clearly anisotropic (SW30 Dump and Coke Beach), these simulations were repeated for K_v/K_h ratios of 10 and 100 for all elements. The resultant values of K were calculated using the single height equation with results shown for both simulations in Figure 4.27. The first two data series are AP and GP values that were discussed in Section 4.7.3 for isotropic and anisotropic soils. The remaining data sets involve isotropic and anisotropic simulations for GP conditions of regions of lower hydraulic conductivity below the well bore (GP: $K_{well\ bottom}/K_{region}$) and surrounding the well bore (GP: K_{well}/K_{region}).

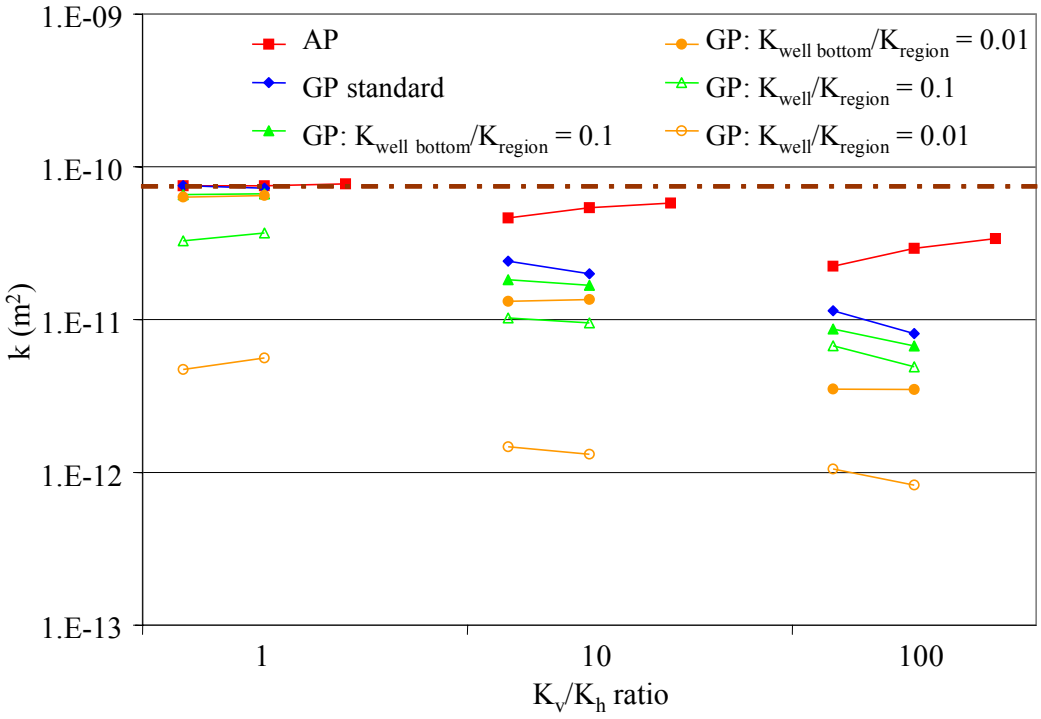

Figure 4.27. Results of two numerical simulations comparing air permeameter values to Guelph permeameters for the cases: 1) smearing of base of well bore and 2) smearing of walls and base of well bore for isotropic and anisotropic conditions.

The results show that if a small layer as thin as 0.5 cm experiences a drop in hydraulic conductivity below the well bore, the resultant permeability calculated with the GP method is not significantly affected for isotropic soil. However, the coupled effect of lowered K below the well bore and anisotropic soil produces values of permeability approximately one order of magnitude lower than those produced by the AP for the case of $K_v/K_h = 100$. This combined effect is possible and could provide some explanations for the differences in permeability measured by the AP and GPs.

For the case of smeared soil around the entire well bore, a drop in K_{well} by a factor of 10 in an isotropic soil causes the resultant K value to drop almost half an order of magnitude. When the lowered K layer ($K_{well}/K_{region} = 0.01$) is coupled with anisotropy ($K_v/K_h = 100$) within the soil region, the values of permeability are up to 2 orders of magnitude lower than those produced by the AP in anisotropic soil. Therefore, if there is any fraction of the well bore face that is not properly treated to remove the smear

layer prior to a GP test, a significant difference in permeabilities calculated by the AP and GP methods should be expected. The GP apparatus has the potential to underestimate the value of K up to half an order of magnitude for an isotropic soil, and almost two orders of magnitude for an anisotropic soil.

As shown in this Chapter, the air permeameter performs well under ideal, controlled conditions when compared with conventional water permeability tests. However, when the air permeameter is used in a field application, some differences in permeability values occur when compared with a method such as the Guelph permeameter. Several possible explanations for these differences were discussed. Numerical simulations were also used to compare these two field methods under different in-situ conditions. There is good potential for the air permeameter to be used as a reclamation monitoring tool. However, the concerns mentioned here must be fully investigated first.

CHAPTER 5
CONCLUSIONS AND RECOMMENDATIONS

5.1 Conclusions

Tracking the changes in hydraulic conductivity is an important step in predicting the long term performance of a reclamation soil cover. The method used to do this must be cost effective and efficient in order to be used extensively. Several methods have been used to measure the saturated hydraulic conductivity of reclamation covers in the past, including laboratory and field methods. However, these methods tend to be very time consuming. The method of air permeability is proposed in this study as an alternative to these methods.

The first objective of this study was to design a prototype air permeameter that could be used to measure the air hydraulic conductivity of reclamation soil covers in the oilsands mining industry of Northern Alberta, Canada. A method was chosen based on the portable air permeameter design of Iversen et al. (2001). A prototype was built prior to the 2005 field season capable of testing to depths of 40 cm.

Improvements were made to the air permeameter design prior to the 2006 field season. Extensive testing was carried out on reclamation covers at three locations: Syncrude Canada Ltd. SW30 Dump, Syncrude Coke Beach and Suncor Energy Coke Stockpile. The method was found to operate efficiently and required approximately 30 minutes to determine the air permeability of a 40 cm profile. This time frame included set up of the apparatus and recovery of the soil profile from the permeameter cylinder.

The second objective of this project was to compare permeability values determined with the air permeameter to traditional methods of measuring saturated hydraulic conductivity in the laboratory and field. First, laboratory column tests using air and water as the test fluids were carried out on a uniform sand to ensure that (intrinsic)

permeability using two different test fluids at identical fluid phase contents was equal. A relative difference of 4% was found between these values of permeabilities. This difference is acceptable for the objectives of this study.

The prototype air permeameter was then used in a tank of the same dry uniform sand, to determine a permeability value for comparison to the standard constant head (water) column test. The permeabilities determined with the full scale air permeability test and the water column test were found to have a difference of 21%. Although this difference is larger than that determined using the air and water column methods, it is seen as acceptable in terms of the objectives of this study. The Guelph permeameter was also used in the sand tank to provide a comparison to the air permeameter. However, the results are not comparable because the upper hydraulic conductivity limit of the Guelph permeameter was exceeded.

Guelph permeameter testing was carried out alongside the air permeameter on the three reclamation soil covers mentioned earlier. When the values of permeability determined using both methods were compared, the behaviour of the results was dependent on material type. Permeabilities calculated from both methods were different by approximately one order of magnitude for the Suncor peat cover. For both of the Syncrude till covers the permeability values calculated from each method were different by approximately two orders of magnitude.

The third objective of this project was to determine the suitability of using the air permeability method as an alternative to the Guelph permeameter. In terms of equipment costs and time requirements, the air permeameter is definitely a more suitable option. However, further investigation into the difference between values of permeability measured with each method is needed before confidence can be established in the air permeameter method.

A difference of one order of magnitude between permeability predictions can be explained by factors such as difference in surface area available to flow and air

entrapment during infiltration using the Guelph permeameter. However, a difference of two orders of magnitude between permeabilities predicted for till soil covers is not acceptable.

There are several factors that could explain the difference of two orders of magnitude in the permeability of the till covers. Fluid flow through these soil covers is dominated by the presence of secondary structure which occurs as macropores or fractures. This flow behaviour creates anisotropy within the soil, likely causing the vertical permeability to be greater than the horizontal permeability. The air permeameter utilizes the vertical direction to flow, whereas the Guelph permeameter uses an average of vertical and horizontal flow.

Smearing of the clay, and the resulting closure of secondary structure during augering of the Guelph permeameter well bore in these fine-grained soils, could be another explanation for the difference. The small surface area used for water infiltration in this method may not intersect a large number of macropores or fractures. If any of these pathways become smeared shut, there is a great potential for underestimating permeability of the soil. Conversely, the air permeameter utilizes the vertical flow direction, and does not disturb the secondary structure, resulting in a larger available transport network.

5.2 Recommendations

The air permeameter holds great potential for use as a reclamation monitoring tool. The capabilities for using the air permeameter on a larger scale could be increased by creating a mechanical system to operate the permeameter. At the present time, the cylinder is inserted by hand, which takes a great amount of effort and also increases the risk of disturbance along the cylinder wall. However, if the cylinder was mounted on a vehicle (e.g. ATV) and inserted smoothly using a hydraulic ram, the chance of disturbance and leakage would be minimized. The test time could also be decreased, likely to approximately ten minutes.

Site-specific factors such as macropore flow effects in fine-grained tills increase the anisotropy of soil, and affect the air permeameter and Guelph permeameter in opposite ways. The results from each method are difficult to compare. To determine whether the difference in permeabilities in this study is due to flow directions and differences in available surface area to flow, the air permeameter could be compared against other methods of measuring saturated hydraulic conductivity. Possible methods may include the velocity and disk permeameters.

As mentioned in Chapter 2, the velocity permeameter involves inserting a cylinder into the ground and measuring flow in the vertical direction. As well, the disk permeameter utilizes a larger sample diameter of 25.4 cm, and forces flow to occur through the soil surface, resulting in minimal disturbance to the secondary structure. Comparison of the permeability measured with these methods and the air permeameter could delineate whether or not the difference in permeability found in this study was solely due to the operation of the air permeameter, or the operating behaviour of both methods.

The 2006 field season testing program included a leakage investigation for the air permeameter method. Following an initial set of permeability measurements, the soil within the cylinder was kneaded against the cylinder wall, and a second set of measurements were made. Although the difference between values before and after kneading was not large, modifications could be made to the apparatus to eliminate leakage at the soil surface. A rubber gasket fitting tightly to the inside wall of the cylinder could be pressed against the soil surface prior to a test to ensure that no air flow occurs along the cylinder wall. However, this would not eliminate the possibility of air traveling along the cylinder wall at depth.

The potential for using the air permeameter as a reclamation monitoring tool is great. Further studies to investigate values of permeability predicted with the method are necessary. If it can be shown that the values of permeability measured using the AP are correct, of if adjustments can be made to the method to decrease the difference in permeability values measured with air and saturated permeability techniques, the air

permeameter will prove to be a valuable alternative to the Guelph permeameter. The air permeameter could then be used in more extensive applications, such as mapping the spatial distribution of permeability across a reclamation cover.

REFERENCES

American Society for Testing and Materials 2005. D2434-68 Standard test method for permeability of granular soils (Constant head). In 2005 Annual Book of ASTM Standards, Volume 04.08. ASTM International, West Conshohocken, PA.

Ankeny, M.D., Kaspar, T.C., and Horton, R. 1988. Design for an automated tension infiltrometer. Soil Science Society of America Journal, 52: 893-896.

Ba-Te, Zhang, L., and Fredlund, D.G. 2005. A general air-phase permeability function for airflow through unsaturated soils. In Geo-Frontiers 2005 Congress. Edited by P.E. Ellen M. Rathje. Austin, TX. January 24-26, 2005. American Society of Civil Engineering.

Baehr, A.L., and Hult, M.F. 1991. Evaluation of unsaturated zone air permeability through pneumatic tests. Water Resources Research, 27(10): 2605-2617.

Bagarello, V. 1997. Influence of well preparation on field-saturated hydraulic conductivity measured with the Guelph permeameter. Geoderma, 80: 169-180.

Bagarello, V., Iovino, M., and Reynolds, W.D. 1999. Measuring hydraulic conductivity in a cracking clay soil using the Guelph permeameter. American Society of Agricultural Engineers, 42(4): 957-964.

Ball, B.C. 1981. Modelling of soil pores as tubes using gas permeabilities, gas diffusivities and water release. Journal of Soil Science, 32: 465-481.

Barbour, S.L. 2005. Lessons from the Southwest 30 Overburden Hill instrumented watershed research program. In Watershed Research Team Annual Meeting. Edmonton, AB. January 25, 2005. Syncrude Canada Limited.

Beven, K., and Germann, P. 1982. Macropores and water flow in soils. Water Resources Research, 18(5): 1311-1325.

Bodhinayake, W., and Si, B. 2004. Near-saturated surface soil hydraulic properties under different land uses in the St. Denis National Wildlife Area, Saskatchewan, Canada. Hydrological Processes, 18: 2835-2850.

Bouma, J., and Wosten, J.H.M. 1979. Flow patterns during extended saturated flow in two, undisturbed swelling clay soils with different macrostructures. Soil Science Society of America Journal, 43: 16-22.

Bouma, J. 1982. Measuring the hydraulic conductivity of soil horizons with continuous macropores. Soil Science Society of America Journal, 46: 438-441.

Bowles, J. 1992. Engineering properties of soils and their measurement. McGraw-Hill Inc.

Campbell, C.M., and Fritton, D.D. 1994. Factors affecting field-saturated hydraulic conductivity measured by the borehole permeameter technique. Soil Science Society of America Journal, 58: 1354-1357.

Constantz, J., Herkelrath, W.N., and Murphy, F. 1988. Air encapsulation during infiltration. Soil Science Society of America Journal, 52: 10-16.

Daniel, D.E. 1989. In situ hydraulic conductivity tests for compacted clay. Journal of Geotechnical Engineering, 115(9): 1205-1226.

Dwyer Instruments Inc. 2005. Series RM Rate-Master flow meters specifications-installations and operating instructions bulletin F-43, Dwyer Instruments Inc., Michigan City, IN 46361, U.S.A.

Elrick, D.E., and Reynolds, W.D. 1992. Infiltration from constant-head well permeameters and infiltrometers. Advances in Measurement of Soil Physical Properties: Bringing Theory into Practice, SSSA Special Publication no. 30: 1-24.

Elrick, D.E., and Reynolds, W.D. 1992. Methods for analyzing constant-head well permeameter data. Soil Science Society of America Journal, 56: 320-323.

Elrick, D.E., Sheard, R.W., and Baumgartner, N. 1981. A simple procedure for determining the hydraulic conductivity and water retention of putting green soil mixtures. In IV Int. Turfgrass Res. Conf. Guelph, pp. 189-200.

Elrick, D.E., Reynolds, W.D., and Tan, K.A. 1989. Hydraulic conductivity measurements in the unsaturated zone using improved well analyses. Ground Water Monitoring Review, 9: 184-193.

Fenske, D. 2008. A Study to Evaluate the Performance of a Reclamation Soil Cover Placed Over an Oil Sands Fluid Coke Deposit. M.Sc. thesis, University of Saskatchewan, Saskatoon, SK, Canada. Pending.

Freeze, R.A., and Cherry, J.A. 1979. Groundwater. Prentice-Hall, Inc., Englewood Cliffs, N.J.

Garbesi, K., Sextro, R.G., Robinson, A.L., Wooley, J.D., and Owens, J.A. 1996. Scale dependence of soil permeability to air: Measurement method and field investigation. Water Resources Research, 32(3): 547-560.

GEO-SLOPE International, L. 2004. GeoStudio 2004, Calgary, AB, Canada.

Giakoumakis, S.G., and Tsakiris, G.P. 1999. Quick estimates of hydraulic conductivity in unsaturated sandy loam soil. Irrigation and Drainage Systems, 13: 349-359.

Grover, B.L. 1955. Simplified air permeameters for soil in place. In Soil Science Society Proceedings, Vol.19, pp. 414-418.

Heid, J.G., McMahon, J.J., Nielsen, R.F., and Yuster, S.T. 1950. Study of the permeability of rocks to homogeneous fluids. A.P.I. Drilling and Production Practice: 230.

Hillel, D. 1998. Environmental Soil Physics. Academic Press, London.

Iversen, B.V., Moldrup, P., and Loll, P. 2004. Runoff modelling at two field slopes: Use of in situ measurements of air permeability to characterize spatial variability of saturated hydraulic conductivity. Hydrological Processes, 18: 1009-1026.

Iversen, B.V., Schjonning, P., Poulsen, T.G., and Moldrup, P. 2001. In situ, on-site and laboratory measurements of soil air permeability: Boundary conditions and measurement scale. Soil Science, 166(2): 97-106.

Iversen, B.V., Moldrup, P., Schjonning, P., and Loll, P. 2001. Air and water permeability in differently textured soils at two measurement scales. Soil Science, 166(10): 643-659.

Iversen, B.V., Moldrup, P., Schjonning, P., and Jacobsen, O.H. 2003. Field application of a portable air permeameter to characterize spatial variability in air and water permeability. Vadose Zone Journal, 2: 618-626.

Kirkham, D. 1946. Field method for determination of air permeability of soil in its undisturbed state. In Soil Science Society Proceedings, Vol.11, pp. 93-99.

Kirkham, D. 1947. Field method for determination of air permeability of soil in its undisturbed state. Soil Science Society of America Proceedings, 11: 93-99.

Klinkenberg, L.J. 1941. The permeability of porous media to liquids and gases. Drilling and Production Practice: 200-213.

Lee, D.M., Reynolds, W.D., Elrick, D.E., and Clothier, B.E. 1985. A comparison of three field methods for measuring saturated hydraulic conductivity. Canadian Journal of Soil Science, 65: 563-573.

Liang, P., Bowers, C.G.J., and Bowen, H.D. 1995. Finite element model to determine the shape factor for soil air permeability measurements. Transactions of the ASAE, 38(4): 997-1003.

Loll, P., Moldrup, P., Schjonning, P., and Riley, H. 1999. Predicting saturated hydraulic conductivity from air permeability: Application in stochastic water infiltration modelling. Water Resources Research, 35(8): 2387-2400.

Massmann, J.W. 1989. Applying groundwater flow models in vapor extraction system design. Journal of Environmental Engineering, 115(1): 129-149.

Meiers, G.P. 2002. The use of field measurements of hydraulic conductivity to characterize the performance of reclamation soil covers with time. M.Eng. report, University of Saskatchewan, Saskatoon, SK, Canada.

Meiers, G.P., Barbour, S.L., and Qualizza, C.V. 2006. The use of in situ measurement of hydraulic conductivity to provide an understanding of cover system performance over time. In 7th International Conference on Acid Rock Drainage (ICARD). Edited by R.I. Barnhisel. St. Louis MO. March 26-30, 2006. American Society of Mining and Reclamation (ASMR).

Merva, G.E. 1987. The velocity permeameter technique for rapid determination of hydraulic conductivity in-situ. In International Workshop on Land Drainage 3rd. Columbus, OH. December 7-11, 1987. Ohio State University, pp. G-55-G-66.

Messing, I., and Jarvis, N.J. 1990. Seasonal variation in field-saturated hydraulic conductivity in two swelling clay soils in Sweden. Journal of Soil Science, 41: 229-237.

Mohanty, B.P., Kanwar, R.S., and Everts, C.J. 1994. Comparison of saturated hydraulic conductivity measurement methods for a glacial-till soil. Soil Science Society of America Journal, 58: 672-677.

Ostle, B., Turner, K.V.J., Hicks, C.R., and McElrath, G.W. 1996. Engineering Statistics. The Industrial Experience. Wadsworth Publishing Company.

Perroux, K.M., and White, I. 1988. Designs for disc permeameters. Soil Science Society of America Journal, 52: 1205-1215.

Reynolds, W.D., and Elrick, D.E. 1985. In situ measurement of field-saturated hydraulic conductivity, sorptivity and the alpha-parameter using the Guelph permeameter. Soil Science, 140(4): 292-302.

Reynolds, W.D., and Elrick, D.E. 1986. A method for simultaneous in situ measurement in the vadose zone of field-saturated hydraulic conductivity, sorptivity and the conductivity- pressure head relationship. Ground Water Monitoring Review, 6(1): 84-95.

Reynolds, W.D., and Zebchuk, W.D. 1996. Hydraulic conductivity in a clay soil: Two measurement techniques and spatial characterization. Soil Science Society of America Journal, 60: 1679-1685.

Riley, H., and Ekeberg, E. 1989. Ploughless tillage in large-scale trials, II, Studies of

soil chemical and physical properties (in Norwegian with English abstract). Norsk Landbrugsforskning, 3: 107-115.

Scanlon, B.R., Nicot, J.P., and Massmann, J.W. 2002. Chapter 8. Soil gas movement in unsaturated systems. In Soil Physics Companion. pp. 297-341.

Schjonning, P. 1986. Soil permeability by air and water as influenced by soil type and incorporation of straw (in Danish with English summary). Tidsskrift for Planteavl, 90: 227-240.

Singh, P., Kanwar, R.S., and Thompson, L. 1991. Macropore characterization for two tillage systems using resin-impregnation technique. Soil Science Society of America Journal, 55: 1674-1679.

Sinha, N., Rodeck, S.A., Omar, M.T., DeVantier, B.A., and Das, B.M. 1995. Soil air permeability: Threshold gradient and anisotropy. Geotechnical Testing Journal, 18(4): 483-492.

Soilmoisture Equipment Corp. 1991. 2800KI Operating Instructions. SPSS, I. 2006. SPSS 15.0 for Windows.

Sollins, P., and Radulovich. 1988. Effects of soil physical structure on solute transport in a weathered topical soil. Soil Science Society of America Journal, 52(4): 1168-1173.

Tukey, J.W. 1977. Exploratory Data Analysis. Addison-Wesley, Reading, MA.

Watson, K.W., and Luxmoore, R.J. 1986. Estimating macroporosity in a forest watershed by use of a tension infiltrometer. Soil Science Society of America Journal, 50: 578-582.

Yu, L.L. 1985. Study of air flow through porous media, University of Connecticut, Storrs.

APPENDIX A
2006 LABORATORY TEST DATA

Table A.1. Raw data from column test using air as the test fluid, October 20, 2006. Trial 1: air flow from bottom to top of column.

		Manometer Readings (cm H_2O)									
		Port 1 (X= 4 cm)		Port 3 (X= 7 cm)		Port 5 (X= 15 cm)		Port 7 (X= 23 cm)		Port 9 (X= 26 cm)	
Q (ft^3/h)	T (°C)	H_1	H_2	H_1	H_2	H_1	H_2	H_1	H_2	H_1	H_2
10	21.4	45.1	51.3	45.5	50.9	45	48.5	46.1	47.4	41.6	42.3
15	21.6	43.7	52.6	44.2	52.2	44.1	49.4	45.9	47.6	41.2	42.7
20	22	42.1	54.3	42.7	53.7	43.1	50.4	45.5	48	41	43
25	22	40.6	55.8	41.4	55	42.2	51.3	44.6	48.8	40.5	43.4
30	22.2	38.8	57.5	39.8	56.6	41	52.5	44.3	49.3	40	43.8
35	22.1	37.8	58.5	38.8	57.6	40.2	53.3	43	50.4	39.6	44.2
40	22.1	35.4	60.8	36.7	59.7	38.7	54.8	42.8	50.7	38.8	45
2	22.1	47.7	48.6	47.7	48.6	46.5	47	46.5	47	41.9	42
4	22.1	47.1	49.2	47.3	49.1	46.2	47.3	46.5	47	41.8	42
8	22.1	46	50.3	46.3	50.1	45.6	47.9	46.2	47.3	41.7	42.1
10	22.1	45.5	50.8	45.8	50.6	45.2	48.3	46	47.5	41.6	42.2

Table A.2. Raw data from column test using air as the test fluid, October 20, 2006. Trial 2: air flow from top to bottom of column.

		Manometer Readings (cm H_2O)									
		Port 1 (X= 4 cm)		Port 3 (X= 7 cm)		Port 5 (X= 15 cm)		Port 7 (X= 23 cm)		Port 9 (X= 26 cm)	
Q (ft^3/h)	T (°C)	H_1	H_2	H_1	H_2	H_1	H_2	H_1	H_2	H_1	H_2
10	22	47.5	48.8	47.2	49.1	44.8	48.6	43.8	49.6	38.6	45
15	22	47	49.2	46.5	49.8	43.8	49.6	42.3	51.2	37	46.6
20	22	46.4	49.9	45.7	50.6	42.5	51	40.5	52.9	35	48.6
25	22	45.7	50.5	45	51.4	41.3	52.1	39	54.4	33.3	50.2
30	22	44.8	51.4	43.9	52.4	39.9	53.5	37.2	56.3	31.3	52.2
40	22	42.5	53.7	41.2	55.1	36.2	57.2	32.5	60.8	26.2	57.3

Table A.3. Raw data from column test using water as the test fluid, October 24, 2006.

		Test Number									
		1	2	3	4	5	6	7	8	9	10
		Flow Rate Readings									
	V (mL)	30	48	98	126	190	218	250	269	321	331
	Time (s)	120	120	135	120	120	120	120	120	120	120
	T (°C)	19.9	20	20	20.2	20.2	20.2	21.1	21.1	21.1	21.1
	X (cm)	Manometer Readings (cm H_2O)									
Port 1	4	33.1	33.7	35	36.3	38.4	39.4	40.3	41	42.6	43.7
Port 2	5.5	32.9	33.6	34.8	36	37.9	38.8	39.8	40.5	42	42.8
Port 3	7	33	33.6	34.8	35.9	37.8	38.7	39.5	40.1	41.5	42.2
Port 4	11	32.9	33.4	34.4	35.3	36.8	37.5	38.3	38.8	39.9	40.5
Port 5	15	32.6	33	33.9	34.5	35.7	36.3	36.9	37.3	38.1	38.6
Port 6	19	32.5	32.8	33.4	33.8	34.6	35	35.5	35.7	36.3	36.7
Port 7	23	32.4	32.6	32.9	33.2	33.7	33.9	34.1	34.2	34.6	34.9
Port 8	24.5	32.5	32.6	32.8	33	33.3	33.5	33.6	33.7	34	34.1
Port 9	26	32.2	32.3	32.5	32.6	32.8	32.9	33	33	33.2	33.2

Table A.4. Raw data from full scale air permeameter tank test, November 3, 2006.

Trial	D (cm)	T (°C)	Q (ft^3/h)	H_1 (cm H_2O)	H_2 (cm H_2O)	P_{atm} (kPa)
1	10	20.8	40	56	52.3	94.87
2	10	20.8	30	55.6	52.8	94.87
3	10	20.8	20	55.15	53.2	94.87
4	10	20.8	10	54.8	53.6	94.87
5	20	20.8	40	57.15	51.15	94.87
6	20	20.8	30	56.5	51.8	94.87
7	20	20.8	20	55.8	52.5	94.87
8	20	20.8	10	55.05	53.3	94.87
9	30	20.5	40	58.95	49.3	94.87
10	30	20.5	30	57.8	50.5	94.87
11	30	20.5	20	56.7	51.7	94.87
12	30	20.5	10	55.5	52.8	94.87
13	40	20.5	40	60.6	47.7	94.87
14	40	20.5	30	59.1	49.2	94.87

15	40	20.5	20	57.55	50.7	94.87
16	40	20.5	10	55.9	52.4	94.87
17	46	20.5	40	62.1	46.2	94.87
18	46	20.5	30	60.1	48.15	94.87
19	46	20.5	20	58.3	50	94.87
20	46	20.5	10	56.3	52	94.87

APPENDIX B
2006 GUELPH PERMEAMETER FIELD TEST DATA

Table B.1. Guelph Permeameter Data Set: Suncor 3:1 Cover Peat I, July 6, 2006. Weather: Overcast, 25C. Hole depth: 18cm. Soil layers present: peat, sand. Cell constant: 35.7 cm2.

5cm Head Data			10cm Head Data		
Time	Water Level (cm)	Δh (cm)	Time	Water Level (cm)	Δh (cm)
0:00:00	6.7	-	0:00:00	16.0	-
0:01:00	6.7	0.0	0:01:00	16.8	0.8
0:02:00	6.7	0.0	0:02:00	17.3	0.5
0:03:00	6.7	0.0	0:03:00	17.8	0.5
0:04:00	7.0	0.3	0:04:00	18.3	0.5
0:05:00	7.2	0.2	0:05:00	18.8	0.5
0:06:00	7.4	0.2	0:06:00	19.3	0.5
0:07:00	7.5	0.1	0:07:00	19.9	0.6
0:08:00	7.7	0.2	0:08:00	20.4	0.5
0:09:00	7.9	0.2	0:09:00	20.9	0.5
0:10:00	8.1	0.2	0:10:00	21.4	0.5
0:11:00	8.3	0.2			
0:12:00	8.6	0.3			
0:13:00	8.7	0.1			
0:14:00	8.9	0.2			
0:15:00	9.2	0.3			
0:16:00	9.5	0.3			
0:17:00	9.7	0.2			
0:18:00	9.8	0.1			
0:19:00	10.2	0.4			
0:20:00	10.4	0.2			
0:21:00	10.5	0.1			
0:22:00	10.8	0.3			
0:23:00	11.1	0.3			
0:24:00	11.4	0.3			
0:25:00	11.6	0.2			
0:26:00	11.8	0.2			
0:27:00	12.0	0.2			
0:28:00	12.3	0.3			
0:29:00	12.6	0.3			

Table B.2. Guelph Permeameter Data Set: Suncor 3:1 Cover Peat II, July 6, 2006. Weather: Overcast, 25C. Hole depth: 25cm. Soil layers present: peat, sand. Cell constant: 35.7 cm^2.

5cm Head Data		
Time	Water Level (cm)	Δh (cm)
0:00:00	6.6	-
0:01:00	6.7	0.1
0:02:00	6.8	0.1
0:03:00	6.8	0.0
0:05:00	7.1	0.3
0:06:00	7.2	0.1
0:08:00	7.4	0.2
0:11:00	7.7	0.3
0:12:00	7.8	0.1
0:13:00	7.9	0.1
0:14:00	8.0	0.1
0:15:00	8.1	0.1
0:16:00	8.2	0.1
0:17:00	8.3	0.1
0:18:00	8.3	0.0
0:19:00	8.4	0.1
0:20:00	8.5	0.1
0:21:00	8.6	0.1
0:22:00	8.7	0.1
0:23:00	8.7	0.0
0:24:00	8.8	0.1
0:25:00	8.9	0.1
0:26:00	9.0	0.1
0:27:00	9.1	0.1

10cm Head Data		
Time	Water Level (cm)	Δh (cm)
0:00:00	12.7	-
0:01:00	13.0	0.3
0:02:00	13.3	0.3
0:03:00	13.6	0.3
0:04:00	13.9	0.3
0:05:00	14.3	0.4
0:06:00	14.6	0.3
0:07:00	14.8	0.2
0:08:00	15.1	0.3
0:09:00	15.4	0.3
0:10:00	15.7	0.3
0:11:00	15.9	0.2
0:12:00	16.2	0.3
0:13:00	16.5	0.3
0:14:00	16.8	0.3
0:15:00	17.0	0.2
0:16:00	17.3	0.3

Table B.3. Guelph Permeameter Data Set: Syncrude D3 Cover Till I, August 16, 2006. Weather: Sunny, 22C. Hole depth: 31cm. Soil layers present: peat, till. Layer boundary present: 10cm. Cell constant: 35.22 cm^2.

5cm Head Data			10cm Head Data		
Time	Water Level (cm)	Δh (cm)	Time	Water Level (cm)	Δh (cm)
0:00:00	9.0	-	0:00:00	14.5	-
0:02:00	9.0	0.0	0:02:00	14.9	0.4
0:04:00	9.2	0.2	0:04:00	15.2	0.3
0:06:00	9.4	0.2	0:06:00	15.5	0.3
0:08:00	9.5	0.1	0:08:00	15.8	0.3
0:10:00	9.6	0.1	0:10:00	16.2	0.4
0:12:00	9.8	0.2	0:12:00	16.5	0.3
0:14:00	9.9	0.1	0:14:00	16.9	0.4
0:16:00	10.1	0.2	0:16:00	17.1	0.2
0:18:00	10.2	0.1	0:18:00	17.5	0.4
0:20:00	10.3	0.1	0:20:00	17.8	0.3
0:22:00	10.5	0.2	0:22:00	18.1	0.3
0:24:00	10.6	0.1	0:24:00	18.4	0.3
0:26:00	10.8	0.2	0:26:00	18.8	0.4
0:28:00	10.9	0.1			
0:30:00	11.1	0.2			

Table B.4. Guelph Permeameter Data Set: Syncrude D3 Cover Till II, August 16, 2006. Weather: Sunny, 22C. Hole depth: 29cm. Soil layers present: peat, till. Layer boundary present: 10cm. Cell constant: 35.47 cm^2.

5cm Head Data			10cm Head Data		
Time	Water Level (cm)	Δh (cm)	Time	Water Level (cm)	Δh (cm)
0:04:00	14.9	-	0:00:00	24.9	-
0:05:00	15.0	0.1	0:01:00	25.7	0.8
0:06:00	15.2	0.2	0:02:00	26.5	0.8
0:07:00	15.5	0.3	0:03:00	27.3	0.8
0:08:00	15.9	0.4	0:04:00	27.9	0.6
0:09:00	16.2	0.3	0:05:00	28.7	0.8
0:10:00	-	-	0:06:00	29.4	0.7
0:11:00	16.7	-	0:07:00	30.0	0.6

0:12:00	17.0	0.3
0:13:00	17.3	0.3
0:14:00	-	-
0:15:00	17.8	-
0:16:00	18.2	0.4
0:17:00	18.4	0.2
0:18:00	18.7	0.3
0:19:00	19.0	0.3
0:20:00	19.3	0.3
0:21:00	19.6	0.3
0:22:00	19.8	0.2
0:23:00	20.1	0.3
0:24:00	20.4	0.3
0:25:00	20.7	0.3

0:08:00	30.8	0.8
0:09:00	31.5	0.7
0:10:00	32.1	0.6
0:11:00	32.7	0.6
0:12:00	33.5	0.8
0:13:00	34.2	0.7
0:14:00	34.8	0.6
0:15:00	35.5	0.7

Table B.5. Guelph Permeameter Data Set: Syncrude Coke Beach Deep Cover Till I, August 17, 2006. Weather: Sunny, 25C. Hole depth: 21cm. Soil layers present: peat, till. Layer boundary present: 2 cm. Cell constant: 35.22 cm^2.

5cm Head Data		
Time	Water Level (cm)	Δh (cm)
0:00:00	27.8	-
0:01:00	28.1	0.3
0:02:00	28.7	0.6
0:03:00	29.1	0.4
0:04:00	29.6	0.5
0:05:00	30.0	0.4
0:06:00	30.4	0.4
0:07:00	31.0	0.6
0:08:00	31.2	0.2
0:09:00	31.8	0.6
0:10:00	32.2	0.4
0:11:00	32.5	0.3
0:12:00	32.9	0.4
0:13:00	33.5	0.6

10cm Head Data		
Time	Water Level (cm)	Δh (cm)
0:00:00	46.2	-
0:01:00	47.1	0.9
0:02:00	48.1	1.0
0:03:00	49.0	0.9
0:04:00	50.0	1.0
0:05:00	51.0	1.0
0:06:00	51.8	0.8
0:07:00	52.9	1.1
0:08:00	53.6	0.7
0:09:00	54.6	1.0
0:10:00	55.6	1.0
0:11:00	56.5	0.9
0:12:00	57.5	1.0
0:13:00	58.5	1.0

0:14:00	33.9	0.4	0:14:00	59.2	0.7
0:15:00	34.2	0.3	0:15:00	60.2	1.0
0:16:00	34.6	0.4	0:16:00	61.2	1.0
0:17:00	35.1	0.5	0:17:00	62.0	0.8
0:18:00	35.4	0.3	0:18:00	63.0	1.0
0:19:00	35.9	0.5	0:19:00	63.9	0.9
0:20:00	36.2	0.3	0:20:00	65.0	1.1
0:21:00	36.6	0.4	0:21:00	65.8	0.8
0:22:00	37.2	0.6	0:22:00	67.0	1.2
0:23:00	37.6	0.4	0:23:00	67.7	0.7
0:24:00	38	0.4	0:24:00	68.7	1.0
0:25:00	38.5	0.5	0:25:00	69.6	0.9
0:26:00	38.9	0.4	0:26:00	71	1.4
0:27:00	39.3	0.4	0:27:00	71.7	0.7
0:28:00	39.8	0.5	0:28:00	72	0.3
0:29:00	40.2	0.4	0:29:00	73.3	1.3
0:30:00	40.6	0.4	0:30:00	74.2	0.9
0:31:00	41	0.4	0:31:00	75.1	0.9
0:32:00	41.4	0.4	0:32:00	76	0.9

Table B.6. Guelph Permeameter Data Set: Syncrude Coke Beach Deep Cover Till II, August 17, 2006. Weather: Sunny, 25C. Hole depth: 28cm. Soil layers present: peat, till. Layer boundary present: 2 cm. Cell constant: 35.22 cm^2.

5cm Head Data			10cm Head Data		
Time	Water Level (cm)	Δh (cm)	Time	Water Level (cm)	Δh (cm)
0:00:00	21.6	-	0:00:00	37.8	-
0:01:00	22.9	1.3	0:01:00	37.8	0.0
0:02:00	23.8	0.9	0:02:00	38.2	0.4
0:03:00	24.9	1.1	0:03:00	38.5	0.3
0:04:00	-	-	0:04:00	38.8	0.3
0:05:00	26.8	-	0:05:00	39.4	0.6
0:06:00	28.1	1.3	0:06:00	39.8	0.4
0:07:00	29.1	1.0	0:07:00	40.0	0.2
0:08:00	30.2	1.1	0:08:00	40.6	0.6

0:09:00	31.1	0.9
0:10:00	31.9	0.8
0:11:00	32.9	1.0
0:12:00	33.8	0.9
0:13:00	34.9	1.1
0:14:00	35.8	0.9
0:15:00	36.8	1.0
0:16:00	37.7	0.9
0:17:00	38.8	1.1
0:18:00	39.8	1.0
0:19:00	40.7	0.9
0:20:00	41.8	1.1
0:21:00	42.6	0.8
0:22:00	43.7	1.1
0:23:00	44.8	1.1
0:24:00	45.7	0.9
0:25:00	46.7	1.0
0:26:00	47.8	1.1
0:27:00	48.7	0.9
0:28:00	49.8	1.1
0:29:00	50.8	1.0
0:30:00	51.9	1.1
0:31:00	52.9	1.0
0:32:00	53.9	1.0

0:09:00	41.0	0.4
0:10:00	41.3	0.3
0:11:00	41.9	0.6
0:12:00	42.2	0.3
0:13:00	42.6	0.4
0:14:00	43.7	1.1
0:15:00	44.0	0.3
0:16:00	44.6	0.6
0:17:00	45.0	0.4
0:18:00	45.5	0.5
0:19:00	46.0	0.5
0:20:00	46.3	0.3
0:21:00	46.9	0.6
0:22:00	47.4	0.5
0:23:00	47.9	0.5
0:24:00	48.5	0.6
0:25:00	48.9	0.4
0:26:00	49.4	0.5
0:27:00	50	0.6
0:28:00	50.5	0.5
0:29:00	51	0.5
0:30:00	51.5	0.5
0:31:00	52	0.5
0:32:00	52.5	0.5
0:33:00	53	0.5

APPENDIX C
2006 AIR PERMEAMETER FIELD DATA

Table C.1. Suncor 3:1 Peat Cover Air Permeameter Trials, August 2006.

Depth (cm)	T (°C)	Q (ft^3/h)	H_1 (cm)	H_2 (cm)	P_{atm} (kPa)
Trial: 3-1-S1. August 11, 2006.					
10	23.3	10	60.1	44.3	96.72
10	23.3	20	69.8	34.6	96.72
10	22.9	30	79.2	25.2	96.72
10	22.7	40	90	14.1	96.72
10	22.7	10	59.5	45.1	96.72
10	22.7	8	58.5	46.6	96.72
10	22.7	6	56.5	48.1	96.72
10	22.7	4	55	49.6	96.72
Trial: 3-1-S2. August 12, 2006.					
10	25.3	10	58	37.9	96.67
10	25.1	8	56	39.8	96.67
10	24.9	6	54	41.9	96.67
10	24.9	4	52.1	43.8	96.67
10	24.8	10	59.1	36.7	96.67
10	24.5	20	70.3	25.3	96.67
10	24.4	30	81.6	13.9	96.67
20	24.5	10	74.2	21.4	96.67
20	24.3	8	69.1	26.6	96.67
20	24.3	6	63.6	32.1	96.67
20	24.3	4	58.6	37	96.67
30	24.7	10	75.3	24.7	96.67
30	24.5	8	70.5	29.5	96.67
30	24.4	6	65.3	34.7	96.67
30	24.4	4	60.4	39.6	96.67
40	25.3	10	81.4	18.4	96.67
40	24.9	8	75.4	24.5	96.67
40	24.9	6	69.1	30.9	96.67
40	24.8	4	62.6	37.2	96.67
46	25.7	10	78.7	21.1	96.67
46	25.6	8	73.6	26.3	96.67
46	25.6	6	67.3	32.6	96.67

Depth (cm)	T (°C)	Q (ft^3/h)	H_1 (cm)	H_2 (cm)	P_{atm} (kPa)
46	25.4	4	61.8	38.1	96.67
Trial: 3-1-S3. August 12, 2006.					
10	34.5	10	54.4	45.4	96.56
10	34.2	8	53.5	46.1	96.56
10	34.1	6	52.5	47.1	96.56
10	33.9	4	51.7	48	96.56
10	33.5	10	55	44.7	96.56
10	33.3	20	60.7	39	96.56
10	33	30	66.8	32.8	96.56
20	30.6	10	92	7.6	96.56
20	30.6	8	84.3	15.4	96.56
20	30.7	6	75.4	24.3	96.56
20	30.8	4	67.3	32.4	96.56
30	29.4	2	54.7	45.1	96.56
30	29.4	4	59.3	40.5	96.56
30	29.2	6	63.9	35.9	96.56
30	28.9	8	69.4	30.3	96.56
30	28.5	10	73.8	25.9	96.56
40	27.3	2	56	43.8	96.56
40	26.9	4	61.8	38	96.56
40	26.5	6	68.1	31.7	96.56
40	26.2	8	74.5	25.2	96.56
40	26	10	80.5	19.2	96.56
Trial: 3-1-S4. August 13, 2006.					
10	27.3	4	50.4	49.5	96.87
10	27.3	6	50.5	49.5	96.87
10	27.4	8	50.7	49.3	96.87
10	27.4	10	50.8	49.2	96.87
10	27.5	10	51.1	48.8	96.87
10	27.4	20	52.2	47.8	96.87
10	27.2	30	53.4	46.6	96.87
Trial: 3-1-S5. August 13, 2006.					
10	28.6	2	56.8	43.1	96.83
10	28.4	4	63.7	36.2	96.83

Depth (cm)	T (°C)	Q (ft^3/h)	H_1 (cm)	H_2 (cm)	P_{atm} (kPa)
10	28	6	70.3	29.6	96.83
10	28.4	8	77.2	22.5	96.83
10	28.7	10	82.5	16.3	96.83
20	28.7	2	61	39	96.83
20	28.8	4	70.7	29.2	96.83
20	28.9	6	80.3	19.5	96.83
20	28.9	8	91.7	8.1	96.83
30	28.6	2	56.5	43.6	96.83
30	28.6	4	63.3	36.7	96.83
30	28.6	6	70	30	96.83
30	28.5	8	77.1	22.7	96.83
30	28.3	10	83.5	16.2	96.83
40	27.8	2	58.8	41.3	96.83
40	27.7	4	66.9	33	96.83
40	27.5	6	75.5	24.4	96.83
40	27.2	8	84.7	15.2	96.83
40	27	10	93	6.6	96.83
Trial: 3-1-S6. August 13, 2006.					
10	34	2	64.2	35.9	96.77
10	32.7	4	77.4	22.4	96.77
10	33.3	6	89.3	10	96.77
10	34.7	1	56.3	43.7	96.77
10	35	0.8	55.9	44.2	96.77
10	35	0.6	54.3	45.6	96.77
20	32.9	2	54	46	96.77
20	33	4	57.8	42.2	96.77
20	32.8	6	61.6	38.3	96.77
20	32.7	8	66.6	33.3	96.77
20	32.6	10	70.8	29.2	96.77
30	31.6	2	53.8	46.3	96.77
30	31.5	4	57.3	42.8	96.77
30	31.5	6	60.6	39.4	96.77
30	31.2	8	64.6	35.4	96.77
30	31.1	10	67.8	32.1	96.77

Depth (cm)	T (°C)	Q (ft^3/h)	H_1 (cm)	H_2 (cm)	P_{atm} (kPa)
30	30.8	2	54.1	46	96.77
30	30.8	4	58	42	96.77
30	30.5	6	62	38	96.77
30	30.2	8	66.2	34.8	96.77
30	30	10	70.1	29.8	96.77
40	30.5	2	55.7	44.3	96.77
40	30.2	4	60.9	39.1	96.77
40	30.1	6	66.4	33.7	96.77
40	30	8	72.6	27.5	96.77
40	30	10	77.7	22.3	96.77
40	29.2	2	55.7	44.5	96.77
40	30	4	61.4	38.7	96.77
40	30.1	6	66.6	33.5	96.77
40	30.1	8	73.2	26.7	96.77
40	30.1	10	78.6	21.3	96.77
Trial: 3-1-S7. August 13, 2006.					
10	31	2	52.5	47.6	96.74
10	31	4	54.9	45.3	96.74
10	30.5	6	57.3	42.8	96.74
10	30.4	8	59.9	40.2	96.74
10	30.3	10	62.1	37.9	96.74
10	30.6	2	52.6	47.6	96.74
10	31.1	4	55	45	96.74
10	31	6	57.7	42.5	96.74
10	30.9	8	60.3	39.8	96.74
10	30.9	10	62.5	37.4	96.74
20	32.6	2	52.6	47.5	96.74
20	32.7	4	55.1	44.9	96.74
20	32.5	6	57.6	42.4	96.74
20	32.3	8	60.6	39.4	96.74
20	32.1	10	62.9	37	96.74
20	32.7	2	52.7	47.4	96.74
20	32.9	4	55.4	45.6	96.74

Depth (cm)	T (°C)	Q (ft^3/h)	H_1 (cm)	H_2 (cm)	P_{atm} (kPa)
20	32.9	6	58.1	42	96.74
20	32.9	8	61.1	38.9	96.74
20	32.9	10	63.4	36.5	96.74
20	32.9	4	55.6	44.5	96.74
Trial: 3-1-S8. August 13, 2006.					
10	34.1	2	53.2	46.8	96.72
10	34.1	4	56.3	43.8	96.72
10	33.9	6	59.4	40	96.72
10	33	8	62.6	37.3	96.72
10	33.8	10	65.3	34.6	96.72
20	32.6	2	61.3	38.7	96.72
20	33.1	4	74.7	25	96.72
20	32.9	6	87.4	12.3	96.72
30	31.9	2	53.8	48.9	96.72
30	32.1	4	56.8	45.9	96.72
30	32.2	6	59.5	43	96.72
30	32.2	8	62.7	39.8	96.72
30	32.2	10	65.5	36.9	96.72
40	31.6	2	54.7	47.8	96.72
40	31.8	4	58.5	44.1	96.72
40	31.8	6	62	40.5	96.72
40	31.7	8	66.2	36.3	96.72
40	31.6	10	69.3	33	96.72

Table C.2. Syncrude D3 Till Cover Air Permeameter Trials, August 2006

Depth (cm)	T (°C)	Q (ft^3/h)	H_1 (cm)	H_2 (cm)	P_{atm} (kPa)
Trial: D3-1. August 14, 2006.					
10	32.2	30	51.5	47.6	96.64
10	32.4	20	50.9	48.2	96.64
10	32.4	10	50.2	48.8	96.64
10	32.4	10	50.1	49	96.64
10	32.4	8	50	49.1	96.64
10	32.4	6	49.9	49.2	96.64
20	30.2	10	50.1	49	96.64
20	30.2	20	50.5	48.6	96.64
20	30.2	30	51	48	96.64
30	30.2	10	50.2	48.9	96.64
30	30.2	20	51	48.1	96.64
30	30.2	30	51.7	47.4	96.64
Trial: D3-2. August 16, 2006.					
10	20.6	10	50.2	48.5	96.81
10	20.6	20	50.8	48	96.81
10	20.6	30	51.6	47.1	96.81
21	20.6	10	50.3	48.6	96.81
21	20.6	20	51	47.8	96.81
21	20.6	30	51.8	46.9	96.81
21	22.4	10	50.5	48.3	96.81
21	22.4	20	51.6	47.1	96.81
21	22.4	30	53	45.7	96.81
21	22.7	20	51.8	46.7	96.81
21	22.7	10	50.6	48.2	96.81
21	22.7	20	51.5	47.1	96.81
21	22.7	30	52.9	45.8	96.81
21	22.7	20	51.7	47	96.81
21	22.7	10	50.6	48.3	96.81
30.5	22.4	10	50.7	48.1	96.81
30.5	22.4	20	53.2	46.5	96.81
30.5	22.4	30	53.7	45	96.81
41	21.7	10	51.1	47.8	96.81
41	21.3	20	52.8	45.9	96.81
41	20.8	30	54.6	44	96.81
41	20.8	30	54.7	44	96.81
41	20.8	20	52.9	45.8	96.81

Depth (cm)	T (°C)	Q (ft^3/h)	H_1 (cm)	H_2 (cm)	P_{atm} (kPa)
41	20.8	10	51	47.7	96.81
41	20.8	20	52.8	45.9	96.81
41	20.8	30	54.6	44	96.81
Trial: D3-3. August 16, 2006.					
10	26.4	10	51	47.8	96.84
10	26.2	20	52.8	45.9	96.84
10	25.9	30	54.7	44	96.84
20	25.8	10	51.6	47.1	96.84
20	25.5	20	54.4	44.3	96.84
20	25.1	30	57.2	41.5	96.84
30	25.4	10	52.4	46.4	96.84
30	25.1	20	55.9	42.7	96.84
30	24.4	30	59.6	39.1	96.84
40	23.6	10	52.7	46	96.84
40	24.1	20	56.6	42.1	96.84
40	24.3	30	60.6	38	96.84
40	24.6	20	56.6	42	96.84
40	24.8	10	52.6	46	96.84
40	24.7	20	56.4	42.2	96.84
40	24.7	30	60.5	38.1	96.84
40	22.5	20	56.6	42	96.84
40	22.7	10	52.6	46	96.84

Table C.3. Syncrude Coke Beach Deep Till Cover Air Permeameter Trials, August 2006

Depth (cm)	T (°C)	Q (ft^3/h)	H_1 (cm)	H_2 (cm)	P_{atm} (kPa)
Trial: CD-1. August 17, 2006.					
13	25.2	10	47.2	46.3	97.4
13	24.7	20	47.5	45.9	97.4
13	24.4	30	48	45.4	97.4
13	24.3	40	48.5	45	97.4
19	24.3	10	47.5	46	97.4
19	23.6	15	47.7	45.8	97.4
19	23.6	20	48.1	45.9	97.4
19	23.3	30	48.8	44.6	97.4
19	23.3	40	49.6	43.8	97.4
19	23.3	30	49	44.5	97.4
19	23.3	20	48.2	45.2	97.4
19	23.3	10	47.5	46	97.4
19	23.3	20	48	45.4	97.4
19	23.3	30	48.7	44	97.4
30	23.2	10	47.9	45.6	97.4
30	23.6	15	48.4	45	97.4
30	23.6	20	49	44.4	97.4
30	23.3	30	50.3	43.2	97.4
30	23.1	40	51.7	41.7	97.4
40	22.7	10	47.7	45.5	97.4
40	22.8	15	48.2	45	97.4
40	22.7	20	48.7	44.4	97.4
40	22.6	30	50	43.3	97.4
40	22.2	40	51.3	42	97.4
Trial: CD-2. August 17, 2006.					
10	27.7	10	46.6	46.1	97.34
10	27.1	20	46.8	45.9	97.34
10	27	30	47.1	45.5	97.34
10	28	40	47.5	45.2	97.34
20	26.6	10	46.7	46	97.34
20	26.6	20	47	45.7	97.34
20	26.6	30	47.4	45.3	97.34
20	26.6	40	47.8	44.8	97.34
31	26	10	46.9	45.9	97.34
31	26	20	47.2	45.5	97.34
31	26	30	47.6	45.6	97.34

Depth (cm)	T (°C)	Q (ft^3/h)	H_1 (cm)	H_2 (cm)	P_{atm} (kPa)
31	26	40	48.2	44.5	97.34
31	26	30	47.8	45	97.34
31	26	20	47.4	45.4	97.34
31	26	10	46.9	45.9	97.34
31	26	20	47.2	45.6	97.34
31	26	30	47.6	45.1	97.34
40	26	10	46.9	45.9	97.34
40	26	20	47.2	45.6	97.34
40	26	30	47.7	45.1	97.34
40	26	40	48.2	44.6	97.34
Trial: CD-3. August 17, 2006.					
10	28	10	47.6	45.2	97.32
10	28	15	48	44.7	97.32
10	28	20	48.5	44.3	97.32
10	28	30	49.7	43.1	97.32
10	28	40	51	41.9	97.32
20	27.5	10	47.2	45.2	97.32
20	27.5	15	48.1	44.8	97.32
20	27.5	20	48.7	44.1	97.32
20	27.5	30	50.1	42.8	97.32
20	27.5	40	51.5	41.8	97.32
20	27.5	30	50.2	42.6	97.32
20	27.5	20	48.9	43.9	97.32
20	27.5	10	47.7	45.2	97.32
20	27.5	20	48.7	44.1	97.32
20	27.5	30	50	42.8	97.32
30	26.3	10	48.2	44.6	97.32
30	26.3	15	49	43.8	97.32
30	26.3	20	49.8	43	97.32
30	26.3	30	51.8	41.2	97.32
30	26.3	40	54	38.8	97.32
40	26	10	48.5	44.4	97.32
40	26	15	49.2	43.6	97.32
40	26	20	50.5	42.5	97.32
40	25.6	30	52.5	40.4	97.32
40	25.6	40	55	37.9	97.32